Author's response:

We thank the Referees for the careful revision and comments which helped in improving the overall quality of the manuscript.

A point-by-point answer (in regular typeset) to the referees' remarks (in the *italic typeset*) follows, while changes to the manuscript are indicated in blue font.

In the following page and lines references refer to the manuscript version reviewed by anonymous referee #1 and #2.

Anonymous Referee #1

This manuscript presents an analysis of the composition and source apportionment of PM$_1$ filters collected at three sites in Lithuania. For this offline technique, the aqueous extracts from filters were nebulized with Ar for introduction into the HR-ToF-AMS. The use of Ar as the nebulization gas enabled an analysis of the CO$^+$/CO$_2^+$ fragment ratio and trends in that ratio with season. Positive matrix factorization was also applied on both the offline AMS data set as well as an offline marker data set collected using the same filters. This manuscript provides a good demonstration of the type of data sets that can be generated via this offline AMS technique and the CO+/CO2+ analysis provides new insights into the interpretation of AMS data from ambient samples. Thus, I see this paper as appropriate for publication in ACP. However, I have a few concerns, mostly related to sampling artifacts that need to be addressed prior to publication.

1) **P2 L9:** *Traffic exhaust OA is listed as a PMF factor from AMS spectra, yet in the*

   experimental it is noted that the contribution is too low to be resolved with PMF and is instead estimated using a CMB approach. I suggest rewording the abstract to clarify this.

We reworded the abstract as follows: "AMS WSOA spectra were analyzed using positive matrix factorization (PMF), which yielded 4 factors. These factors included biomass burning OA (BBOA), local OA (LOA) contributing significantly only in Vilnius, and two oxygenated OA (OOA) factors, summer OOA (S-OOA) and background OOA (B-OOA) distinguished by their seasonal variability. The contribution of traffic exhaust OA (TEOA) was not resolved by PMF due to both low concentrations and low water solubility. Therefore, the TEOA concentration was estimated using a chemical mass balance approach, based on the concentrations of hopanes, specific markers of traffic emissions."

Changes in text:

2) **P5 L24:** *The nebulizer used was operated at 60°C, how long are the aerosols in this heated region? Was this temperature in the nebulizer also used in the Daellenbach et al. analysis? What effect might this high temperature have on the composition of the organics measured with the AMS compared to online analysis? If this temperature was not used for the Daellenbach analysis, what effect might this have on the factor specific*

recoveries of this work compared to the results from that previous analysis?

The nebulizing Ar flow was 0.4 L min^{-1}. Considering the internal diameter (6 mm) and the length of our lines, we can estimate an aerosol residence time in our lines (from nebulization to AMS detection) of ca. 2 s. The aerosol residence time in the 60°C zone is significantly shorter (~100ms). A set of 40 PM$_1$ filter samples collected in Lithuania (not included within the source apportionment presented in this work) was measured using both the Apex Q nebulizer (Elemental Scientific Inc., Omaha NE 68131 USA) operated at 60°C and using a custom-built nebulizer (Daellenbach et al., 2016). The comparable WSOA/SO$_4^{2-}$ ratio registered using the two systems indicates a negligible loss of volatile organics (Fig. Discussion 1 (Fig. D1)).

We compared organic mass spectral time series and fragments fractional contributions retrieved from the two different nebulization systems. Mass spectra revealed a good correlation for all fragments (R = 0.94 on average), similarly the total organic signal showed a correlation of R = 0.94 (Fig. D1). Excluding CO$_2^+$ and the related fragments (CO$^+$, H$_2$O$^+$, HO$^+$, and O$^+$, Aiken et al., 2008; Canagaratna et al., 2007), the intensity of which can be affected by the vaporizer history (Fröhlich et al., 2015, Pieber et al., 2016), we observed a good agreement between the normalized AMS mass spectral fingerprints obtained with the two different nebulizers, with 95% of the i, j elements not statistically different within 2σ. As stated in the manuscript, here i, and j represent a generic filter sample and a generic AMS fragment, respectively, while the uncertainty considered here includes blank variability, repeatability, uncertainty related to ion counting statistics and ion-to-ion signal variability at the detector. Overall the new nebulization system revealed a ~7 times higher sensitivity. Given the high correlation and the similarity in the mass spectral fingerprints, we can exclude substantial effects on the recoveries of the different factors.
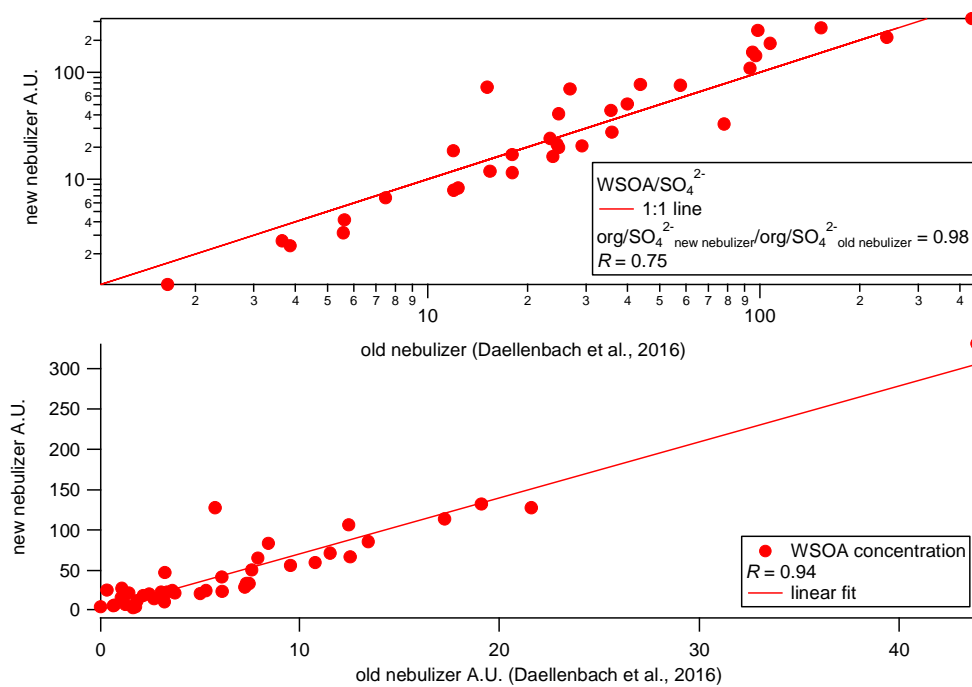
Figure D1. Top: WSOA/SO$_4^{2-}$ ratio registered with a custom-made nebulizer (Daellenbach et al. 2016, here marked as "old nebulizer") and our nebulization system ("new nebulizer"). Bottom: OA signal comparison.

3) **P18 L25:** *PM$_1$ composition discussed here and shown in Figure 1 shows ions that can be measured with both the AMS and IC (e.g. SO4, NO3, etc.). Do the contributions shown in Figure 1 correspond to the IC measurements or AMS? For ions that can be quantified with both techniques, how do the values compare between the AMS and IC?*

Author's response:

As mentioned at P6, L30-31, the ion concentrations are from IC if not differently specified. For the sake of clarity we added this information in the Figure 1 caption.

Following the recommendations of anonymous referees #1 and #2 we added in the revised SI a comparison between offline-AMS and IC:

Offline-AMS comparison with IC and WSOC determination by TOC analyzer

Overall, the comparison between offline-AMS and IC concentrations of NH$_4^+$, SO$_4^{2-}$, and NO$_3^-$ reveals a non-linear relation due to the lower IC detection limits. This is

1 most likely related to the low transmission efficiency of the AMS lens for small
2 particles, particularly predominant for diluted filter extracts.

3 Nevertheless, considering internally mixed nebulized particles, the composition of the
4 particles is not supposed to change with the solution concentration, as also
5 confirmed by dilution tests conducted on our filter extracts (Fig. D2).
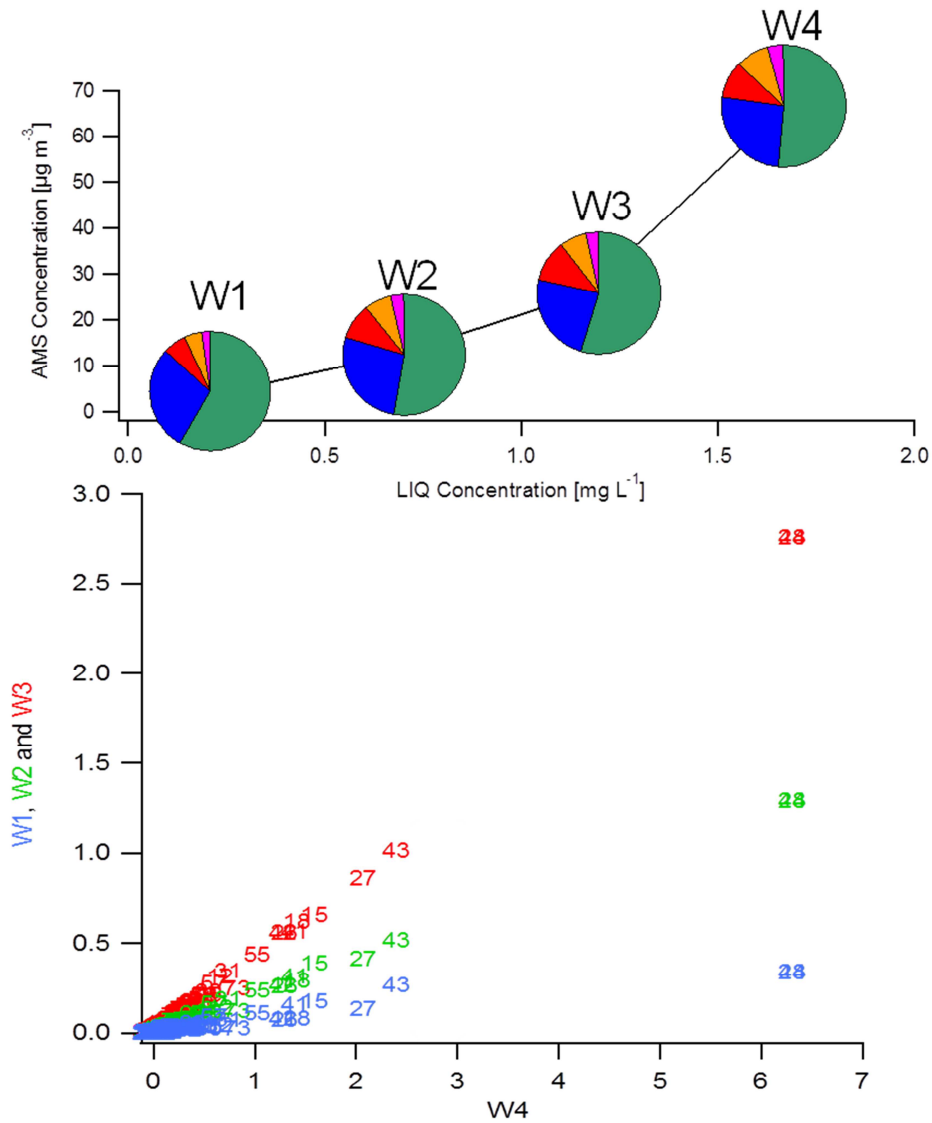
Figure D2. Dilution tests: NR PM composition and comparison of mass spectra registered at different dilutions.
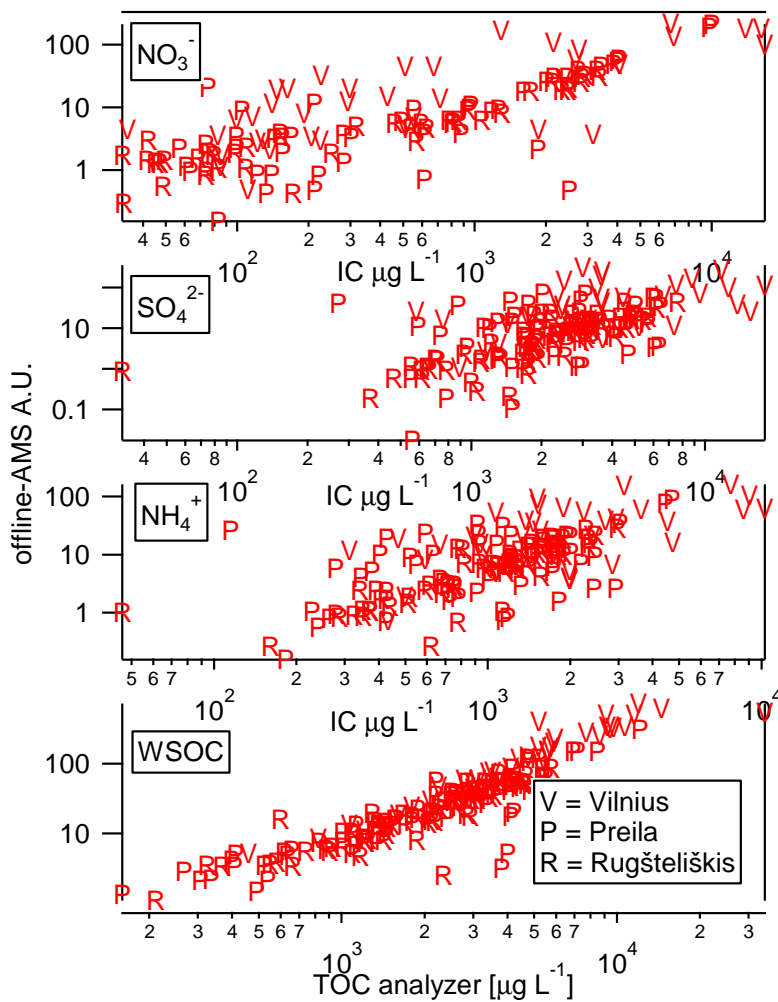
Figure D3. Offline-AMS comparison with different techniques with IC and WSOC measurements by TOC analyzer.

Figure D2 and D3 were added to the SI as Fig. S16 and S17:

The following paragraph was added to Fig. S17 caption:

This low particle transmission efficiency for diluted solutions results in a high scattering at low concentration. Additional scattering is observed in the relation between offline-AMS and IC SO_4^{2-}. This is related to the presence of refractory sulfate salts (e.g. Na_2SO_4, ammonium sulfate) which are detectable by IC, but not with the AMS, consistent with lower slope obtained between offline-AMS and IC SO_4^{2-}, compared to the other species.

These species are likely formed during nebulization, e.g.

$$(NH4)_2SO_4 + CaCl_2 \rightleftharpoons CaSO_4 + 2NH_4Cl$$

For these reasons we only reported inorganic ion concentrations from IC.

6

1

2

3   *4)*   **P19 L14-20:** *The nitrate concentration shows clear seasonality with larger*
4   *contributions in the winter and the sulfate concentration looks relatively*
5   *constant throughout the year. However, in Figure 1, the ammonium*
6   *concentration appears to also be relatively constant throughout the year. Is*
7   *this correct? If so, can the authors comment on potential counter ions for*
8   NO_3 *?*

9

10 **Author's response:**

11 Considering the NH_4^+, SO_4^{2-} and NO_3^- concentrations in μEq m^{-3}, the agreement
12 between (NH_4^+) and (SO_4^{2-} + NO_3^-) is high, with an average (SO_4^{2-} + NO_3^-)/NH_4^+ ratio
13 of 0.99 over the year and 1.02 during winter. The Pearson correlation coefficient *R*
14 between (SO_4^{2-} + NO_3^-) and NH_4^+ was 0.92 considering the whole year and 0.84
15 considering only winter. Therefore, the role of other counter ions is negligible.

16

17

7
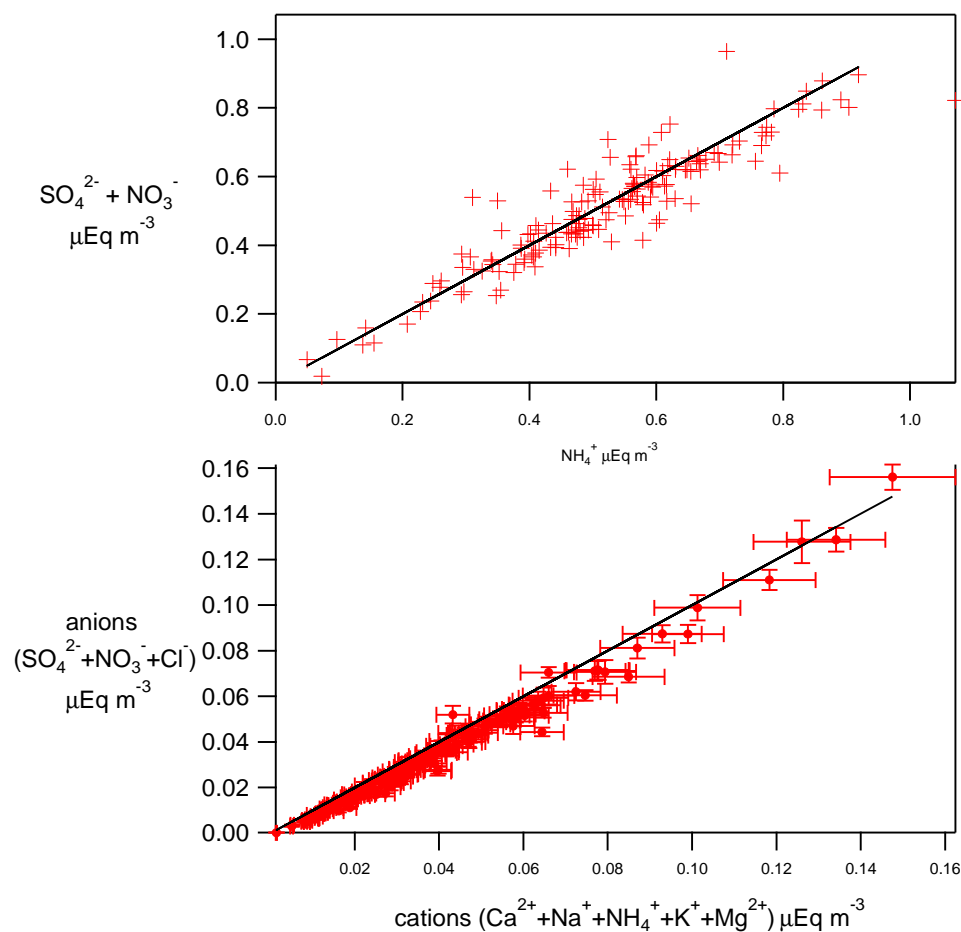
1
2　Figure D4. NH_4^+ correlation with $SO_4^{2-} + NO_3^-$. Data in $\mu Eq\ m^{-3}$ (top); ion balance (bottom).

3　Figure D4 was added to Fig. S11.

4
5　　*5)*　　**P20 L 28-31:** *The background-OOA factor appears to correlate with NH_4^+*
6　　　　　*much better at Preila and Vilnius than Rugsteliskes (Figure S11). Are there*
7　　　　　*any potential reasons for the lower apparent correlation at Rugsteliskes?*
8　　　　　*How much uncertainty is there in the NH_4^+ measurement? What is the*
9　　　　　*significance of a correlation of B-OOA with NH_4^+?*

10

11　**Author's response:**

12　The B-OOA factor correlation with NH_4^+ is significant at all stations: $R = 0.82$ ($R^2 =$
13　0.67) for Vilnius, 0.87 ($R^2 = 0.76$) for Preila, and 0.71 ($R^2 = 0.50$) for Rūgšteliškis. The
14　correlation of B-OOA with a secondary inorganic component such as NH_4^+ could
15　suggest the secondary origin of B-OOA, as also inferred by the comparison with the
16　marker-source apportionment (section 4.4.2). The repeatability of NH_4^+ IC
17　measurements was 10%, while according to our error estimate (Section 3.1.3), the
18　average relative uncertainty on the B-OOA factor for Rūgšteliškis was 12%. We

8

estimated that up to half of the total unexplained variability in the relationship between NH_4^+ and B-OOA in Rūgšteliškis can be due to the abovementioned errors, while in Preila and Vilnius the B-OOA *vs* NH_4^+, most of the unexplained variability can be attributed to the errors. For Rūgšteliškis the remaining unexplained variability (27%) may be related to variability in the precursor composition and/or in the air masses photochemical age.

This information was added to Fig. S11 caption.

6) ***Section 2.1 and P21 L1-17:*** *Were the High-Volume samplers located in temperature controlled rooms? If not, what effect could higher summer temperatures have on the composition of the organic compared to the winter samples? Could the S-OOA factor be complicated by collection differences caused by the loss (on the filter) of more volatile organic molecules during summer months?*

Author's response:

High volume were equipped with temperature control systems maintaining the filter storage temperature always below 25°C, which is lower or comparable to the maximum daily temperature during summer (Fig. 3b). This should prevent large negative artifacts involving the most volatile fraction.

We added this information in P4, L16:

In order to prevent large negative filter artifacts, the high-volume samplers were equipped with temperature control systems maintaining the filter storage temperature always below 25°C, which is lower or comparable to the maximum daily temperature during summer.

7) ***P2 L6:*** *the CO_2^+:CO^+ ratios reported in section 4.5 are greater than 1. The less than sign should be switched.*

Corrected as suggested

8) ***P10 L22-23:*** *a verb such as "was used" is missing.*

Corrected as "was constrained"

9) ***P22 L3:*** *I suggest some mention directing the reader to Figure 5 be made in the text as the time series for the factors are discussed in this section but no mention of Figure 5 is made.*

We introduced a reference to Figure 5 at P22 L3

10) **P25 L13:** *"Using the ratio (1.88) calculated from offline-AMS". Suggest adding*

OM/OC$_{BBOA}$ *ratio to communicate what ratio is being used in the calculation here.*

Corrected as suggested

11) **P30 L 25-26:** *suggest rephrasing, the double negative "unlikely return uncertain CO+ values" is confusing.*

Rephrased as: "should return accurate CO$^+$"

12) **P45 Figure 2 and P46 Figure 4:** *Suggest either writing out the factor names in the labels (background-OOA instead of B-OOA etc.) or giving the names and labels in the caption.*

Factor names and labels added in Figure 2 and Figure 4 captions.

Anonymous Referee #2

General Comments:

This manuscript reported an analysis of PM$_1$ compositions and sources at three different sites in Lithuania based on filter samples. The authors applied AMS and other instruments to analyze the filter samples, and then performed PMF analysis to study the sources of OA and PM$_1$. This study presented a method/case to study the sources of total ambient OA based on the measurements of water soluble OA only. That is, apply PMF analysis on the water soluble organic mass spectra, identify multiple factors, and rescale the water soluble concentration to total concentration by applying recovery ratios. This is an interesting method but has large uncertainties,

1 *which arise from the recovery ratio. I think this manuscript is suitable for publication*
2 *in ACP once the following comments have been addressed.*

3

4

5 ***Source Apportionment***

6

7

8 We thank Anonymous Referee #2 for the careful review which indeed helped to
9 improve the overall quality of our work. We want to state that while the uncertainty
10 deriving from the recovery application is substantial, we do demonstrate that this
11 uncertainty is comparable to that from PMF rotational uncertainty. The overall
12 uncertainty of our source apportionment is factor dependent and is on average 14%
13 for BBOA, 15% for B-OOA, 28% for S-OOA, and 100% for LOA, with the latter mostly
14 due to the low concentrations during winter and . As a comparison, the R_{BBOA} relative
15 uncertainty (σR_{BBOA}) was 10%, σR_{OOA} was 7%, and σR_{LOA} 14%. Our factor
16 uncertainties are comparable to the AMS mass uncertainty, which is commonly
17 considered to be 30%, but does not affect our results, and instead affects online-
18 AMS source apportionment studies. Therefore the uncertainty relative to the offline-
19 AMS methodology is high, yet comparable to the online-AMS source apportionment.

20

21

22 **Major comments**
23   *1)*   *Ambient total OA source apportionment based on the measurement of*
24   *water soluble OA.*

25

26   *The major uncertainty of this method arises from the recovery ratio (Rz),*
27   *which is a reflection of the bulk extraction efficiency and water solubility of*
28   *OA factors. It is not clear how the Rz values are obtained in this study. As I*
29   *understand, the authors randomly selected Rz from Daellenbach et al.*
30   *(2016) as initial conditions and fit Eq. (6) to get RLOA. If so, how are*
31   *RBBOA and ROOA obtained? Why are they different from the values in*
32   *Daellenbach et al. (2016). Also, it is not clear which Rz values are*
33   *eventually applied, from Daellenbach et al. (2016) or the values calculated*
34   *in this study?*

35

36 As anonymous referee #2 mentioned, factor recoveries were randomly selected from
37 the combinations reported in Daellenbach et al. (2016). The randomly selected R_Z
38 combinations were perturbed assuming possible biases in the OC and WSOC
39 measurements in Daellenbach et al. (2016) and in this study. The perturbed
40 randomly selected R_Z combinations were then used as input to fit R_{LOA} according to
41 Eq. (6). Only R_Z combinations leading to unbiased OC fit residuals were retained (i.e.
42 OC fitting residuals not statistically different from 0 within 1σ for summer and winter
43 individually and for the whole period). The retained R_Z combinations were displayed
44 as PDF in Fig. S8. The newly obtained R_{BBOA} and R_{OOA} are systematically lower than
45 those reported in Daellenbach et al. (2016), by 5.6% and 12.3% respectively, within

the expected biases of the different measurements. L23 P12- L6, P13 were modified as follows:

For each of the 95 retained PMF solutions, Eq. (6) was fitted 100 times by randomly selecting a set of 100 R_{BBOA}, R_{OOA} value combinations from those determined by Daellenbach et al. (2016). Each fit was initiated by perturbing the input OC_i and $TEOC_i$ within their uncertainties, assuming a normal distribution of the errors. Additionally, in order to explore the effect of possible bulk extraction efficiency (WSOC/OC) systematic measurement biases on our R_Z estimates, we also perturbed the OC, WSOC (Daellenbach et al., 2016) inputs. Specifically, we assumed an estimated accuracy bias of 5% for each of the perturbed parameters, which corresponds to the OC and WSOC measurement accuracy. In a similar way, we also perturbed the input R_{BBOA} and R_{OOA} assuming an accuracy estimate of 5% deriving from a possible OC measurement bias in Daellenbach et al. (2016) which could have affected the R_Z determination. In total $9.5·10^3$ fits were performed (Eq. 6) and we retained only solutions (and corresponding perturbed R_Z combinations) associated with average OC residuals not statistically different from 0 within 1σ for each station individually and for summer and winter individually (~8% of the $9.5·10^3$ fits, Fig. S6). The OC residuals of the accepted solutions did not manifest a clear correlation with the LOA concentration (Fig. S7), indicating that the estimated R_{LOA} was properly fitted, without compensating for unexplained variability of the PMF model or biases from the other R_z. Fig. S8 shows the probability density functions (PDF) of the retained perturbed R_z which account for all uncertainties and biases mentioned above.

> *2)* *The authors mentioned that the bulk extraction efficiency in this study is lower than that in Daellenbach et al. (2016). This result is not surprising since one OA factor likely has contribution from multiple sources and the water solubility of OA factors may vary with site and season. For example, the water solubility of BBOA ranges from 64% to 80% (Sciare et al., 2011; Timonen et al., 2008). In addition, this method is not sensitive to primary OA factors (e.g., HOA and Cooking OA), which is largely water insoluble. This is another reason why HOA cannot be resolved from the PMF analysis. The limitations should be better discussed in the manuscript.*
>
> *What suggestions do the authors have for researchers who want to use the method as proposed in this manuscript? For example, should they follow the same filter extraction procedures as in this study? How to calculate the Rz?*

Indeed, Bulk EE (WSOC/OC) can vary between site and seasons and WSOC ranges reported in the literature for the different sources (e.g. BBOA, *(Sciare et al., 2011; Timonen et al., 2008)* cover the ranges obtained here and in Daellenbach et al. (2016). However, it is unexpected that all primary and secondary factors determined in this study in both seasons have systematically lower water solubility than those in Daellenbach et al. (2016). By contrast, the Bulk EE differences found between this work and Daellenbach et al. (2016) can be fully explained by the WSOC and OC accuracy measurements.

The following recommendations for future offline-AMS users were added at P13 L19:

In general the recovery estimates reported in Daellenbach et al. (2016) represent the most accurate estimates available, being constrained to match the online-ACSM source apportionment results. The R_Z combinations reported by Daellenbach et al. (2016) demonstrated to positively apply to this dataset, enabling properly fitting the measured Bulk EE (WSOC/OC) with unbiased residuals and therefore providing a further confidence on their applicability (we note that in Eq. 6 we fitted OC as function of $1/R_Z$ and $WSOC_{Z,i}$, therefore R_Z fitted WSOC/OC = Bulk EE). In general further R_Z determinations calculated comparing offline-AMS and online-AMS source apportionments would be desirable in order to provide more robust R_Z estimates. In absence of a-priori R_Z values for specific factors (e.g. for LOA in this study) we recommend constraining the R_Z combinations reported by Daellenbach et al. (2016) as a-priori information to fit the unknown recoveries, with the caveat that the R_Z combinations reported by Deallenbach et al. (2016) were determined for filter samples water extracted following a specific procedure; therefore we recommend adopting these R_Z combinations for filter samples extracted in the same conditions. Nevertheless the R_Z combinations reported by Daellenbach et al. (2016) should be tested also for filters extracted with water in different conditions to verify whether they can properly fit the Bulk EE. In case the R_Z combinations reported by Daellenbach et al. (2016) would not apply for a specific location or extraction procedure (i.e. not enabling a proper fit of Bulk EE) we recommend a R_Z redetermination by comparing the offline-AMS source apportionment results with well-established source apportionment techniques. In absence of data to perform a well-established source apportionment, we recommend to fit all the R_Z to match the bulk EE (i.e. fitting all the recoveries similarly as in Eq. 6 without constraining any a-priory R_Z value).

In general, the offline-AMS technique assesses less precisely the contribution of the lower water soluble factors. The higher uncertainty mostly stems from the larger PMF rotational ambiguity when separating a factor characterized by low concentration in the aqueous filter extracts. Nevertheless, the uncertainty is dataset dependent, as the separation of source components with low water solubility can be improved in case of distinct time variability characterizing those sources in comparison with the other aerosol sources. The low aqueous concentration of scarcely water soluble sources in fact can be partially overcome by the large signal/noise characterizing the offline-AMS technique (170 on average for this dataset).

3) *Discussions on instruments comparison are required.*

Inorganic ions such as NH4+, NO3-, and SO42- are measured by both AMS and IC. The authors should present the instruments comparison.

The comparison between offline-AMS and IC ion concentrations was discussed and added to the SI, according also to Anonymous Referee #1 question (question 5). We note though that offline AMS data are not used for quantification, which will be the subject of an up-coming study.

4)   Page 9 Line 29-30. The AMS measured concentration is scaled to match the WSOC measurement. What's the scale ratio? Is the scale ratio the same for all filter samples?

Similarly to NH_4^+, SO_4^{2-}, and NO_3, and for the same reasons discussed above (Anonymous referee #1, question 5), the WSOC signal from offline-AMS does not follow a linear relation. Therefore the scaling factor is not constant. We would like to note once again that the AMS has not been used for quantification, specifically because of these issues related to particle transmission efficiency; moreover, as displayed in Fig. D2 the WSOM AMS mass spectral fingerprint does not show large changes when diluting our filter extracts. This comparison was inserted in the revised SI.
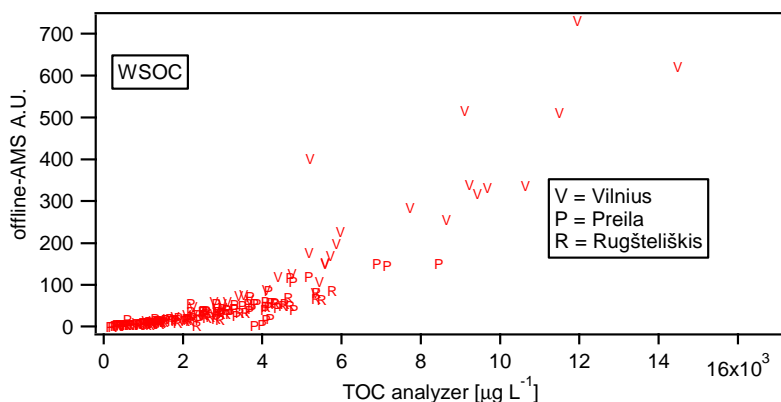
Figure D5. Correlation between WSOC offline-AMS signal and WSOC measurements by TOC analyzer.

5)   The difference in separation and classification of OA factors between online and offline-AMS (Page 20 Line 14-27).

I disagree with the statement that "online-AMS OOA factors are commonly classified based on their volatility", because chemistry and sources also affect the factor separation. For example, the separation of IEPOX-OA factor (Budisulistiorini et al., 2013; Hu et al., 2015) or called isoprene-OA factor (Xu et al., 2015) is driven by IEPOX chemistry, but not volatility. Also, Xu et al. (2015) showed that nighttime monoterpene oxidation by nitrate radical contributes to less-oxidized OOA (as termed SV-OOA in this study).

Following the suggestion of anonymous referee #2 we modified the lines at P20 L17-18 as follows:

Few online-AMS studies reported the separation of isoprene-related OA factor (Budisulistiorini et al., 2013; Hu et al., 2015, Xu et al., 2015) mostly driven by isoprene epoxides chemistry. Xu et al. (2015) showed that nighttime monoterpene oxidation by nitrate radical contributes to less-oxidized OOA. However, the large majority of online-AMS OOA factors are commonly classified based on their volatility

14

(semi-volatile OOA and low-volatility OOA) rather than on their sources and formation mechanisms.

6)   *The authors stated that "the offline-AMS sources apportionment separates factors by seasonal trends rather than volatility". However, sometimes, seasonal trend affects the source apportionment through volatility. For example, Page 23 Line 26-27 discussed that higher NO3--related SA exhibits higher concentration in winter than summer, which is due to the semi-volatile nature of NO3- (Page 19 Line 20).*

Concerning the relation between seasonality and volatility, we agree that OOA factors with different seasonal behaviors can be characterized by different volatilities. However in this work the offline-AMS OOA separation is not driven by volatility, given the low correlation between NO_3^- and our OOA factors (this is also reflected by the low NO_3^--related SOA correlation with B-OOA and S-OOA, Table 2). Additionally, the partitioning of semi-volatile OA at low temperatures would lead to a less oxidized OOA fingerprint during winter; however, this is not the case here. We observed a less oxidized OOA factor during summer, whose fingerprint closely resembles that of SOA from biogenic precursors, while similar to OOA from biomass burning emissions OOA during the cold season is more oxidized. This has been also reported from online-ACSM monitoring campaigns (Canonaco et al., 2015),

7)   *OM/OC ratio.*

In this study, the OM/OC is calculated by Aiken method (Page 12 Line 20). However, a recent study by Canagaratna et al. (2015) improved the estimation from Aiken method by including composition-dependent correction factors. The Canagaratna method is recommended to use. Since many calculations in this study depend on the OM/OC ratio, how would it affect the results/conclusions if the authors use Canagaratna method to calculate the OM/OC ratio?

Following the suggestion of anonymous referee #2 we included following discussion within the SI.

We recalculated the OM:OC ratio for the water soluble collected spectra according to the new parametrization reported by Canagaratna et al. (2015). Consistently with Canagaratna et al. (2015), the newly calculated OM:OC ratio was on average 9% higher than the OM:OC ratio calculated according to Aiken method. More specifically, the OM:OC ratio was on average 9% higher during summer, and 10% during winter. The two methods reported well correlated OM:OC values ($R = 0.98$ over the whole monitoring period, $R = 0.99$ during winter, $R = 0.97$ during summer). In our study, the OM:OC ratios of our water soluble mass spectra were mostly used to determine the total WSOM concentrations. Considering the high correlations between the Aiken and Canagaratna OM:OC ratios, we can exclude large effects on the WSOM variability and therefore on the source apportionment. Nevertheless the WSOM estimated concentrations would be 10 % larger, when assuming the Canagaratna

OM:OC parametrization. In general Aiken assumed a $CO_2^+:CO^+$ ratio of 1, while Canagaratna stated that such an assumption would underestimate CO^+. From our dataset, we observed a $CO_2^+:CO^+$ of 1.75_{med} suggesting that the Aiken OM:OC parametrization would represent more accurately our data although both parametrizations are uncertain for this dataset.

> *8)*   *Background-OOA (B-OOA) factor.*
>
> *When the authors selected solutions, one criterion is the correlation between B-OOA and NH4+ (Page 12 Line 8). The authors should explain the use of NH4+. SO42- is regional and usually used as background OA. What's the correlation between B-OOA and SO42-? In Page 20 Line 30, it is stated that B-OOA correlates well with NH4+. However, the correlation between B-OOA and NH4+ varies with site as shown in Fig. S11. For example, the correlation is really weak for the Rugsteliskis site.*

The lower correlation between NH_4^+ and B-OOA in Rūgšteliškis (R^2 = 0.5 vs R^2 > 0.7 at other locations) and its possible explanation were discussed in the response to anonymous referee #1 (question 5). The repeatability of NH_4^+ measurements is estimated to be around 10%, while according to our error estimate (Section 3.1.3), the average relative uncertainty on the B-OOA factor for Rūgšteliškis was 12%. We estimated that up to half of the total unexplained variability in the relationship between NH_4^+ and B-OOA in Rūgšteliškis can be due to the abovementioned errors, while for the B-OOA *vs* NH_4^+ relationship in Preila and Vilnius most of the unexplained variability can be attributed to these errors. For Rūgšteliškis the remaining unexplained variability (27%) can be related to variability in the secondary precursor composition and/or in the air masses photochemical age.

The criterion based on the NH_4^+ *vs* B-OOA correlation did not reveal any negative correlation for each station individually and for all the stations together, therefore no PMF solution was discarded according to this criterion as well as for the criterion based on the correlation of levoglucosan with BBOA (this information was added to the manuscript). As previously discussed, NH_4^+ [μEq m^{-3}] matches the sum of SO_4^{2-} and NO_3^- [μEq m^{-3}]. Therefore NH_4^+ variability well represents the variability of inorganic secondary components of different origin (local: NO_3^- and regional: SO_4^{2-}) formed at different time scales. Nevertheless, similar to B-OOA retrieved from the offline-AMS PMF, NH_4^+ correlates most significantly with sulfate (R = 0.80) and the sulfate-rich factor from the marker-PMF, indicating that these species represent the background long range transported aerosols.

> *9)*   *If B-OOA represents background OA, why is B-OOA lower in urban site than the other sites? I disagree with the authors' argument that this difference is caused by PMF residual uncertainties or biases (Page 29 Line 10). The authors' argument is flawed because it is based on circular assumptions. When the authors calculate B-OOAmarker, the LOA and S-OOA are based on PMF analysis without considering "some residual uncertainties or biases". If the authors considered "some residual uncertainties or biases" and re-performed PMF analysis, the concentrations of LOA and S-OOA would change, which would influence*

and concentration of B-OOAmarker. In that circumstance, B-OOAoffline-AMS may agree among all three sites, but B-OOAmarker may be different among all three sites.

Showing that PMF results are affected by model residuals is exactly the point we wanted to make with this comparison. Therefore, drawing strong conclusions on site-to-site differences should be done with caution. In the current version of the manuscript we elaborate further on these issues, as we discuss below. The discussion regarding B-OOA differences at different sites was modified as follows (added in P26, L31):

Another advantage obtained in coupling the two source apportionment results is the possibility to study the robustness of the factor analyses by evaluating the consistency of the two approaches as we already discussed for the primary OA and Other-OA fractions. Figure S14a displays the PMF modelled WSOC:measured WSOC PMF for the offline-AMS case, indicating a clear bias between Vilnius and the rural sites, with a WSOC overestimation of ~5% in Preila and Rūgšteliškis. While this overestimation is negligible for WSOC mass, it might have significant consequences on single factor concentrations. By contrast, OM residuals are more homogeneous for the case of markers PMF (Fig. S14b). As we show in Fig. S6, these residuals marginally affect the apportionment of combustion sources, as suggested by the well comparing estimates of BBOA and TEOA using the two methods. Therefore, these residuals are more likely affecting non-combustion sources (LOA, S-OOA and B-OOA). For the common days, the S-OOA concentration is not statistically different at the different stations during summer (confidence interval of 95%), indicating that the residuals are more likely affecting LOA and B-OOA, which instead show site-to-site differences. Now, the PMF WSOC residuals appear at all seasons, also during periods without significant LOA contribution in Vilnius. Therefore, we conclude that B-OOA is the factor most significantly affected by the difference in the WSOC residuals. We could best assess the residual effects by comparing the B-OOAoffline-AMS with that estimated using the other technique that seem to yield more homogeneous residuals: B-OOAmarker. Here B-OOAmarker is estimated as Other-OAmarkers - LOA - S-OOA. While B-OOAoffline-AMS shows site-to-site differences, B-OOAmarkers did not show statistically different concentrations at all stations within a confidence interval of 95%. Based on these observations, we conclude that observed site-to-site differences in B-OOA concentrations are likely to be related to model uncertainties.

1
2 Figure D6. a) Modelled OM : input OM for the markers-PMF. b) Modelled WSOC :
3 measured WSOC for the offline-AMS PMF

4 Figure D6 was added to revised SI as Fig. S14

5
6 *Minor comments*
7   *10)   TEOA is resolved from CMB, not PMF. This needs to be clarified in*
8   *multiple places in the manuscript, such as Page 2 Line 9 and Page 23 Line*
9   *30. Considering that the TEOA concentration is small and only one filter*
10   *has statistical significant TEOA concentration (Page 22 Line 27), I suggest*
11   *the authors to remove the comparison about TEOA concentration between*
12   *sites (for example, Page 32 Line 15-17).*

13 We clarified in P2, L9, P25, L14, and P 23 L30 that PMF returned 4 factors, and
14 TEOA was estimated by CMB. We replaced the TEOA comparison between sites
15 with the comparison of the hopanes concentration at the different locations (P 25
16 L19, P25, L31-32, and P32 L 15-17).

18

11)   Page 2 Line 10. Please rephrase to "two oxygenated OA factors, summer OOA (S-OOA) and background OOA (B-OOA)".

Corrected as suggested.

12)   Page 2 Line 16 vs. Line 18. Use OA or OM. Be consistent.

Corrected as suggested.

13)   Page 4 Line 3. Please rephrase to "source apportionment on the submicron water soluble OA" in order to be precise about the method.

We agree with anonymous referee #2 that our method access only the water soluble fraction, however the water soluble factor concentrations obtained from PMF analysis were subsequently rescaled for the corresponding factor recoveries enabling accessing the total OA concentrations (as also previously pointed out by anonymous referee #2, the recovery correction increases the uncertainty of our source apportionment).

14)   Page 5 Line 24. The nebulizer temperature is 60°C, which is different from Daellenbach et al. (2016). Also, the nebulizer system in this study is different from that in Daellenbach et al. (2016). Would these differences cause the difference in Rz between studies?

As previously discussed (anonymous referee #1, question 2), the use of two different nebulizing setups are unlikely to significantly affect our source apportionment results and therefore our *Rz* estimates. This is due to the well comparing time series of fragments and mass spectral fingerprints. The differences in the *Rz* estimates stem from the different bulk EE (WSOC/OC) values measured for the two different datasets. We note that those differences can be fully ascribed to WSOC and/or OC measurement biases assuming a mass accuracy of 5% for both measurements.

15)   Page 5 Line 27-28. The correction of blank is not appropriate. This is because the particles generated from nebulizing DI water only are too small to be detected by AMS. However, the organics associated with DI water will be detected by AMS when nebulizing real filter extracts because the particles are big. I suggest the authors to nebulize ammonium sulfate solution (i.e. dissolve ammonium sulfate in DI water with similar concentration as ambient filters) and use the detected organic concentration as blank.

In this study we nebulized twice per day a NH_4NO_3 solution. We compared our blank OA mass spectra with the OA mass spectra collected during NH_4NO_3 nebulization. Excluding CO_2^+ and the related fragments, which can be affected by NH_4NO_3 induced non-OA CO_2^+ signal, (Pieber et al. 2016, Friedel et al., 1953, Friedel et al., 1959), none of the other OA AMS fragments showed significantly different concentration from our blanks (ultrapure water nebulization) within 2σ. Our average signal to blank ratio was 170, indicating that the blank represented only a small fraction of the total signal. . Therefore, we consider that under our conditions the nebulization of pure water and NH_4NO_3 solution yield equivalent results. Nevertheless, we recognize that nebulizing $(NH_4)_2SO_4$ or NH_4NO_3 solutions would provide a better estimate of the OA blank. This methodology can be indeed implemented for future studies.

16) *Page 9 Line 7-9. Although the detailed procedures have been discussed in Daellenbach et al. (2016), it is still helpful to briefly discuss the method in the manuscript, especially how the recovery ratios are calculated.*

Rephrased as: "The offline-AMS source apportionment returns the water soluble PMF factor concentrations. Daellenbach et al. (2016) determined factor specific recoveries (including PMF factor extraction efficiencies), by comparing offline-AMS and online-ACSM OA source apportionments. In particular, the filter samples were collected for one year during an online-ACSM monitoring campaign conducted at the same sampling station. Briefly, the factor recoveries were determined as the ratio between the water soluble OA PMF-factor concentrations retrieved from offline-AMS source apportionment divided by the OA PMF factor concentrations obtained from ACSM OA source apportionment. Factor specific recoveries and corresponding uncertainties were determined for HOA, BBOA, COA, and OOA".

17) *Page 10 Line 28. Please rephrase to "this factor has too small contribution in the water extracts to be resolved".*

Corrected as suggested.

18) *Page 12 Line 6. This sentence has been repeated twice. Delete.*

Sentence deleted as suggested

19) *Page 12 Line 13-16. AMS measures OM, instead OC. Please be clear that the conversion from OM to OC is for the carbon mass closure in Eq. (6).*

The information was added to the manuscript as suggested: "Here the water-soluble OA factor concentrations were converted to the corresponding water-soluble OC concentrations to fit the measured OC."

20) *Page 12 Eq. (6). WSW-OOA should be WSB-OOA. Is Rz the same for S-OOA and B-OOA since the same ROOA is applied for both factors?*

WSW-OOA was corrected as WSB-OOA

In this study we assumed $R_{S\text{-}OOA} = R_{B\text{-}OOA}$ because the recoveries of the OOA factors reported in Daellenbach et al. (2015), were determined from the sum of two OOA factors. The two recoveries were not determined individually in Daellenbach et al. (2015) due to the dissimilar OOA classification between offline-AMS and online ACSM source apportionments, which prevented an unambiguous attribution of the offline-AMS OOA factors to the online-AMS ones.

21) *Page 14 Line 20. What's the OMres/OM ratio?*

The information was added to the manuscript: "OM_{res} represented on average 95±2% of total OM."

22) *Page 15 Line 21. List the non-source specific variables.*

The information was added to the text: "(EC, OM_{res}, (Me-)PAHs, S-PAHs, inorganic ions, oxalate, alkanes)".

1 The entire list is reported here below:

2 (EC, SO_4^{2-}, NO_3^-, Cl^-, NH_4^+, Na^+, K^+, Ca^{2+}, Mg^{2+}, oxalate, MSA, Phenanthrene,

3 anthracene, fluoranthene, pyrene, benzo[a]anthracene, chrysene, triphenylene,

4 retene, benzo[b,k]fluoranthene, benzo[j]fluoranthene, benzo-e-pyrene,

5 benzo[a]pyrene, indeno[1,2,3 - cd]pyrene, dibenzo[a,h]anthracene,

6 benzo[ghi]perylene, coronene, dibenzothiophene, phenanthro(4,5-bcd)thiophene,

7 Benzo(b)naphtho(2,1-d)thiophene, Benzo(b)naphtha(1,2-d)thiophene,

8 Benzo(b)naphtho(2,3-d)thiophene, Dinaphtho(2,1-b;1',2'-d)thiophene,

9 Benzo(b)phenantho(2,1-d)thiophene, 2-methylnaphtalene, 1-methylfluoranthene, 3-

10 methylphenanthrene, 2-methylphenanthrene, 2-methylanthracene, 4/9

11 methylphenanthrene, 1-methylphenanthrene, 4-methylpyrene, 1-methylpyrene, 1+3-

12 methylfluoranthene, methylfluoranthene/pyrene, 3-methylchrysene,

13 methylchrysene/benzoanthracene, Cholesterol, 6,10,14-trimethyl-2-pentadecanone,

14 Undecane (C11), dodecane (C12), tridecane (C13), tetradecane (C14), pentadecane

15 (C15), exadecane (C16), heptadecane (C17), octadecane (C18), nonadecane (C19),

16 eicosane (C20), heneicosane (C21), docosane (C22), tricosane (C23), tetracosane

17 (C24), pentacosane (C25), hexacosane (C26), heptacosane (C27), octacosane

18 (C28), nonacosane (C29), triacontane (C30), untricontane (C31), totriacontane

19 (C32), tritriacontane (C33), tetratriacontane (C34), pentatriacontane (C35),

20 hexatriacontane (C36), heptatriacontane (C37), octatriacontane (C38),

21 nonatriacontane (C39), tetracontane (C40), pristane, phytane, OM_{res})

22

23 *23) What's the Hopanessum/OC ratio in the traffic exhaust factor? Is it*
24 *consistent with the CMB method (i.e., 0.0012 in Page 11 Line 15)?*

25 Since our HOA matches between the two methods within our uncertainty, also the
26 Hopanes$_{sum}$:OC ratio will be not statistically different. Note that the hopanes were
27 constrained to contribute only to traffic in the markers source apportionment (Section
28 5.3.2.2).

29 *24) Page 16 Line 25. Should be "EC/OMres" ratio.*

30 Text corrected as "while EC:BB ratio was constrained to 0.1".

31 *25) Page 17 Line 10-16. The discussion is not clear. Suggest re-wording.*

32 Lines 10-16 were reformulated as:

33 As discussed in section 3.2.2, we assumed the contribution of specific markers to be
34 0 in different factor profiles. Such assumptions preclude the PMF model to vary the

21

contributions of these variables from 0 (Eq. 3). In order to explore the effect of such assumptions on our PMF results we loosened all these constraints assuming variable contributions equal to 50%, 37.5%, 25%, and 12.5% of their average relative contribution to measured PM_1. In all cases the *a*-value was set to 1.

26) *Page 20 Line 1-3. List the levoglucosan/BBOC range in the literature. Similar suggestions for other places. For example, list the non-fossil primary organic carbon in Page 25 Line 13 and average fossil primary OC in Page 25 Line 29.*

Information added to the manuscript.

27) *Page 21 Line 2. I disagree with that S-OOA increases exponentially with average daily temperature from the data points in this study (Fig. S12). For example, many data points with T > 25°C do not have high S-OOA concentration and do not follow the exponential fit.*

Indeed data show a certain scattering. This scattering can stem from other parameters affecting the biogenic SOA concentrations, such as the photochemical aging of the air parcel, RH, rain, solar radiation, NO_x concentration, accumulation during the previous days, and wind speed. When binning the data from Lithuania and Payerne in temperature steps of 5 degrees the exponential relation of S-OOA *vs* average daily temperature reveals a good agreement with the exponential relation reported by Leaitch et al. (2011). We also modified Fig. S12 adding the error bars and binning the S-OOA concentration in 5°C temperature steps.
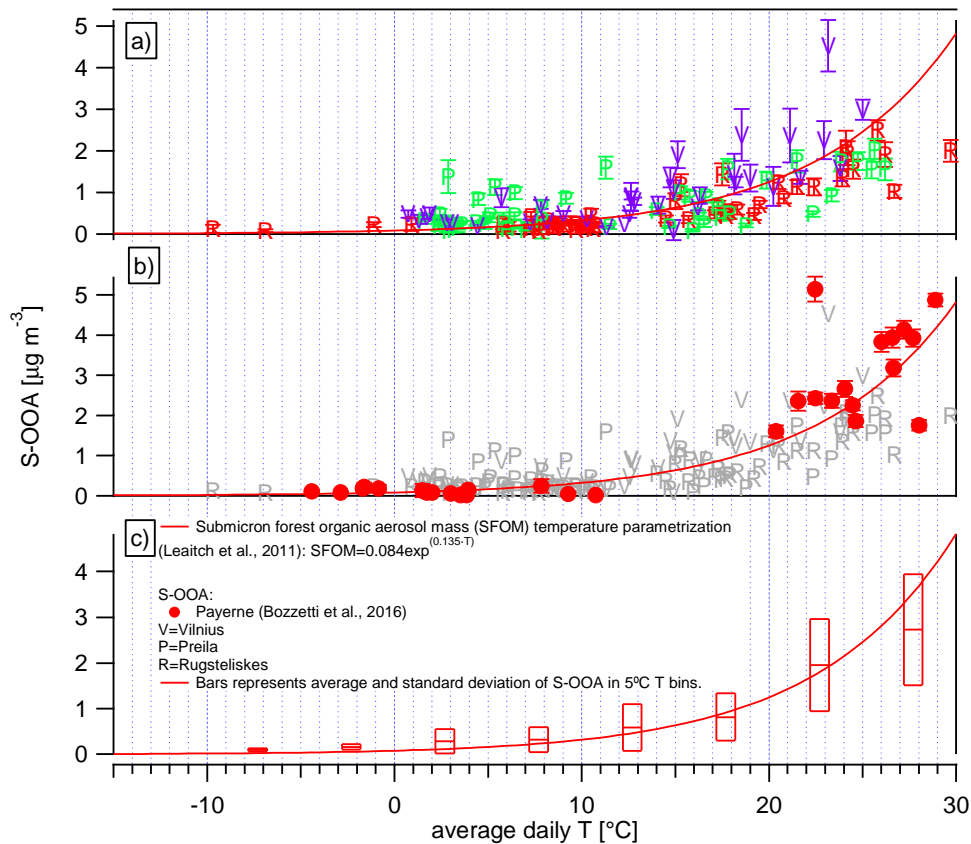
Figure D7. S-OOA temperature dependence and submicron forest organic aerosol mass (SFOM) temperature parameterization by Leaitch et al. (2015). a) Lithuania; b) rural site of Payerne (Switzerland), Bozzetti et al. (2016); c) Binned S-OOA concentrations (average and standard deviation).

28) *Page 22 Line 13-15. This has been mentioned previously in Page 20 Line 1-3. It is not proper to discuss BBOC here because this section focuses on the marker-PMF, instead of offline AMS. Similar problem for Page 22 Line 23-24.*

The levoglucosan:BBOC ratios discussed in this section (P22 L13-15 and 23-24) actually refer to the marker-PMF source apportionment. In order to estimate the BBOC concentration from the marker source apportionment we used the OM:OC$_{BBOA}$ ratio retrieved from offline-AMS.

29) *Page 23 Line 14-15. The observation that nitrate concentration is higher in urban site than rural site has been shown in many previous studies (Xu et al., 2016; McMeeking et al., 2012), which should be cited here.*

Citations added as suggested

30) *Page 23 Line 30-31. This sentence is confusing. The remaining OM fraction is termed as OMres in Page 10 Line 20, but termed as Other-OA here. It should be clearly stated that Other-OA refers to OA after excluding BB and TE.*

Text corrected as suggested: "(Other-OA = OA – BBOA - TEOA)"

31) *Page 24 Line 18. Should be "higher"*

Text corrected as suggested

32) *Page 24 Line 21-23. (1) Which method did the authors use to get the BBOA concentration and correlation in this sentence? (2) It would be helpful to include a scatter plot between Preila and Vilnius. (3) I disagree with "the importance of regional meteorological conditions" as stated in this sentence and Page 32 Line 31-32. Firstly, the BBOA concentrations are different between two sites. Secondly, the BBOA in the Rugsteliskis site does not correlate with the other two sites.*

(1) The BBOA concentration reported at P24 L21-23 was estimated by offline-AMS. Information added to the text.

(2-3) For this comparison we considered only filter samples collected simultaneously during winter at the different stations. In this case we observed high correlations between the winter BBOA concentrations estimated for Preila and Vilnius (R = 0.91), and significantly positive correlations between Preila and Rūgšteliškis (R = 0.72) and between Vilnius and Rūgšteliškis (R = 0.66). We do not mean that BBOA has a regional origin, as also confirmed by the different concentrations observed at the different stations. The high correlations between the sites only suggest either a common accumulation/depletion of pollutants due to similar meteorological conditions, or a concomitant increment/decrease of residential wood combustion activity at the different stations. We could exclude the latter hypothesis because, as mentioned in the text, most of the BBOA spikes were not directly related to a decrease of temperature (Section 4.4.1)y. Therefore the BBOA daily variability in the region seem to be mostly driven by regional meteorological patterns (rain episodes and anticyclonic conditions), however, the proximity to biomass burning emission spots can influence the total concentration, therefore not surprisingly Vilnius and Preila show higher concentrations than Rūgšteliškis.

winter BBOA concentration [μg m⁻³]

1

25
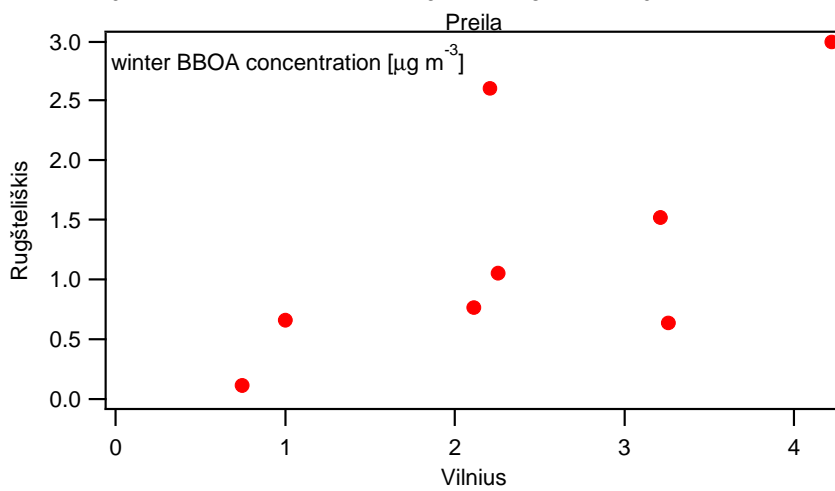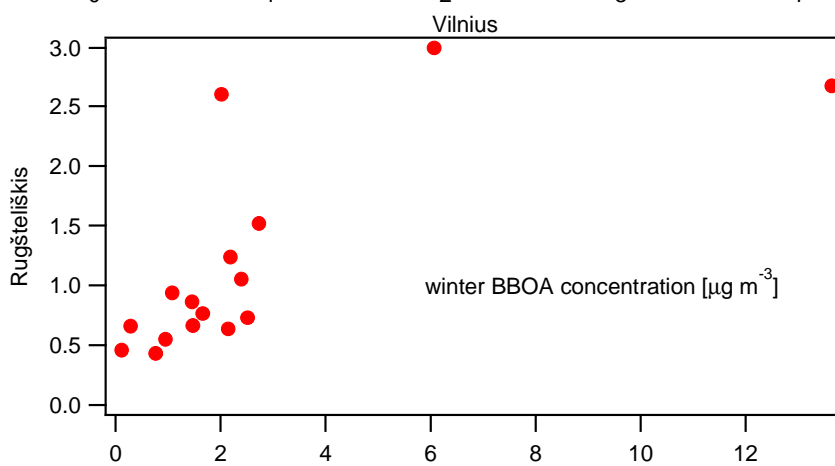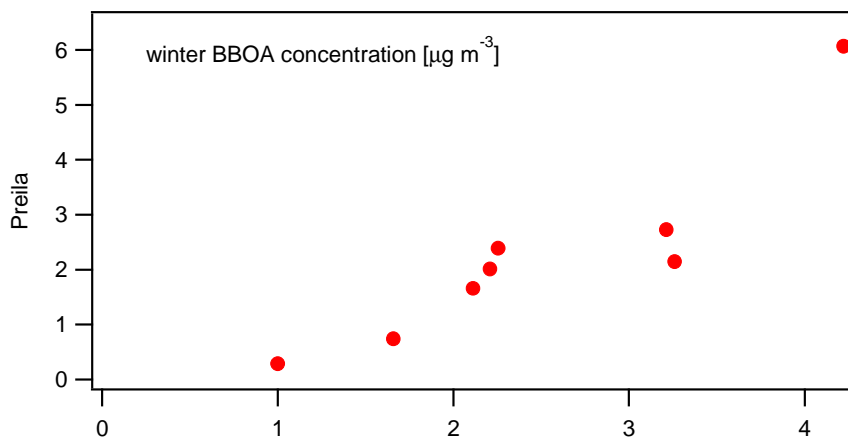
Figure D8. S-OOA temperature dependence and submicron forest organic aerosol mass (SFOM) temperature parameterization by Leaitch et al. (2015). a) Lithuania; b) rural site of Payerne (Switzerland), Bozzetti et al. (2016); c) Binned S-OOA concentrations (average and standard deviation).

P24 Lines 21-23 were corrected as:

During winter, considering only the samples collected concomitantly, Preila and Vilnius showed well correlated BBOA time series (R = 0.91) and significantly positive correlations were observed for also for Preila and Rūgšteliškis (R = 0.72) and for Vilnius and Rūgšteliškis (R = 0.66) (offline-AMS BBOA time series). These results highlight the effect of regional meteorological conditions on the BBOA daily variability in the south east Baltic region.

33) *Page 24 line 29. Both methods have the same time resolution (one filter per day).*

As mentioned in the main text in Table 1, Table S1, section 2.3 and section 3.2.1 this is not the case as the marker-source apportionment is based on composite samples which were created by merging two consecutively collected filter samples, and therefore the time resolution is 48 h.

34) *Page 25 line 15. In the statistical significance test, why is sometimes 1σ is used but sometimes 3σ is used (for example, Page 26 Line 28).*

We homogenized all the statistical significances to the confidence interval of 3σ.

35) *Page 26 Line 30. Should be "factor" instead of "fraction".*

Corrected as suggested

36) *Table 2. The correlation coefficient R between NO3-related SOA and B-OOA is only 0.21. Thus, it is not meaningful to discuss the relationship between NO3-related SA and B-OOA (Page 28 Line 17). Similar problem for the relationship between MSA-related SOA and S-OOA (Page 28 Line 21).*

The NO_3-related SOA correlation with B-OOA is indeed small, however the correlation with LOA and S-OOA is negative, suggesting that the mass attributed to NO_3-related SOA by the markers source apportionment is fully attributed to the B-OOA factor in the offline-AMS source apportionment. This is also confirmed by the fact that the sum of LOA and S-OOA concentrations during winter (when the NO_3-related SOA substantially contributes) can't explain the NO_3^--related SOA mass, which therefore has to be attributed to B-OOA. We believe that this result is relevant because it relates the NO_3^--related SOA factor, typically resolved from a marker source apportionment, to the OOA factor typically resolved by AMS source apportionment in winter datasets. In a similar way we found that large part of MSA-related SOA is related to S-OOA, which provides more insight into the S-OOA precursors, moreover the precursor emissions of both factors (dimethyl sulfide, isoprene, and terpenes) are known to be strongly related to temperature, and not surprisingly the two factors increase during summer.

1

2 Lines 17-20, P28 were modified as follows:

3 The NO_3^--related SOA and the PBOA were mostly related to the B-OOA factor as
4 they showed higher correlations with B-OOA than with S-OOA. The B-OOA factor
5 therefore may explain a small fraction of primary sources (PBOA), which however
6 represents only $0.6\%_{avg}$ of the total OA. In detail, the NO_3-related SOA correlation
7 with B-OOA was poor (R = 0.21), however the correlation with LOA and S-OOA was
8 negative (Table 2), suggesting that the mass attributed to NO_3-related SOA by the
9 markers source apportionment was fully attributed to the B-OOA factor in the offline-
10 AMS source apportionment. This is also confirmed by the fact that the sum of LOA
11 and S-OOA concentrations during winter (when the NO_3-related SOA substantially
12 contributes) can't explain the NO_3^--related SOA mass, which therefore has to be
13 attributed to B-OOA.

14

15 We added the following discussion at P 28, L26.

16

17 The correlation between the two factors is therefore not surprising as the precursor
18 emissions (dimethyl sulfide, isoprene and terpenes) are strongly related to
19 temperature leading to higher summer MSA-related SOA and S-OOA concentrations.
20

21 *37) Page 29 Line 18. Please rephrase to "fCO2 value is higher than fCO".*

22 Corrected as suggested

23 *38) Page 29 Line 24-25. The logic is not clear. Why does higher CO2+/CO+*
24 *ratio of gas CO2 suggest a minor contribution from WSOM decarboxylation*
25 *to CO+.*

26 L24-25, P29 were modified as follows:

27 The fragmentation of pure gaseous CO_2 returned a CO_2^+:CO^+ ratio of 8.21_{avg} which is
28 significantly higher than our findings for the water-soluble bulk OA (1.75_{med}).
29 Assuming thermal decarboxylation of organic acids as the only source of CO_2^+ does
30 not explain the observed CO_2^+:CO^+ ratio of 1.75_{med} and another large source of CO^+
31 has to be assumed. Therefore, the carboxilic acid decarboxylation into CO_2can be
32 considered as a minor source of CO^+.

33 *39) Page 30 Line 7. Many data points from the Rugsteliskis site are outside the*
34 *triangle range in Fig. 7a.*

35 As discussed in Fig. 7 caption, some points from Rūgšteliškis lie outside the triangle,
36 suggesting that CO^+ and CO_2^+ variabilities are not well explained by our PMF model
37 for those specific filter samples. However, Fig. S5 displays flat residuals for
38 Rūgšteliškis, indicating an overall good WSOM explained variability by the model.

39 *40) Page 31 Line 4. The correlation between CO+ and C2H3O+ is not shown*
40 *in Fig. 7b. It would be helpful to show a scatter plot.*

41 We added to Fig. 7 the scatter plot fCO^+ *vs.* $fC_2H_3O^+$ as suggested.

41)   Page 31 Line 16. Canagaratna et al. (2015) carefully discussed the CO2+/CO+ ratio of a number of standards, which should be discussed and mentioned more in the manuscript.

As mentioned in the manuscript (P31, L24), we can observe that the most representative standards of our aqueous filter extracts in terms of $CO^+:CO_2^+$ ratio were multifunctional carboxylic acids (only hydroxyl mono and poly-acids and keto acids) and 2 diacids used by Canagaratna et al. (2015) . Specifically, These include citric acid, malic acid tartaric acid, ketobutyric acid, hydroxyl methylglutaric acid, pyruvic acid, oxaloacetic acid, tartaric acid, oxalic acid and malonic acid. Considering that the median OA bulk extraction efficiency was 0.59, and considering that the CO^+ and CO_2^+ fragmentation precursors tend to be more water soluble than the bulk OA, the listed compounds could be representative of large part of the CO^+ and CO_2^+ fragmentation precursors.

Lines 23-28, P31 were modified as follows:

With the exception of some multifunctional compounds (citric acid, malic acid tartaric acid, ketobutyric acid, hydroxyl methylglutaric acid, pyruvic acid, oxaloacetic acid, tartaric acid, oxalic acid and malonic acid), the water-soluble single compounds analyzed by Canagaratna et al. (2015) mostly showed $CO_2^+:CO^+$ ratios <1, systematically lower than the $CO_2^+:CO^+$ ratios measured for the bulk WSOM in Lithuania (1st quartile 1.50, median 1.75, 3rd quartile 2.01), which represents a large fraction of the total OM (bulk EE: median = 0.59, 1st quartile = 0.51, 3rd quartile = 0.72). Considering the relatively high extraction efficiency, and considering that the CO^+ and CO_2^+ fragmentation precursors tend to be more water soluble than the bulk OA, the aforementioned compounds could be representative of a large part of the CO^+ and CO_2^+ fragmentation precursors.

42)   Figure 5. The grey caps of traffic exhaust are not clear in this figure.

Traffic grey caps were highlighted with a marker
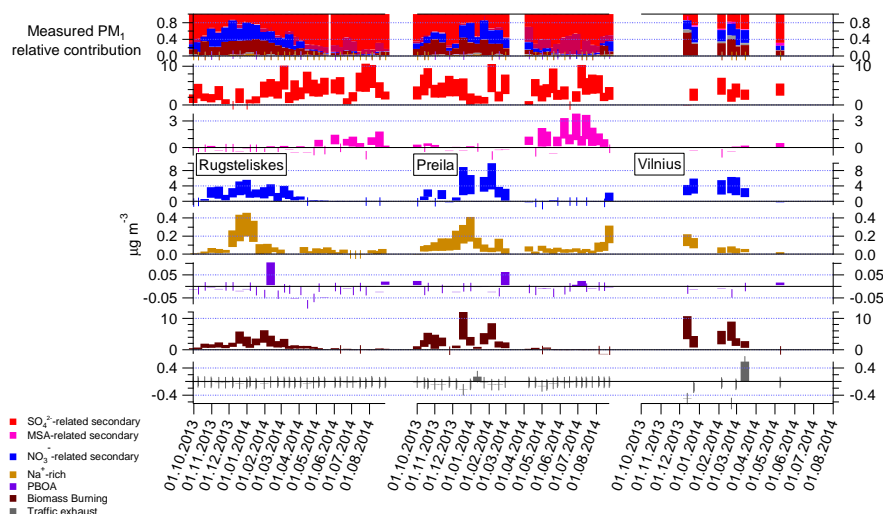
1 Figure D9. Figure 5. PM$_1$ marker source apportionment: factor time series and
2 relative contributions. Shaded areas indicate uncertainties (standard deviation) of 20
3 bootstrap runs.

4

5 References:

6 Budisulistiorini, S. H., Canagaratna, M. R., Croteau, P. L., Marth, W. J.,
7 Baumann, K., Edgerton, E. S., Shaw, S. L., Knipping, E. M., Worsnop, D. R.,
8 Jayne, J. T., Gold, A., and Surratt, J. D.: Real-Time Continuous Characterization
9 of Secondary Organic Aerosol Derived from Isoprene Epoxydiols in Downtown
10 Atlanta, Georgia, Using the Aerodyne Aerosol Chemical Speciation Monitor,
11 Environ Sci Technol, 47, 5686-5694, Doi 10.1021/Es400023n, 2013.

12 Friedel, R. A., Sharkey, A. G., Shultz, J. L., and Humbert, C. R.: Mass
13 spectrometric analysis of mixtures containing nitrogen dioxide, Anal. Chem., 25,
14 1314-1320, 1953.

15 Friedel, R. A., Shultz, J. L., and Sharkey Jr, A. G.: Mass spectrum of nitric acid,
16 Anal. Chem., 31, 1128, 1959.

17 Fröhlich, R., Crenn, V., Setyan, A., Belis, C. A., Canonaco, F., Favez, O., Riffault,
18 V., Slowik, J. G., Aas, W., Aijälä, M., Alastuey, A., Artiñano, B., Bonnaire, N.,
19 Bozzetti, C., Bressi, M., Carbone, C., Coz, E., Croteau, P. L., Cubison, M. J.,
20 Esser-Gietl, J. K., Green, D. C., Gros, V., Heikkinen, L., Herrmann, H., Jayne, J.
21 T., Lunder, C. R., Minguillón, M. C., Mocnik, G., O'Dowd, C. D., Ovadnevaite, J.,
22 Petralia, E., Poulain, L., Priestman, M., Ripoll, A., Sarda-Estève, R.,
23 Wiedensohler, A., Baltensperger, U., Sciare, J., and Prévôt, A. S. H.: ACTRIS
24 ACSM intercomparison – Part 2: Intercomparison of ME-2 organic source
25 apportionment results from 15 individual, co-located aerosol mass spectrometers,
26 Atmos. Meas. Tech., 8, 2555–2576, 2015.

27 Hu, W. W., Campuzano-Jost, P., Palm, B. B., Day, D. A., Ortega, A. M., Hayes,
28 P. L., Krechmer, J. E., Chen, Q., Kuwata, M., Liu, Y. J., de Sá, S. S., McKinney,
29 K., Martin, S. T., Hu, M., Budisulistiorini, S. H., Riva, M., Surratt, J. D., St. Clair, J.
30 M., Isaacman-Van Wertz, G., Yee, L. D., Goldstein, A. H., Carbone, S., Brito, J.,
31 Artaxo, P., de Gouw, J. A., Koss, A., Wisthaler, A., Mikoviny, T., Karl, T., Kaser,
32 L., Jud, W., Hansel, A., Docherty, K. S., Alexander, M. L., Robinson, N. H., Coe,
33 H., Allan, J. D., Canagaratna, M. R., Paulot, F., and Jimenez, J. L.:
34 Characterization of a real-time tracer for isoprene epoxydiols-derived secondary

organic aerosol (IEPOX-SOA) from aerosol mass spectrometer measurements, Atmos. Chem. Phys., 15, 11807-11833, 10.5194/acp-15-11807-2015, 2015.

McMeeking, G. R., Bart, M., Chazette, P., Haywood, J. M.,, Hopkins, J. R., McQuaid, J. B., Morgan, W. T., Raut, J.-C., Ryder, C. L., Savage, N., Turnbull, K., and Coe, H.: Airborne measurements of trace gases and aerosols over the London metropolitan region, Atmos. Chem. Phys., 12, 5163–5187, 2012.

Pieber, S. M., El Haddad, I., Slowik, J. G., Canagaratna, M. R., Jayne, J. T., Platt, S. M., Bozzetti, C., Daellenbach, K. R., Fröhlich, R., Vlachou, A., Klein, F., Dommen, J., Miljevic, B., Jimenez, J. L., Worsnop, D. R., Baltensperger, U., and Prévôt A. S. H.: Inorganic salt interference on CO2+ in Aerodyne AMS and ACSM organic aerosol composition studies, Environ. Sci. Tech., http://dx.doi.org/10.1021/acs.est.6b01035, 2016.

Xu, L., Guo, H., Boyd, C. M., Klein, M., Bougiatioti, A., Cerully, K. M., Hite, J. R., Isaacman-VanWertz, G., Kreisberg, N. M., Knote, C., Olson, K., Koss, A., Goldstein, A. H., Hering, S. V., de Gouw, J., Baumann, K., Lee, S.-H., Nenes, A., Weber, R. J., and Ng, N. L.: Effects of anthropogenic emissions on aerosol formation from isoprene and monoterpenes in the southeastern United States, Proceedings of the National Academy of Sciences, 112, 37-42, 10.1073/pnas.1417609112, 2015.

Xu, L., Williams, L. R., Young, D. E., Allan, J. D., Coe, H., Massoli, P., Fortner, E., Chhabra, P., Herndon, S., Brooks, W. A., Jayne, J. T., Worsnop, D. R., Aiken, A. C., Liu, S., Gorkowski, K., Dubey, M. K., Fleming, Z. L., Visser, S., Prévôt, A. S. H., and Ng, N. L.: Wintertime aerosol chemical composition, volatility, and spatial variability in the greater London area, Atmos. Chem. Phys., 16, 1139-1160, 10.5194/acp-16-1139-2016, 2016.

Field Code Changed

Minor revisions:

Anonymous Referee #1

43) *I recommend that the authors should add a short bit of text, either to the manuscript or the supplemental that addresses the reviewer 2's comment- that volatility and seasonal trends are linked.*

In the revised manuscript we replaced P22, L21-22 with the following discussion:

In general, OOA factors with different seasonal behaviors can be characterized by different volatilities. However in this work the offline-AMS OOA separation is not driven by volatility, given the low correlation between NO_3^- and our OOA factors (also reflected by the low NO_3^--related SOA correlation with B-OOA and S-OOA, Table 2). Additionally, the partitioning of semi-volatile OA at low temperatures would lead to a less oxidized OOA fingerprint during winter than in summer; however, this was not the case. We observed a less oxidized OOA factor during summer, whose mass spectral fingerprint closely resembles that of SOA from biogenic precursors. Meanwhile similar to OOA from aging of biomass burning emissions, OOA during the cold season is more oxidized. This has been also reported in an urban environment in central Europe (Zurich) using an online-ACSM (Canonaco et al., 2015).

Table 2 was moved below this section.

Formatted: English (U.S.)

Anonymous Referee #2

Received and published: 07 October 2016

General Comments:
I thank the authors for taking time to revise the manuscript. The authors have addressed the comments adequately. However, I have two minor comments.

44)   *1. OM/OC ratio. While I agree with the authors that both Aiken and Canagaratna parameterizations are uncertain for this dataset, I want to point out that the OM/OC ratio would affect the recovery ratios determined by Eq. (6). Higher OM/OC ratio from Canagaratna parameterization would lead to lower recovery ratio and hence higher ambient concentration of factors.*

The recovery estimates are independent of the choice of Aiken or Canagaratna's OM:OC parameterizations. Indeed the recovery fitting equation (Eq. 6) explicitly contains the PMF factors OM:OC ratio. However the water-soluble PMF factor concentrations (Eq. 6) implicitly depend on the bulk OM:OC ratio used to determine the bulk WSOM concentration ($WSOM_i = WSOC_i \cdot OM/OC_i$) which was used as input for our PMF model. This leads to canceling corrections making the recovery estimates independent of the choice of the Aiken's or Canagaratna's OM:OC parameterizations.
This information was added in the revised SI.

45)   *2. It is important to discuss why the same Rz is selected for both B-OOA and S-OOA (i.e.,response to comment#20) and mention that the Rz of OOA factors warrants further investigation in the manuscript.*

The factor recoveries determined in this work enabled properly fitting the OC time series according to Eq. (6). The OC fitting residuals were unbiased within our uncertainty in different seasons (summer and winter) and at the different stations. Therefore there's no reason to consider statistically different recoveries for S-OOA and W-OOA. We also fitted the factor recoveries according to Eq. (6) without any *a-priori* constrain from Daellenbach et al. (2016), and assuming different recoveries for S-OOA and B-OOA. The measured OC *vs.* fitted OC correlation was not statistically higher (95% confidence interval) than the correlation obtained when constraining the OOAs and BBOA factor recoveries according to Daellenbach et al. (2016). This suggests that the measured OC is equally well explained by the two fits.
The completely unconstrained fit returned a wide $R_{S\text{-}OOA}$ range (Fig. D10, only solutions associated to unbiased OC residuals and R_ks values comprised between 0 and 1 were retained). This occurs despite the considerable contribution of S-OOA, at all sites. This suggests that the least square algorithm fails to independently estimate the recoveries of factors and a priori constrains are needed to get unambiguous results. We have assumed $R_{S\text{-}OOA} = R_{B\text{-}OOA}$ based on the comparison between offline-AMS and online ACSM, although obtained at another site, especially that this assumption fits our knowledge of OOA water solubility and returned a mathematically equivalent OC reconstruction compared to the completely unconstrained model.
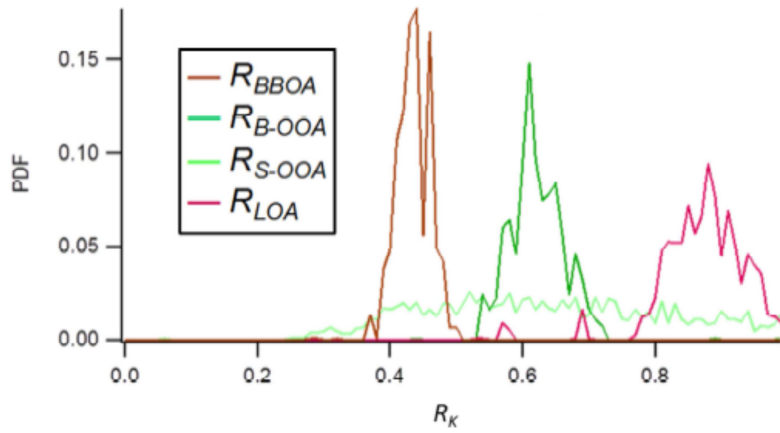
1
2   Fig. D10. R_k probability density functions obtained by fitting Eq. (6) assuming $R_{\text{S-OOA}}$
3    $\neq R_{\text{B-OOA}}$ and without a-priori R_k information.

List of all relevant changes made in the manuscript

In the following page numbers and lines refer to the originally submitted version of the manuscript.

1) As suggested by both anonymous referee #1 and #2 we clarified in several points that TEOA concentrations and uncertainties were not resolved by offline-AMS source apportionment, but by a CMB approach using hopanes as molecular markers. (P2, L9, P25, L14, and P23 L30).

2) A more complete description of the offline-AMS methodology was introduced in section 3.1 according to the suggestion of anonymous referee #2.

3) A cleared description of Offline-AMS PMF factor recoveries (R_k) estimates was introduced in section 3.1.3 as suggested by anonymous referee #2.

4) Recommendations for future offline-AMS users were added at P13 L19 according to the suggestion of anonymous referee #2.

5) Following the suggestion of anonymous referee #2 we modified P20 L17-18 in order to explicitly mention AMS-PMF works which resolved secondary aerosol factors according to their sources or formation mechanisms.

6) We discussed more in depth the relation between NO_3^--related SOA and B-OOA (L 17-20, P28) in order to reply to a question raised by anonymous referee #2.

7) We discussed more in details the relation between PMF residuals and B-OOA site-to-site differences observed in Vilnius (P26, L31), in order to answer a question raised by anonymous referee #2.

8) We explicitly listed the standards most representative of observed water-soluble ambient CO^+/CO_2^+ ratios (Lines 23-28, P31), as suggested by anonymous referee #2.

9) We added the CO^+ *vs.* $C_2H_3O^+$ scatter plot in Fig. 7, as suggested by anonymous referee #2.

1

Argon offline-AMS source apportionment of organic aerosol over yearly cycles for an urban, rural and marine site in Northern Europe

5

C. Bozzetti[1], Y. Sosedova[1], M. Xiao[1], K. R. Daellenbach[1], V. Ulevicius[2], V. Dudoitis[2], G. Mordas[2], S. Byčenkienė[2], K. Plauškaitė[2], A. Vlachou[1], B. Golly[3], B. Chazeau[1], J.-L. Besombes[4], U. Baltensperger[1], J.-L. Jaffrezo[3], J. G. Slowik[1], I., El Haddad[1], I., and A. S. H. Prévôt[1]

[1] {Laboratory of Atmospheric Chemistry, Paul Scherrer Institute (PSI), 5232 Villigen-PSI, Switzerland}

[2] {Department of Environmental Research, SRI Center for Physical Sciences and Technology, LT-02300 Vilnius, Lithuania}

[3] {Université Grenoble Alpes, CNRS, LGGE, 38000 Grenoble, France}

[4] {Université Savoie Mont-Blanc, LCME, F-73000 Chambéry, France}

16

Correspondence to: A. S. H. Prévôt (andre.prevot@psi.ch); I. El Haddad (imad.el-haddad@psi.ch)

19

Abstract

The widespread use of Aerodyne aerosol mass spectrometers (AMS) has greatly improved real-time organic aerosol (OA) monitoring, providing mass spectra that contain sufficient information for source apportionment. However, AMS field deployments remain expensive and demanding, limiting the acquisition of long-term datasets at many sampling sites. The offline application of aerosol mass spectrometry entailing the analysis of nebulized water extracted filter samples (offline-AMS) increases the spatial coverage accessible to AMS measurements, being filters routinely collected at many stations worldwide.

PM$_1$ (particulate matter with an aerodynamic diameter <1 μm) filter samples were collected during an entire year in Lithuania at three different locations representative of three typical environments of the South-East Baltic region: Vilnius (urban background), Rūgšteliškis (rural terrestrial), and Preila (rural coastal). Aqueous filter extracts were nebulized in Ar, yielding the first AMS measurements of water-soluble atmospheric organic aerosol (WSOA) without interference from air fragments. This enables direct measurement of the CO$^+$ fragment contribution, whose intensity is typically assumed to be equal to that of CO$_2^+$. Offline-AMS spectra reveal that the water soluble CO$_2^+$:CO$^+$ ratio not only shows values systematically $\leq$1 but is also dependent on season, with lower values in winter than in summer.

AMS WSOA spectra were analyzed using positive matrix factorization (PMF), which yielded 4 factors. These factors included biomass burning OA (BBOA), local OA (LOA) contributing significantly only in Vilnius, and two oxygenated OA (OOA) factors, summer OOA (S-OOA) and background OOA (B-OOA) distinguished by their seasonal variability. The contribution of traffic exhaust OA (TEOA) was not resolved by PMF due to both low concentrations and low water solubility. Therefore, the TEOA concentration was estimated using a chemical mass balance approach, based on the concentrations of hopanes, specific markers of traffic emissions. ~~AMS WSOA spectra were analyzed using positive matrix factorization (PMF), yielding 5 factors: traffic exhaust OA (TEOA), biomass burning OA (BBOA), local OA (LOA) contributing significantly only in Vilnius, and two oxygenated OA (OOA) factors distinguished by seasonal variability.~~ AMS-PMF source apportionment results were consistent with those obtained from PMF applied to marker concentrations (i.e. major inorganic ions, OC/EC, and organic markers including polycyclic aromatic hydrocarbons and their derivatives, hopanes, long-chain alkanes, monosaccharides, anhydrous sugars, and lignin fragmentation products). OA was the largest fraction of PM$_1$ and was dominated by BBOA during winter with an average concentration of 2 μg m^{-3} (53% of ~~OA~~OM), while summer-OOA (S-OOA), probably related to biogenic emissions was the prevalent OA source during summer with an average concentration of 1.2 μg m^{-3} (45% of OM).

PMF ascribed a large part of the CO$^+$ explained variability (97%) to the OOA and BBOA factors. Accordingly we discuss a new CO$^+$ parameterization as a function of CO$_2^+$, and C$_2$H$_4$O$_2^+$ fragments, which were selected to describe the variability of the OOA and BBOA factors.

36

1 Introduction

Atmospheric aerosols affect climate (Lohmann et al., 2004, Schwarze et al., 2006), human health (Dockery et al., 2005, Laden et al., 2000), and ecosystems on a global scale. Quantification and characterization of the main aerosol sources are crucial for the development of effective mitigation strategies. The Aerodyne aerosol mass spectrometer (AMS, Canagaratna et al., 2007) and aerosol chemical speciation monitor (ACSM, Ng et al., 2011, Fröhlich et al., 2013) have greatly improved air quality monitoring by providing real-time measurements of the non-refractory (NR) submicron aerosol (PM_1) components. Analysis of organic mass spectra using positive matrix factorization (PMF, Paatero, 1997; Paatero and Tapper, 1994) has enabled the quantitative separation of OA factors, which can be subsequently related to major aerosol sources and formation processes (e.g. Lanz et al., 2007; Lanz et al., 2010; Zhang et al., 2011; Ulbrich et al., 2009; Elser et al., 2016 a). Despite its numerous advantages, AMS field deployment remains expensive and demanding, and therefore most of the studies are typically restricted to short-time periods and a single (or few) sampling site(s). The limited amount of long-term datasets suitable for OA source apportionment severely limits model testing and validation (Aksoyoglu et al., 2011; Aksoyoglu et al., 2014; Baklanov et al., 2014), as well as for the development of appropriate pollution mitigation strategies. AMS analysis of aerosol filter samples (Lee et al., 2011; Sun et al., 2011; Mihara and Mochida, 2011; Daellenbach et al., 2016), which are routinely collected at many stations worldwide, broadens the temporal and spatial scales available for AMS measurements.

In this study we present the application of the offline-AMS methodology described by Daellenbach et al. (2016) to yearly cycles of filter samples collected in parallel at three different locations in Lithuania between September 2013 and August 2014. The methodology consists of water extraction of filter samples, followed by nebulization of the liquid extracts, and subsequent measurement of the generated aerosol by high-resolution time-of-flight AMS (HR-ToF AMS). In this work, organic aerosol water extracts were nebulized in Ar, permitting direct measurement of the CO^+ ion (Fig. S1), which is typically not directly quantified in AMS data analysis due to interference with N_2^+, but is instead estimated as being equal to CO_2^+ (Aiken et al., 2008). Direct measurement of CO_2^+ better captures the variability in the total OA mass and its elemental composition as well as potentially improving source apportionment of ambient aerosol. Aerosol elemental ratios and oxidation state are of

1 particular relevance as they provide important constraints for understanding aerosol sources,

2 processes, and for the development of predictive aerosol models (Canagaratna et al., 2015).

3 Aerosol composition in the south-east Baltic region has so far received little attention. To our

4 knowledge the only investigation of OA sources in this area was during a five-day period of

5 intense land clearing activity occurring in the neighboring Russian enclave of Kaliningrad

6 (Ulevicius et al., ~~2015~~2016; Dudoitis et al., 2016), in which transported biomass burning

7 emissions dominated the aerosol loading. OA source contributions under less extreme

8 conditions remain unstudied, with the most relevant measurements performed in Estonia with

9 a mobile lab during March 2014 at two different locations (Elser et al., 2016b). On-road

10 measurements revealed large traffic contributions with an increase of 20% from rural to urban

11 environments. Also, residential biomass burning (BB) and oxygenated OA (OOA)

12 contributions were found to be substantial.

13 In this study we present a complete source apportionment of the submicron OA fraction

14 following the methodology described by Daellenbach et al. (2016) in order to quantify and

15 characterize the main OA sources affecting the Lithuanian air quality. The three sampling

16 stations were situated in the Vilnius suburb (urban background), Preila (rural coastal

17 background), and Rūgšteliškis (rural terrestrial background), covering a wide geographical

18 domain and providing a good overview of the most typical Lithuanian and south-eastern

19 Baltic air quality conditions and environments. PMF analysis of offline-AMS measurements

20 are compared with the results reported by Ulevicius et al. (~~2015~~2016) and with PMF analysis

21 of chemical marker measurements obtained from the same filter samples.

2 Sampling and offline measurements

2.1 Site description and sample collection

24 We collected 24-h integrated PM_1 filter samples at 3 different stations in Lithuania from 30

25 September 2013 to 2 September 2014 using 3 High-Volume samplers (Digitel DHA80, and

26 DH-77) operating at 500 L min^{-1}. In order to prevent large negative filter artifacts, the high

27 volume samplers were equipped with temperature control systems maintaining the filter

28 storage temperature always below 25°C, which is lower or comparable to the maximum daily

29 temperature during summer. The particulate matter was collected on 150-mm diameter quartz

30 fiber filters (Pallflex Tissuquartz 2500QAT-UP / pure quartz, no binder) pre-baked at 800°C

31 for 8 h. Filter samples were wrapped in pre-baked aluminum foils (400°C for 6 h), sealed in

1 polyethylene bags and stored at -20°C after exposure. Field blanks were collected and stored

2 following the same procedure.

3 Sampling was conducted at urban (Vilnius), rural terrestrial (Rūgšteliškis) and rural coastal

4 (Preila) monitoring sites (Fig. 1). The rural terrestrial site of Rūgšteliškis serves as a baseline

5 against which urban-specific sources in the major population center of Vilnius can be

6 compared. The rural coastal site of Preila provides an opportunity to distinguish terrestrial and

7 marine sources.

8 The sampling station in Vilnius is located at the Center for Physical Sciences and Technology

9 campus (54°38' N, 25°10' E, 165 m a.s.l.) 12 km southwest of the city center (population:

10 535000) and is classified as an urban background site. The site is relatively far from busy

11 roads, and surrounded by forests to the north/northeast, and by a residential zone to the

12 south/east. It is ca. 350 km distant from the Baltic coast, and 98 km from the Rūgšteliškis

13 station (Fig. 1).

14 The station in Preila (55°55' N, 21°04' E, 5 m a.s.l.) is a representative rural coastal

15 background site, situated in the Curonian Spit National Park on the isthmus separating the

16 Baltic Sea from the Curonian Lagoon. The monitoring station is located <100 m from the

17 Baltic shore. The closest populated area is the village of Preila (population: 200 inhabitants),

18 located 2 km to the south.

19 The rural terrestrial station of Rūgšteliškis (55°26' N and 26°04' E, 170 m a.s.l.) is located in

20 the eastern part of Lithuania, about 350 km from the Baltic Sea. The site is surrounded by

21 forest and borders the Utenas Lake in the southwest. The nearest residential areas are

22 Tauragnai, Utena (12 km and 26 km west of the station, population: 32000 inhabitants) and

23 Ignalina (17 km southeast of the station, population: 6000 inhabitants).

24 **2.2 Offline-AMS analysis**

25 The term *offline-AMS* will be used herein to refer to the methodology described by

26 Daellenbach et al. (2016) and summarized below. For each analyzed filter sample, four 16-

27 mm diameter filter punches were subjected to ultrasonic extraction in 15 mL of ultrapure

28 water (18.2 MΩ cm at 25°C, total organic carbon (TOC) < 3 ppb) for 20 min at 30°C.

29 The choice of water instead of an organic solvent is motivated by two arguments:

- Water yields the lowest offline-AMS background and hence the highest signal to noise compared to other highly pure solvents (including methanol, dichloromethane and ethyl acetate).
- In contrast to the water extraction, the use of organic solvents precludes the quantification of the organic content in the extracts (e.g. by using a total OC analyzer), which in turn prevents a quantitative source apportionment.

Liquid extracts were then filtered and atomized in Ar ($\geq$99,998 % Vol. abs., Carbagas, CH-3073 Gümligen, Switzerland) using an Apex Q nebulizer (Elemental Scientific Inc., Omaha NE 68131 USA) operating at 60°C. The resulting aerosol was ~~then~~ dried by passing through a Nafion drier (Perma Pure, Toms River NJ 08755 USA), and subsequently analyzed by a HR-ToF-AMS. 12 mass spectra per filter sample were collected (AMS V-mode, m/z 12-232, 30 s collection time per spectrum). A measurement blank was recorded before and after each sample by nebulizing ultrapure water for 12 minutes. Field blanks were measured following the same extraction procedure as the collected filter samples, yielding a signal not statistically different from that of nebulized milliQ water. Finally we registered the AMS fragmentation spectrum of pure gaseous CO_2 ($\geq$99,7 % Vol, Carbagas, CH-3073 Gümligen, Switzerland), in order to derive its CO_2^+:CO^+ ratio.

Offline-AMS analysis was performed on 177 filter samples in order to determine the bulk water-soluble organic matter (WSOM) mass spectral fingerprints. In total, 63 filters from Rūgšteliškis, 42 from Vilnius, and 71 from Preila were measured in Ar. The reader is referred to DeCarlo et al. (2006) for a thorough description of the AMS operating principles and calibration procedures.

HR-ToF-AMS analysis software SQUIRREL (SeQUential Igor data RetRiEvaL, D. Sueper, University of Colorado, Boulder, CO, USA) v.1.53G and PIKA (Peak Integration by Key Analysis) v.1.11L for IGOR Pro software package (Wavemetrics, Inc., Portland, OR, USA) were utilized to process and analyze the AMS data. HR analysis of the AMS mass spectra was performed in the m/z range 12-115.

2.3 Supporting measurements

Additional offline analyses were carried out in order to validate and corroborate the offline-AMS source apportionment results. This supporting dataset was also used as input for PM_1 source apportionment as discussed below. The complete list of the measurements performed

40

1   can be found in Table 1 and Table S1. Briefly, major ions were measured by ion
2   chromatography (IC; Jaffrezo et al., 1998); elemental and organic carbon (EC, OC) were
3   quantified by thermal optical transmittance following the EUSAAR2 protocol (Cavalli et al.,
4   2010); water-soluble OC (WSOC) was measured by water extraction followed by catalytic
5   oxidation and non-dispersive infrared detection of CO_2 using a total organic carbon analyzer
6   (Jaffrezo et al., 2005). Organic markers were determined for 67 composite samples by gas
7   chromatography-mass spectrometry (GC-MS; Golly et al., 2015); high performance liquid
8   chromatography (HPLC) associated with a fluorescence detector (LC 240 Perkin Elmer) and
9   HPLC-pulsed amperometric detection (PAD; Waked et al., 2014) for 67 composite samples.
10   Composites were created merging two consecutive filter samples, but no measurements are
11   available for Vilnius during summer. Organic markers measurements Measurements included
12   18 polycyclic aromatic hydrocarbons (PAHs), alkanes (C21-C40), 10 hopanes, 13
13   methoxyphenols, 13 methyl-PAHs (Me-PAHs), 6 sulfur-containing-PAHs (S-PAHs), 3
14   monosaccharide anhydrides, and 4 monosaccharides (including glucose, mannose, arabitol,
15   and mannitol). In this work ion concentrations always refer to the IC measurements if not
16   differently specified.

17   Table 1. Overview of supporting measurements. A complete list of measured compounds can
18   be found in table S1.

Analytical Method	Measured compounds	Filters measured
IC (Jaffrezo et al., 1998)	Ions	All
Thermal optical transmittance using Sunset Lab Analyzer (Birch and Cary, 1996) using EUSAAR2 protocol (Cavalli et al., 2010)	EC/OC	All
TOC analyzer using persulphate oxidation at 100°C of the OM, followed by CO_2 quantification with a non-dispersive infrared spectrophotometer (Jaffrezo et al., 1998)	WSOC	All
HPLC associated with fluorescence detector (LC 240 Perkin Elmer)	PAHs (table S1)	67 composite samples

(Golly et al., 2015, Besombes et al., 2001)		
GC-MS (with and without derivatization step) (Golly et al., 2015)	S-PAHs, Me-PAHs, alkanes, hopanes, methoxyphenols, others	67 composite samples
HPLC-PAD, (Waked et al., 2014)	Anhydrous sugars, sugars alcohols, monosaccharides	67 composite samples
Chemiluminescence (Environnement S.A., Model AC31M)	NO_x	Online (Vilnius only)

1 In the following, subscripts *avg*, and *med* will denote average and median values,
2 respectively.

3 **3 Source apportionment**

4 Positive matrix factorization (PMF, Paatero and Tapper, 1994) is a bilinear statistical model
5 used to describe the variability of a multivariate dataset as the linear combination of a set of
6 constant factor profiles and their corresponding time series, as shown in Eq. (1):

7 $x_{i,j} = \sum_{z=1}^{p}(g_{i,z} \cdot f_{z,j}) + e_{i,j}$ (1)

8 Here *x*, *g*, *f*, and *e* denote elements of data, factor time series, factor profiles and residual
9 matrices, respectively, while subscripts *i,j* and *z* are indices for time, measured variables, and
10 factor number. The value *p* represents the total number of factors chosen for the PMF
11 solution. The PMF algorithm iteratively solves Eq. (1) by minimizing the objective function
12 *Q*, defined in Eq. (2) Only non-negative $g_{i,z}$ and $f_{z,j}$ values are permitted:

13 $Q = \sum_i \sum_j \left(\frac{e_{i,j}}{s_{i,j}}\right)^2$ (2)

14 Here the $s_{i,j}$ elements represent entries in the input error matrix.

15 In this work the PMF algorithm was run in the robust mode in order to dynamically
16 downweigh the outliers. The PMF algorithm was solved using the multilinear engine-2 (ME-
17 2) solver (Paatero, 1999), which enables an efficient exploration of the solution space by *a*

1 *priori* constraining the $g_{i,z}$ or $f_{z,j}$ elements within a certain variability defined by the scalar *a*

2 ($0 \leq a \leq 1$) such that the modelled $g_{i,z}$' and $f_{z,j}$' satisfy Eq. (3):

3 $$\frac{(1-a)f_{z,n}}{(1+a)f_{z,nm}} \leq \frac{f_{z,n}'}{f_{z,m}'} \leq \frac{(1+a)f_{z,n}}{(1-a)f_{z,m}} \qquad (3)$$

4 Here *n* and *m* are any two arbitrary columns (variables) in the normalized F matrix. The

5 Source Finder toolkit (SoFi, Canonaco et al., 2013, v.4.9) for Igor Pro software package

6 (Wavemetrics, Inc., Portland, OR, USA) was used to configure the ME-2 model and for post-

7 analysis. PMF analysis was applied to two complementary datasets: (1) organic mass spectra

8 from offline-AMS measurements for the apportionment of OM sources and (2) molecular

9 markers for the apportionment of the measured PM_1 mass. These two analyses are discussed

10 separately below.

11

12 ## 3.1 Offline-AMS PMF

13 In the following section we describe the offline-AMS source apportionment implementation,

14 optimization and uncertainty assessment. Briefly, we selected the number of PMF factors

15 based on residual analyses and solution interpretability; subsequently we explored the

16 rotational uncertainty of our source apportionment model and discarded suboptimal solutions

17 providing insufficient correlation of factor time series with external tracers. The offline-AMS

18 source apportionment returns the water soluble PMF factor concentrations. Daellenbach et al.

19 (2016) determined factor specific recoveries (including PMF factor extraction efficiencies),

20 by comparing offline-AMS and online-ACSM OA source apportionments. In particular, the

21 filter samples were collected for one year during an online-ACSM monitoring campaign

22 conducted at the same sampling station. Briefly, the factor recoveries were determined as the

23 ratio between the water soluble OA factor concentrations retrieved from offline-AMS PMF

24 divided by the OA factor concentrations obtained from online-ACSM PMF. Factor specific

25 recoveries and corresponding uncertainties were determined for HOA, BBOA, COA, and

26 OOA. ~~The offline-AMS source apportionment returns the water soluble PMF factor~~

27 ~~concentrations. Daellenbach et al. (2016) determined factor specific recoveries (including the~~

28 ~~extraction efficiencies), by comparing offline-AMS and online-ACSM source~~

29 ~~apportionments.~~ In this work we applied the factor recoveries from Daellenbach et al. (2016)

30 to scale the water soluble factor concentrations retrieved from offlne-AMS PMF to the

31 corresponding bulk OA concentrations. We conducted a sensitivity analysis on the applied

recoveries (Section 3.1.3)~~Applying these recoveries enabled scaling the water soluble factor concentrations to the corresponding bulk OA concentrations. A sensitivity analysis of these recoveries was reported in Section 3.1.3,~~ and the corresponding uncertainty was propagated to the source apportionment results.

A second solution selection step was carried out on the rescaled solutions as described in section 3.1.3. In general, the offline-AMS technique assesses less precisely the contribution of the low water soluble factors. The higher uncertainty mostly stems from the larger PMF rotational ambiguity when separating factors characterized by low concentration in the filter extracts (i.e. low water solubility). Nevertheless, the uncertainty is dataset dependent, as the separation of such sources can be improved in case of distinct time variability of these sources. The low aqueous concentration of scarcely water soluble sources in fact can be partially overcome by the large signal/noise characterizing the offline-AMS technique (170 on average for this dataset).

The offline-AMS source apportionment results presented in this study represent the average of the retained rescaled PMF solutions, while their variability represents our best estimate of the source apportionment uncertainty.

3.1.1 Inputs

The offline-AMS input matrices include in total 177 filter samples (62 filters from Rūgšteliškis, 42 from Vilnius, and 73 from Preila). Each filter sample was represented on average by 12 mass spectral repetitions to explore the effect of AMS and nebulizer stability on PMF outputs. A corresponding measurement blank was subtracted from each mass spectrum. The input PMF matrices included 269 organic fragments fitted in the mass range (12-115). The input error $s_{i,j}$ elements include the blank variability ($\sigma_{i,j}$) and the uncertainty related to ion counting statistic and ion-to-ion signal variability at the detector ($\delta_{i,j}$, Allan et al., 2003; Ulbrich et al., 2009):

$$s_{i,j} = \sqrt{\delta_{i,j}^2 + \sigma_{i,j}^2} \tag{4}$$

We applied a minimum error to the $s_{i,j}$ matrix elements according to Ulbrich et al. (2009), and a down-weighting factor of 3 to all fragments with an average signal to noise lower than 2 (Ulbrich et al., 2009). Input data and error matrices were rescaled such that the sum of each row is equal to the estimated $WSOM_i$ concentration, which is calculated as the product of the

44

measured $WSOC_i$ multiplied by the $(OM:OC)_i$ ratios determined from the offline-AMS PMF results.

3.1.2 Overview of retrieved factors and estimate of traffic exhaust OA (TEOA)

We used a 4-factor solution to represent the variability of the input data. The 4 separated OA factors included the following:

1/ a biomass burning OA (BBOA) factor highly correlated with levoglucosan originating from cellulose pyrolysis;

2/ a local OA (LOA) factor explaining a large fraction of N-containing fragments variability and contributing mostly in Vilnius during summer and spring;

3/ a background oxygenated-OA (B-OOA) factor showing relatively stable contributions at all seasons;

4/ a summer-OOA (S-OOA) factor showing increasing concentrations with the average daily temperature.

If the number of factors is decreased to 3, a mixed BBOA/B-OOA factor is retrieved, and significant structure appears in the residuals during winter (Fig. S2, S3, S4). Increasing the number of factors to 5 and 6, leads to a splitting of OOA factors that cannot be interpreted in terms of specific aerosol sources/processes (Fig. S2, S3). The further separated OOA factor in the 5-factor solution possibly derived from the splitting of B-OOA; in fact the sum of the newly separated OOA and B-OOA in the 5-factor solution correlated well with the B-OOA time series from the 4-factor solution ($R = 0.93$). Overall, a clear structure removal in the residual time-series was observed until a number of factors equal to 4 (Fig. S4, S5).

We also explored a 5-factor solution in which a hydrocarbon-like OA (HOA) profile from Mohr et al. (2012) was constrained to estimate the TEOA contribution. However, using hopanes as traffic tracers, the water-soluble TEOA (WSTEOA) contribution to WSOM was estimated as $0.2\%_{avg}$ (section 3.1.4), likely too small for PMF to resolve. We performed 100 PMF runs by randomly varying the HOA a-value. The obtained results showed a low TEOA correlation with hopanes ($R_{max} = 0.25$, $R_{min} = -0.15$) with 45% of the PMF runs associated with negative Pearson correlation coefficients, supporting the hypothesis that this factor has too small contribution in the water extracts to be resolved.this factor has too small a contribution to be resolved. Therefore, we selected the 4-factor solution as our best

45

representation of the data, while TEOA was instead estimated by a chemical mass balance (CMB) approach and not based on AMS mass spectral features.

TEOA concentrations ~~are~~ were estimated ~~using a CMB approach that~~ assum~~ing~~es hopanes, present in lubricant oils engines, (Subramanian et al., 2006) to be unique tracers for traffic. However, hopanes can also be emitted upon combustion of different types of fossil fuel, in particular by coal combustion (Rutter et al., 2009), therefore the traffic contribution estimated here, although very small (as discussed in the result section), should be considered as an upper estimate. Still, the EC~~/~~:hopanes ratio determined in this work (900 ± 100) is consistent with EC~~/~~:hopanes for TE (1400 ± 900: He et al., 2006; He et al., 2008; El Haddad et al., 2009; Fraser et al., 1998) and not with the coal EC/hopanes from literature profiles (300 ± 200: Huang et al., 2014; supplementary information (SI)). To assess the traffic exhaust OC (TEOC) contribution we used the sum of the four most abundant hopanes (17a(H),21b(H)-norhopane, 17a(H),21b(H)-hopane, 22S,17a(H),21b(H)-homohopane, and 22R,17a(H),21b(H)-homohopane (hopanes$_{sum}$)). The TEOC contribution was estimated from the average hopanes$_{sum}$~~/~~:TEOC ratio (0.0012 ± 0.0005) from tunnel measurements reported by He et al. (2006), He et al. (2008), El Haddad et al. (2009), and Fraser et al. (1998), where the four aforementioned hopanes were also the most abundant. In order to rescale TEOC to the total TEOA concentration we assumed an OM:OC$_{TEOA}$ ratio of 1.2 ± 0.1 (Aiken et al., 2008, Mohr et al., 2012, Docherty et al., 2011, Setyan et al., 2012). The uncertainty of the estimated TEOA concentration was assessed by propagating the uncertainties relative to the (OM:OC)$_{TEOA}$ ratio (8.3%), the hopanes$_{sum}$/TEOC ratio (41.7%), the hopane measurement repeatability (11.5%), and detection limits (7 pg m^{-3}).

3.1.3. Source apportionment uncertainty

A common issue in PMF is the exploration of the rotational ambiguity, here addressed by performing 100 PMF runs initiated using different input matrices. We adopted a bootstrap approach (Davison and Hinkley, 1997) to generate the new input data and error matrices (Brown et al., 2015). Briefly, the bootstrap algorithm generates new input matrices by randomly resampling mass spectra from the original input matrices. As already mentioned, the input matrices contained ca. 12 mass spectral repetitions per filter sample; therefore the bootstrap approach was implemented in order to resample random filter sample mass spectra together with the corresponding measurement repetitions. Each newly generated PMF input

46

1   matrix had a total number of samples equal to the original matrices (177 samples), although

2   some of the original 177 filter samples are represented several times, while others are not

3   represented at all. Overall we resampled on average 63±2% of the filter samples per bootstrap

4   run. The generated data matrices were finally perturbed by varying each $x_{i,j}$ element within

5   twice the corresponding uncertainty ($s_{i,j}$) assuming a normal distribution of the errors.

6   ~~Solutions were selected and retained according to three acceptance criteria.~~ Solutions were

7   selected and retained according to three acceptance criteria based on PMF factor correlations

8   with corresponding tracers: BBOA vs. levoglucosan, B-OOA vs. NH_4^+, and S-OOA vs.

9   average daily temperature. In order to discard suboptimal PMF runs, we only retained

10   solutions associated with positive Pearson correlation coefficients for each criterion, for both

11   the individual stations and the entire dataset. In total 95% of the solutions were retained

12   following this approach. <u>We note that no solution was discarded based on the first two</u>

13   <u>criteria.</u>

14   The offline-AMS PMF analysis provides the water-soluble contribution of the identified

15   aerosol sources. <u>Rescaling the water soluble OA factor concentrations to the total OA</u>

16   <u>concentrations induce an uncertainty which was propagated to our source apportionment</u>

17   <u>results as describes hereafter.</u> In order to rescale the water-soluble organic carbon

18   concentration of a generic factor z (WSZOC) to its total OC concentration (ZOC) we used the

19   factor recoveries (R_Z) determined by Daellenbach et al. (2016) according to Eq. (5):

20
$$ZOC_i = \frac{WSZOC_i}{R_z} \tag{5}$$

21   <u>Here for each PMF factor, the</u>~~For each PMF factor (BBOA, W-OOA, and S-OOA), the~~ water-

22   soluble organic carbon <u>time series (WSZOC)$_i$ were</u>~~contribution was~~ determined <u>dividing the</u>

23   <u>WSZOAi time series by the</u> ~~from the~~ OM:OC ratio calculated from the (water-soluble) factor

24   mass ~~spectrum~~ <u>spectra</u> (Aiken et al. 2008). For LOA, whose recovery was not previously

25   reported, R_{LOA} was estimated from a single parameter fit according to Eq. (6)

26
$$OC = TEOC + \frac{WSBBOA}{(OM\!:\!OC)_{WSBBOA} \cdot R_{BBOA}} + \frac{WS\mathrm{B}W\!-\!OOA}{(OM\!:\!OC)_{WSS\!-\!OOA} \cdot R_{OOA}} + \frac{WSS\!-\!OOA}{(OM\!:\!OC)_{WSB\!-\!OOA} \cdot R_{OOA}} + \frac{WSLOA}{(OM\!:\!OC)_{LOA} \cdot \mathbf{R_{LOA}}} \tag{6}$$

27   <u>Here the water-soluble OA factor concentrations were converted to the corresponding water-</u>

28   <u>soluble OC concentrations to fit the measured OC. For each of the 95 retained PMF solutions,</u>

29   <u>Eq. (6) was fitted 100 times by randomly selecting a set of 100 R_{BBOA}, R_{OOA} combinations</u>

30   <u>from those determined by Daellenbach et al. (2016). Each fit was initiated by perturbing the</u>

31   <u>input OC_i and $TEOC_i$ within their uncertainties, assuming a normal distribution of the errors.</u>

Additionally we also perturbed the OC and WSOC inputs (Eq. 6) in order to explore the effect of possible bulk extraction efficiency (WSOC:OC) systematic biases on our R_Z estimates. Specifically, we assumed an estimated accuracy bias of 5% for each of the perturbed parameters, which corresponds to the OC and WSOC measurement accuracy. In a similar way, we also perturbed the input R_{BBOA} and R_{OOA} assuming an accuracy estimate of 5% deriving from a possible OC measurement bias in Daellenbach et al. (2016) which could have affected the R_Z determination. In total $9.5 \cdot 10^3$ fits were performed (Eq. 6) and we retained only solutions (and corresponding perturbed R_Z combinations) associated with average OC residuals not statistically different from 0 within 1σ for each station individually and for summer and winter individually (~8% of the $9.5 \cdot 10^3$ fits, Fig. S6). The OC residuals of the accepted solutions did not manifest a clear correlation with the LOA concentration (Fig. S7), indicating that the estimated R_{LOA} was properly fitted, without compensating for unexplained variability of the PMF model or biases from the other R_z. Fig. S8 shows the probability density functions (PDF) of the retained perturbed R_z which account for all uncertainties and biases mentioned above. ~~For each of the 95 retained PMF solutions, Eq. (6) was fitted 100 times by randomly selecting a set of 100 R_{BBOA}, R_{OOA} value combinations from those determined by Daellenbach et al. (2016). Each fit was initiated by perturbing the input OC_i and $TEOC_i$ within their uncertainties, assuming a normal distribution of the errors. In order to explore the effect of possible bulk extraction efficiency (WSOC/OC) systematic measurement biases on our R_Z estimates, we also perturbed the OC, WSOC, R_{BBOA}, and R_{OOA} (Daellenbach et al., 2016) inputs. Specifically, we assumed an estimated accuracy bias of 5% for each of the perturbed parameters, which corresponds to the OC and WSOC measurement accuracy. In total $9.5 \cdot 10^3$ fits were performed (Eq. 6) and we retained only solutions with average OC residuals not statistically different from 0 within 1σ for each station individually and for summer and winter individually (~8% of the $9.5 \cdot 10^3$ fits, Fig. S6). The OC residuals of the accepted solutions did not manifest a clear correlation with the LOA concentration (Fig. S7), indicating that the estimated R_{LOA} was properly fitted, without compensating for unexplained variability of the PMF model or biases from the other R_z. R_z distributions shown in Fig. S8 accounted for all uncertainties and biases mentioned above.~~ $R_{LOA,med}$ was estimated to be equal to 0.66 (1st quartile 0.61, 3rd quartile 0.69, Fig. S8), while the retained R_{BBOA} and R_{OOA} values ($R_{BBOA,med}$ 0.57, 1st quartile 0.55, 3rd quartile 0.60; $R_{OOA,med}$ 0.84, 1st quartile 0.81, 3rd quartile 0.88) were systematically lower than those reported by Daellenbach et al. (2016), reflecting the lower bulk extraction efficiency (bulk EE = WSOC:OC) measured for this dataset

(median = 0.59, 1st quartile = 0.51, 3rd quartile = 0.72 *vs.* median = 0.74, 1st quartile = 0.66, 3rd quartile 0.90 in Daellenbach et al. (2016)). All the retained R_k combinations are available at DOI: doi.org/10.5905/ethz-1007-53.

Source apportionment uncertainties ($\sigma_{S.A.}$) were estimated for each sample i and factor z as the standard deviation of all the retained PMF solutions (~8% of the $9.5 \cdot 10^3$ fits). In addition to the rotational ambiguity of the PMF model (explored by the bootstrap technique) and R_Z uncertainty, each PMF solution included on average 10 repetitions for each filter sample, and hence $\sigma_{S.A.}$ accounted also for measurement repeatability. In this work, the statistical significance of a factor contribution is calculated based on $\sigma_{S.A.,z,i}$ (Tables S2 and S3).

Overall the recovery estimates reported in Daellenbach et al. (2016) represent the most accurate estimates available, being constrained to match the online-ACSM source apportionment results. The R_Z combinations reported by Daellenbach et al. (2016) demonstrated to positively apply to this dataset, enabling properly fitting the measured Bulk EE (WSOC:OC) with unbiased residuals and therefore providing a further confidence on their applicability (we note that in Eq. 6 we fitted OC as function of $(R_Z)^{-1}$ and $WSOC_{Z,i}$, therefore R_Z fitted WSOC/OC = Bulk EE). In general further R_Z determinations calculated comparing offline-AMS and online-AMS source apportionments would be desirable in order to provide more robust R_Z estimates. In absence of a-priori R_Z values for specific factors (e.g. for LOA in this study) we recommend constraining the R_Z combinations reported by Daellenbach et al. (2016) as a-priori information to fit the unknown recoveries (similarly to Eq. 6), with the caveat that the R_Z combinations reported by Deallenbach et al. (2016) were determined for filter samples water extracted following a specific procedure; therefore we recommend adopting these R_Z combinations for filter samples extracted in the same conditions. Nevertheless the R_Z combinations reported by Daellenbach et al. (2016) should be tested also for filters water extracted in different conditions to verify whether they can properly fit the Bulk EE. In case the R_Z combinations reported by Daellenbach et al. (2016) would not apply for a specific location or extraction procedure (i.e. not enabling a proper fit of Bulk EE) we recommend a R_Z redetermination by comparing the offline-AMS source apportionment results with well-established source apportionment techniques (e.g. from online-AMS or ACSM data). In absence of data to perform a well-established source apportionment, we recommend to fit all the R_Z to match the bulk EE (i.e. fitting all the recoveries similarly as in Eq. 6 without constraining any a-priory R_Z value).

3.1.4. Sensitivity of PMF to the un-apportioned TEOA fraction

Despite representing only a small fraction, the un-apportioned water-soluble TEOA (WSTEOA) contribution could in theory affect the apportionment of the other sources in the offline-AMS PMF model. To assess this, we performed a PMF sensitivity analysis by subtracting the estimated WSTEOA concentration from the input PMF data matrix, and by propagating the estimated WSTEOA uncertainty (section 3.1.2) in the input error matrices. To estimate the WSTEOA concentration we assumed R_{TEOA} of 0.11±0.01 (Daellenbach et al., 2016) and we used the HOA profile reported by Mohr et al. (2012) as surrogate for the TEOA mass spectral fingerprint. This approach is equivalent to constraining both the WSTEOA time series and factor profile. Overall the WSTEOA contribution to WSOM was estimated as 0.2%$_{avg}$, making a successful retrieval of WSTEOA unlikely (Ulbrich et al., 2009). Consistently, PMF results obtained from this sensitivity analysis indicated that BBOA and B-OOA were robust, showing only 1% difference from the average offline-AMS source apportionment results, with BBOA increased and B-OOA decreased. S-OOA and LOA instead showed larger deviations from the average source apportionment results (S-OOA increased by 8% and LOA decreased by 15%), yet within our source apportionment uncertainties. These results highlight the marginal influence of the un-apportioned WSTEOA fraction on the other factors.

3.2 Marker-PMF: measured PM$_1$ source apportionment

In the following section we describe the implementation of source apportionment using chemical markers (marker-PMF), as well as its optimization and uncertainty assessment. We discuss the number of factors and the selection of specific constraints to improve the source separation. Subsequently we discuss the source apportionment rotational uncertainty, and the sensitivity of our PMF results to the number of source specific markers, and to the assumed constraints.

3.2.1 Inputs

The marker-PMF yields a source apportionment of the entire measured PM$_1$ fraction (organic and inorganic). Measured PM$_1$ is defined here as the sum of EC, ions measured via IC, and OM estimated from OC measurements multiplied by the (OM:OC)$_i$ ratio determined from the

1 offline-AMS PMF results by summing the factor profiles OM:OC ratios weighted by the time

2 dependent factor relative contributions (rescaled by the recoveries). PMF was used to analyze

3 a data matrix consisting of selected organic molecular markers, ions measured by IC, EC, and

4 the remaining OM fraction (OM_{res}) calculated as the difference between total OM and the sum

5 of the organic markers already included in the input matrix. (OM_{res} represented on average

6 95±2% of total OM). The marker-PMF analysis in this work is limited by the lack of

7 elemental measurements (e.g. metals and other trace elements) typically used to identify

8 mineral dust and certain anthropogenic sources. All Overall we selected as input variables all

9 markers showing concentrations above the detection limits for more than 25% of the samples

10 were selected as input variables (72 in total). The PMF input matrices contain 67 composite

11 samples (31 for Rūgšteliškis, 29 for Preila, and 7 for Vilnius). The errors ($s_{i,j}$) were estimated

12 by propagating for each j variable the detection limits (DL) and the relative repeatability (RR)

13 multiplied by the $x_{i,j}$ concentration according to Eq. (7) (Rocke and Lorenzato, 1995):

14 $$s_{i,j} = \sqrt{(DL_j{}^2 + (x_{i,j} \cdot RR_{i,j})^2)} \tag{7}$$

3.2.2 Number of factors and constraints

16 We selected a 7-factor solution to explain the variability of the measured PM_1 components.

17 The retrieved factors were biomass burning (BB), traffic exhaust (TE), primary biological

18 organic aerosol (PBOA), SO_4^{2-}-related secondary aerosol (SA), NO_3^--related SA, methane

19 sulfonic acid (MSA)-related SA, and a Na^+-rich factor explaining the variability of inorganic

20 components typically related to resuspension of mineral dust, sea salt, and road salt.

21 We first tested an unconstrained source apportionment. This led to a suboptimal separation of

22 the aerosol sources, with large mixings of PMF factors associated with contributions of

23 markers originating from different sources. In particular we observed mixing of BB markers

24 (e.g. levoglucosan) with fossil fuel combustion markers such as hopanes, as well as with

25 inorganic ions such as NO_3^- and Ca^{2+}. All these markers, although related to different

26 emission/formation processes, are characterized by similar seasonal trends, i.e. higher

27 concentrations during winter than in summer. Specifically, the BB tracers increase during

28 winter because of domestic heating activity, hopanes presumably because of the accumulation

29 in a shallower boundary layer and lower photochemical degradation, NO_3^- because of the

30 partitioning into the particle phase at low temperatures, and Ca^{2+} because winter was the

31 windiest season and therefore was associated with the most intense resuspension.

51

1   We subsequently exploited the markers' source-specificity to set constraints for the profiles

2   output by our model: for each individual source, we treated the contribution of the unrelated

3   source-specific markers as negligible (e.g. we assumed that TE, SA, Na-rich factor and PBOA

4   do not contribute to levoglucosan). In contrast, the non-source specific variables (EC, OM$_{res}$,

5   (Me-)PAHs, S-PAHs, inorganic ions, oxalate, alkanes) were freely apportioned by the PMF

6   algorithm. In a similar way we set constraints for primary markers (e.g. K^+ and Ca^{2+}) and

7   combustion related markers (e.g. PAHs), which are not source-specific but the contribution of

8   which can be considered as negligible in the SA factors. In this case the algorithm can freely

9   apportion these markers to all the primary factors and combustion-related factors,

10 respectively.

11 In details, EC, PAHs, and methyl-PAHs were constrained to zero in non-combustion sources,

12 i.e. all profiles but TE and BB. While EC could partially derive from dust resuspension,

13 literature profiles for this source suggest an EC contribution below 1% (Chow et al., 2003).

14 This is expected to be also the case here given the distance of the three stations from

15 residential areas and busy roads. Methoxyphenols and sugar anhydrides, considered to be

16 unique BB markers, were constrained to zero in all sources but BB. Similarly, hopanes were

17 constrained to zero in all factors but TE. We also assumed no contribution from glucose,

18 arabitol, mannitol, and sorbitol to all secondary factors, and traffic exhaust. The SO_4^{2-}

19 contribution from primary traffic emissions was estimated to be negligible, given the use of

20 desulfurized fuel for vehicles in Lithuania. Likewise, alkane contributions were assumed to be

21 zero in the SA factors, similar to the contribution of Ca^{2+}, Na^+, K^+ and Mg^{2+} in the SA factors

22 and TE.

23 The number of factors was increased until no mixing between source-specific markers for

24 different aerosol sources/processes was observed any more. Secondary sources instead were

25 explained by three factors because of the distinct seasonal and site-to-site variability of MSA,

26 NO_3^- and SO_4^{2-}. Oxalate correlated well with NH_4^+ (R=0.62) and the latter well with the sum

27 of SO_4^{2-} and NO_3^- equivalents (R=0.98). Note that the aforementioned secondary tracers were

28 not constrained in any factor with the exception of SO_4^{2-} contributions which were assumed to

29 be negligible in the TE factor. Moreover the 7-factor solution showed unbiased residuals

30 (residual distribution centered at 0 within 1σ) for all the stations together and for each station

31 individually, while lower order solutions showed biased residuals for at least one station or all

32 the stations together.

1 PMF results obtained assuming only the aforementioned constraints returned suboptimal
2 apportionments of OM_{res} and Na^+ between the BB and the Na^+-rich factor, with unusually
3 high OM_{res} fractional contributions in the Na^+-rich factor and unusually high Na^+
4 contributions in the BB profile in comparison with literature profiles (Chow et al., 2003;
5 Huang et al., 2014 and references therein; Schauer et al., 2001). Similarly the EC/:OM_{res}
6 value for TE was substantially lower than literature profiles (El Haddad et al., 2013 and
7 references therein). Other constraints were therefore introduced to improve the separation of
8 these three variables. Specifically, EC and OM_{res} were constrained in the traffic profile to be
9 equal to 0.45 and 0.27 (*a*-value = 0.5) according to El Haddad et al. (2013), while EC:BB
10 ratio was constrained to 0.1~~while EC was constrained to 0.1~~ (*a*-value = 1) ~~in the BB profile~~
11 according to Huang et al. (2014) and references therein. Na^+ was constrained to 0.2% (*a*-value
12 = 1) in BB according to Schauer et al. (2001), while OM_{res} was constrained to zero in the Na^+-
13 rich factor to avoid mixing with BB. Although this represents a strict constraint, we preferred
14 avoiding constraining OM_{res} to a specific value for the Na^+-rich factor which could not be
15 linked to a unique source but possibly represents different resuspension-related sources (e.g.
16 sea salt, mineral dust and road dust). However, we expect none of the aforementioned sources
17 to explain a large fraction of the submicron OM_{res} (the OC:dust ratio for dust profiles is 1-
18 15% according to Chow et al., 2003). The sensitivity of our source apportionment to the
19 constraints listed in this section is discussed in the next section.

20

21 ### 3.2.3. Source apportionment uncertainty and sensitivity analyses

22 We explored the model rotational uncertainty by performing 20 bootstrap PMF runs, and by
23 perturbing each input $x_{i,j}$ element within $2 \cdot s_{i,j}$ assuming a normal distribution of the errors.
24 Results and uncertainties of the PMF model reported in this paper represent the average and
25 the standard deviation of the bootstrap runs.

26 As discussed in section 3.2.2, we assumed the contribution of specific markers to be 0 in
27 different factor profiles. Such assumptions preclude the PMF model to vary the contributions
28 of these variables from 0 (Eq. 3). In order to explore the effect of such assumptions on our
29 PMF results we loosened all these constraints assuming variable contributions equal to 50%,
30 37.5%, 25%, and 12.5% of their average relative contribution to measured PM_1. In all cases
31 the *a*-value was set to 1.~~We tested the sensitivity of our solution to the constraints listed in~~
32 ~~section 3.2.2. All the constraints assuming variable contributions equal to zero were loosened,~~

assuming for each variable a contribution equivalent to 50%, 37.5%, 25%, and 12.5% of its average relative contribution to measured PM_1. In all cases the *a* value was set to 1. As expected, results showed better agreement with the fully constrained solution in the cases of stronger constraints, meaning that the highest agreements were observed for the 12.5% case both in terms of mass balance and factor time series correlations (Fig. S9). The average factor concentrations for the 12.5% case and the fully constrained average bootstrap PMF solutions were not statistically different (confidence interval of 95%, Fig. S9). Statistically significant differences arose for the of the SO_4^{2-}-related SA in the 50% and 37.5% cases, and the Na^+-rich factor in the 25% and 37.5% cases, indicating that loosening the constraints allowed additional rotational uncertainty in comparison to the uncertainty explored by the bootstrap approach. By contrast, the factors associated with large relative uncertainties from the marker source apportionment (TE and PBOA, Table S3) showed the best agreement in terms of concentrations (Fig. S9) with the fully constrained solution, suggesting that the variability introduced by loosening the constraints did not exceed that already accounted for by the bootstrap approach. As previously mentioned, the largest contribution discrepancies were observed for the SO_4^{2-}-related SA and Na^+-rich factor. Looser constraints increased the explained variability of primary components such as EC, arabitol, sorbitol, K^+, Mg^{2+}, and Ca^{2+} by the (secondary) SO_4^{2-}-related SA factor. The Na^+-rich factor showed increasing contributions from OM_{res} and from BB components such as methoxyphenols, and anhydrous sugars, which exhibited similar seasonal trends as the Na^+-rich factor. None of the marker-PMF factors showed statistically different average contributions (confidence interval of 95%) when tolerating a variability of the constrained variables within 12.5% of their relative contribution to PM_1. Note that with this degree of tolerance the contribution of OM to the Na^+-rich was 28%, which is unrealistically high compared to typically reported values for OM:dust ratios (<15% Chow et al., 2003). Therefore, we consider the fully constrained PMF solution to represent best the average composition of the contributing sources.

The marker-PMF source apportionment depends strongly on the input variables (i.e. measured markers), as these are assumed to be highly source specific. That is, minor sources, such as MSA-related SA and PBOA, are separated because source-specific markers were used as model inputs. Meanwhile, more variables were used as tracers for TE and BB (methoxyphenols (5 variables), sugar anhydrides (3 variables), and hopanes (5 variables)), which gives more weight to these specific sources. We explored the sensitivity of the PMF results to the number and the choice of traffic and wood burning markers, by replacing them

54

1 with randomly selected input variables. In total 20 runs were performed and the average

2 contribution of the different sources to OM_{res} was compared with the marker source

3 apportionment average results, where bootstrap was applied to resample time points. Results

4 displayed in Fig. S10 are in agreement the apportionment of OM_{res} from BB within $11\%_{avg}$,

5 highlighting its robustness. The agreement for TE was lower, which is not surprising given

6 the lower contribution of this source and the smaller number of specific markers (hopanes).

7 However, these uncertainties were within the marker source apportionment uncertainty (Fig.

8 S10), implying that the results were not significantly sensitive to the number and the choice of

9 input markers for BB and traffic exhaust.

10

4   Results and Discussion

4.1 PM$_1$ composition

13 An overview of the measured PM$_1$ composition can be found in Fig. 1. Measured PM$_1$

14 average concentrations were in general low, with lower values detected at the rural terrestrial

15 site of Rūgšteliškis (5.4 µg m^{-3}$_{avg}$) than in Vilnius (6.7 µg m^{-3} $_{avg}$) and Preila (7.0 µg m^{-3} $_{avg}$).

16 OM represented the major fraction of measured PM$_1$ for all seasons and stations, with $57\%_{avg}$

17 of the mass. The average OM concentrations were higher during winter (4.2 µg m^{-3}) than in

18 summer (3.0 µg m^{-3}) at all sites probably due to a combination of domestic wood burning

19 activity and accumulation of the emissions in a shallower boundary layer. For similar reasons,

20 EC average concentrations showed higher values during winter (0.42 µg m^{-3}) than in summer

21 (0.25 µg m^{-3}). During summer, the average EC concentration was ∼5 times higher in Vilnius

22 (0.54 µg m^{-3}) than in Preila and Rūgšteliškis (0.12 and 0.11 µg m^{-3}, respectively), indicating

23 an enhanced contribution from combustion emissions. In the absence of domestic heating

24 during this period, a great part of these emissions may be related to traffic. During winter, EC

25 concentrations were comparable at all sites (only 25% higher in Vilnius than in Preila and

26 Rūgšteliškis). This suggests that a great share of wintertime EC may be related to BB, the

27 average contribution of which is significant at all stations within 3σ (table S2). It should be

28 noted that the highest measured PM$_1$ concentrations were detected at the remote rural coastal

29 site of Preila during three different pollution episodes. In particular, the early March episode

30 corresponded to the period analyzed by Ulevicius et al. (~~2015~~2016) and Dudoitis et al.

31 (~~2015~~2016), and was attributed to regional transport of polluted air masses associated to an

55

1 intense land clearing activity characterized by large scale grass burning in the neighboring

2 Kaliningrad region. SO_4^{2-} represented the second major component of measured PM_1

3 ($20\%_{med}$) at all sites and seasons. Its average concentration remained rather constant with only

4 slightly higher concentrations in summer than in winter (1.2 ± 0.7 μg m^{-3}, and 1.1 ± 0.6 μg m^{-3}

5 respectively). Overall SO_4^{2-} concentrations did not show large differences from site-to-site,

6 suggestive of regional sources. By contrast NO_3^- showed a clear seasonality with larger

7 contributions in winter (average 0.9 ± 0.8 μg m^{-3} equivalent to 12% of measured PM_1) than in

8 summer (0.03 ± 0.03 μg m^{-3}), as expected from its semi-volatile nature.

9 **4.2 OM source apportionment (Offline-AMS PMF)**

10 The apportioned PMF factors were associated to aerosol sources/processes according to their

11 mass spectral features, seasonal contributions and correlations with tracers. The four

12 identified factors were BBOA, LOA, B-OOA, and S-OOA, which are thoroughly discussed

13 below. The TEOA contributions instead were determined using a CMB approach.

14 BBOA was identified by its mass spectral features, with high contributions of $C_2H_4O_2^+$, and

15 $C_3H_5O_2^+$ (Fig. 2), typically associated with levoglucosan fragmentation from cellulose

16 pyrolysis (Alfarra et al., 2007), accordingly the BBOA factor time series correlated well with

17 levoglucosan (Pearson correlation coefficient: R=0.90, Fig. S11). BBOA contributions were

18 higher during winter and lower during summer (Fig. 3a). We determined the biomass burning

19 organic carbon (BBOC) concentration from the BBOA time series divided by the

20 OM:OC$_{BBOA}$ ratio determined from the corresponding HR spectrum. The winter

21 levoglucosan/:BBOC ratio was 0.16_{med}, consistent with values reported in continental Europe

22 for ambient BBOC profiles (levoglucosan/BBOC range: 0.10-0.21, Zotter et al., 2014;

23 Minguillón et al., 2011; Herich et al., 2014).

24 The second factor was defined as LOA because of its statistically significant contribution

25 (within 3σ) only in Vilnius during summer (table S2), in contrast to other potentially local

26 primary (e.g. BBOA) and secondary (S-OOA) sources which contributed at all sites. The

27 LOA mass spectrum was characterized by a high contribution of N-containing fragments

28 (especially $C_5H_{12}N^+$, and $C_3H_8N^+$), with the highest N:C ratio (0.049) among the apportioned

29 PMF factors (0.029 for BBOA, 0.013 for S-OOA, 0.023 for B-OOA). This factor could be

30 related to the activity of theA similar factor was also observed by Byčenkienė et al. (2016)

31 using an ACSM at the same station. In that work, high LOA concentrations were associated

with ~~wind directions from N NW, and the authors suggested~~ the sludge utilization system of Vilnius (UAB Vilniausvandenys) situated 3.9 km NW from the sampling station as a probable source.

Two different OOA sources (S-OOA and B-OOA) were resolved and exhibited different seasonal trends. ~~Separation~~ The separation and classification of OOA sources from offline-AMS is typically different from that of ~~online~~ online-AMS and ACSM measurements, mainly due to the different time resolution. In this section we describe the separation and classification of OOA factors retrieved from online- and offline-AMS.

Few online-AMS studies reported the separation of isoprene-related OA factor (Budisulistiorini et al., 2013; Hu et al., 2015, Xu et al., 2015) mostly driven by isoprene epoxides chemistry. Xu et al. (2015) showed that nighttime monoterpene oxidation by nitrate radical contributes to less-oxidized OOA. However, the large majority of online-AMS OOA factors are commonly classified based on their volatility (semi-volatile OOA and low-volatility OOA) rather than on their sources and formation mechanisms.~~Online-AMS OOA factors are commonly classified based on their volatility (semi-volatile OOA and low-volatility OOA).~~ This differentiation is typically achieved only for summer datasets when the temperature gradient between day and night is sufficiently high, yielding a detectable daily partitioning cycle of the semi-volatile organic compounds and NO_3^- between the gas and the particle phases. Online-AMS datasets have higher time resolution than filter sampling, but sampling periods typically cover only a few weeks. Therefore the apportionment is driven by daily variability rather than seasonal differences. By contrast, in the offline-AMS source apportionment, given the 24-h time resolution of the filter sampling and the yearly cycle time coverage, the separation of the factors is driven by the seasonal variability of the sources and by the site-to-site differences.

In general, OOA factors with different seasonal behaviors can be characterized by different volatilities. However in this work the offline-AMS OOA separation is not driven by volatility, given the low correlation between NO_3^- and our OOA factors (also reflected by the low NO_3^--related SOA correlation with B-OOA and S-OOA, Table 2). Additionally, the partitioning of semi-volatile OA at low temperatures would lead to a less oxidized OOA fingerprint during winter than in summer; however, this was not the case. We observed a less oxidized OOA factor during summer, whose mass spectral fingerprint closely resembles that of SOA from biogenic precursors. Meanwhile similar to OOA from aging of biomass burning emissions,

OOA during the cold season is more oxidized. This has been also reported in an urban environment in central Europe (Zurich) using an online-ACSM (Canonaco et al., 2015). Therefore, the offline-AMS source apportionment tends to separates OOA factors by seasonal trends rather than volatility.

Table 2: Pearson correlation coefficients between non-combustion factors (Other-OA components) from offline-AMS and marker-source apportionment.

		Other-OA$_{marker}$			
		SO_4^{2-}-related SOA	MSA-related SOA	NO_3^--related SOA	PBOA
Other-OA$_{offline-AMS}$	LOA	0.33	0.16	-0.08	0.10
	B-OOA	0.70	0.22	0.21	0.47
	S-OOA	0.60	0.45	-0.47	0.05

In this work, Tthe resolved B-OOA factor explained a higher fraction than S-OOA. It was associated with background oxygenated aerosols as no systematic seasonal pattern was observed. However, B-OOA correlated well with NH_4^+ (R=0.69, Fig. S11), and had the highest OM:OC ratio among the apportioned PMF factors (2.21).

Analyzing the B-OOA and S-OOA time series and seasonal trends, we could obtain more insights into the origin of two factors. Unlike B-OOA, S-OOA showed a clear seasonality with higher contributions during summer, increasing exponentially with the average daily temperature (Fig. S12a). During summer the site-to-site S-OOA concentrations were not statistically different within a confidence interval of 95%, while during winter the site-to-site agreement was lower, possibly due to the larger model uncertainty associated with the low S-OOA concentrations. A similar S-OOA *vs.* temperature relationship was reported by Leaitch et al. (2011) for a terpene dominated Canadian forest using an ACSM and by Daellenbach et al. (2016) and Bozzetti et al. (2016) for the case of Switzerland (Fig. S12b), using a similar source apportionment model. This increase in S-OOA concentration with temperature is consistent with the exponential increase in biogenic SOA precursors (Guenther et al., 2006). Therefore, even though the behavior of S-OOA at different sites might be driven by several parameters, including vegetation coverage, available OA mass, air masses photochemical age and ambient oxidation conditions (e.g. NO_x concentration), temperature seems to be the main driver of S-OOA concentrations. Overall more field observations at other European locations are needed to validate this relation. While the results indicate a probable secondary biogenic origin of the S-OOA factor, the precursors of the B-OOA factor are not identified. In section

58

4.4.2 more insights into the OOA sources deriving from the comparison with the markers source apportionment will be discussed.

The B-OOA and S-OOA mass spectra were also compared with OOA profiles from literature. The S-OOA profile showed a $CO_2^+/C_2H_3O^+$ ratio of 0.61_{avg}, placing it in the region of semi-volatile SOA from biogenic emissions in the $f44/f43$ space (Ng et al., 2011), as attributed by Canonaco et al. (2015). Despite the higher summer photochemical activity, the water-soluble bulk OA showed more oxidized mass spectral fingerprints during winter (O:C=0.61_{avg}) than in summer (O:C=0.55_{avg}), similar to the results presented by Canonaco et al. (2015) for Zurich. Accordingly, the S-OOA profile also showed a less oxidized water-soluble mass spectral fingerprint than B-OOA, with an O:C ratio of 0.40_{avg}, in comparison with 0.80_{avg} for B-OOA. Considering the sum of B-OOA and S-OOA, the median OOA:NH_4^+ ratios for Rūgšteliškis, Preila, and Vilnius were 3.2, 2.4, and 2.5 respectively, higher than the average but within the range of the values reported by Crippa et al. (2014) for 25 different European rural sites (2.0_{avg}; minimum value 0.3; maximum 7.3).

4.3 PM$_1$ source apportionment (marker-PMF)

The PMF factors in this analysis were associated with specific aerosol sources/processes according to their profiles, seasonal trends and relative contributions to the key variables. Fig. 4 displays factor profiles, and the relative contribution of each factor to each variable. The Na^+-rich factor explained a large part of the variability of Ca^{2+}, Mg^{2+}, and Na^+ (Fig. 4) and showed higher contributions during winter than in summer (Fig. 5), suggesting a possible resuspension of sand and salt typically used during winter in Lithuania for road de-icing. This seasonal trend is also consistent with wind speed, which showed the highest monthly values during December 2013 and January 2014. We cannot exclude the possibility that this factor may include contributions from sea salt, although Na^+ and Cl^- were not enhanced at the marine station in comparison with the other stations. The overall contribution of this Na^+-rich factor to measured PM$_1$ was relatively small ($1\%_{avg}$), but may be larger in the coarse fraction.

The BB factor showed a well-defined seasonality, with high contributions during winter. This factor explained a large part of the variability of typical wood combustion tracers such as methoxyphenols, sugar anhydrides (including levoglucosan, mannosan, and galactosan), K^+, Cl^-, EC, PAHs, and methyl-PAHs (Fig. 4). Using the OM:OC$_{BBOA}$ ratio (1.88) calculated from offline-AMS, we estimated the levoglucosan:BBOC ratio to be 0.18_{avg}, which is within

59

the range of previous studies (Ulevicius et al., ~~2015~~ 2016 and references therein). Note that this factor explained also large fractions of variables typically associated with non-vehicular fossil fuel combustion, such as benzo(b)naphtho(2,1-d)thiophene (BNT[2,1]) and 6,10,14-trimethyl-2-pentadecanone (DMPT, Fig. 4, Manish et al., 2007; Subramanian et al., 2007), indicating a potential mixing of BB with fossil fuel combustion sources. However, the fossil fuel combustion contribution to BB is unlikely to be large, considering the low concentrations of fossil fuel tracers such as hopanes (66% of the samples below quantification limit (<QL)), BNT[2,1] (64%<QL), and DMPT (55%<QL). Moreover, the above mentioned agreement of the levoglucosan:BBOC ratio with previous studies corroborates the BB estimate from the marker-PMF.

The traffic exhaust factor explained a significant fraction of the alkane variability, with a preferential contribution from light alkanes (Fig. 4). Its contribution was never statistically significant within ~~1σ~~ 3σ ~~only for one filter collected in Vilnius~~. However on average the concentration was higher in Vilnius than at the other stations and in general higher in winter than in summer.

The PBOA factor explained the variability of the primary biological components, such as glucose, mannitol, sorbitol, arabitol, and alkanes with an odd number of carbon atoms (consistent with Bozzetti et al., 2016 and references therein). Highest PBOA concentrations were observed during spring, especially at the rural site of Rūgšteliškis. Overall the contribution of this factor was uncertain with an average relative model error of 160% probably due to the small PBOA contributions ($0.6\%_{avg}$ of the total OM), which hampers a more precise determination by the model. In particular OM_{res} was the variable showing the highest mass contribution to the PBOA factor~~.~~, ~~H~~however, the large contribution and the large uncertainty of OM_{res} to this factor (0.3 ± 0.4) resulted in a large uncertainty in the PBOA estimated concentration.

The last three factors were related to SA, as indicated by the large contributions of secondary species such as oxalate, SO_4^{2-}, MSA, and NO_3^- to the factor profiles (Fig. 4). The three factors showed different spatial and temporal contributions.

The NO_3^--related SA exhibited highest contributions during winter, suggesting temperature-driven partitioning of secondary aerosol components. Moreover the NO_3^--related SA, similarly to BB and TE, showed the highest concentrations in Vilnius, and the lowest in

Rūgšteliškis suggesting its possible relation with anthropogenic gaseous precursors (e.g. NO_x), as already reported in other studies (e.g. Xu et al., 2016; McMeeking et al., 2012).

The MSA-related SA factor manifested the highest concentrations at the marine site of Preila during summer, and in general larger contributions during summer than winter, suggesting its relation with marine secondary aerosol. MSA has been reported to be related to marine secondary biogenic emissions deriving from the photo-oxidation of dimethyl sulfide (DMS) emitted by the phytoplankton bloom occurring during the warm season (Li et al., 1993, Crippa et al., 2013 and references therein).

The last factor (SO_4^{2-}-related SA) showed higher contributions during summer than in winter without clear site-to-site variability, following the seasonal behavior of SO_4^{2-} showing slightly higher concentrations during summer than in winter, which is probably driven by the secondary formation from gaseous photochemical reactions and aqueous phase oxidation. This factor explained the largest part of the oxalate and SO_4^{2-} variability and represented $48\%_{avg}$ of the measured PM_1 by mass.

4.4 Comparison of the source apportionment methods

In this section we compare the offline-AMS PMF and marker-PMF results. We begin with BBOA and TEOA emissions which were resolved by marker-PMF and offline-AMS (as already mentioned TEOA was actually not resolved by offline-AMS but determined through a CMB approach)both approaches. The remaining OM fraction (Other-OA = OA – BBOA - TEOA) was apportioned by the offline-AMS source apportionment to B-OOA, S-OOA and LOA (Other-OA$_{offline-AMS}$). However, the LOA contribution was statistically significant (within 3σ) only in Vilnius during summer (Table S2), while no data were available for these periods from the marker source apportionment. The marker source apportionment instead attributed the Other-OA mass fraction to 4 factors (Other-OA$_{marker}$): PBOA, as well as to SO_4^{2-}, NO_3^-, and MSA-related secondary organic aerosols (SOA, Fig. S13). The OA concentrations of the factors retrieved from the PM_1 markers source apportionment were obtained by multiplying the factor time series by the sum of the organic markers and OM$_{res}$ contributions to the normalized factor profiles. The PM concentrations from the marker PMF factors are displayed in Fig. 5.

4.4.1 Primary OA sources

Offline-AMS and marker source apportionments provided comparable BBOA estimates, with concentrations agreeing within a 95% confidence interval (Fig. 6). Results revealed that BBOA contributed the largest fraction to the total OM during winter in Preila and Vilnius, while in Rūgšteliškis the largest OA source derived from B-OOA. The average winter BBOA concentration was 1.1 ± 0.8 µg m^{-3} in Rūgšteliškis and 2 ± 1 µg m^{-3} in Vilnius (errors in this section represent the standard deviation of the temporal variability). Overall the average BBOA concentrations were higher at the urban background site of Vilnius and lower at the rural terrestrial site of Rūgšteliškis. Preila showed ~~the highes~~higher values (3 ± 3 µg m^{-3}) driven by the grass burning episode occurred at the beginning of March (Ulevicius et al., 2016). Excluding this episode, the BBOA winter concentration was lower than in Vilnius (1.8 µg m^{-3}). During winter, considering only the samples collected concomitantly, Preila and Vilnius showed well correlated BBOA time series ($R = 0.91$) and significantly positive correlations were observed for also for Preila and Rūgšteliškis ($R = 0.72$) and for Vilnius and Rūgšteliškis ($R = 0.66$) (offline-AMS BBOA time series). These results highlight the effect of regional meteorological conditions on the BBOA daily variability in the south east Baltic region.~~During winter, Preila and Vilnius showed well correlated BBOA time series (R=0.91). These results highlight the important role of regional meteorological conditions on the air quality in the south east Baltic region.~~

By contrast, during summer BBOA concentrations were much lower, with 40% of the points showing statistically not significant contributions within 3σ for the offline-AMS source apportionment and 100% for the marker source apportionment. Between late autumn and early March the offline-AMS source apportionment revealed three simultaneous episodes with high BBOA concentrations at the three stations, while the maker source apportionment which is characterized by lower time resolution did not capture some of these episodes. The first episode occurred between 19 and 25 December 2013 during a cold period with an average daily temperature drop to -9.7 °C as measured at the Rūgšteliškis station (no temperature data were available for the other stations). The third episode occurred between 5 and 10 March 2014 and was associated with an intense grass burning episode localized mostly in the Kaliningrad region (Ulevicius et al., ~~2015~~2016, Dudoitis et al., ~~2015~~2016, Mordas et al., 2016). The episode was not associated with a clear temperature drop, with the highest concentration (14 µg m^{-3}) found at Preila on 10 March 2014, the closest station to the

1 Kaliningrad region. Similarly, at the beginning of February high BBOA concentrations were

2 registered at the three stations, without a clear temperature decrease. Other intense BBOA

3 events were detected but only on a local scale, with intensities comparable to the regional

4 scale episodes. Using the $OM:OC_{BBOA}$ ratio calculated from the HR water-soluble BBOA

5 spectrum (1.88), we estimated the $BBOC_{avg}$ concentrations during the grass burning episode

6 (5-10 March 2014) to span between 0.8 and 7.2 $\mu g\ m^{-3}$. On a daily basis our BBOC

7 concentrations are consistent with the estimated ranges reported by Ulevicius et al.

8 (~~2015~~2016) for non-fossil primary organic carbon (0.6-6.9 $\mu g\ m^{-3}$ during the period under

9 consideration), showing also a high correlation (R=0.98).

10 TEOA estimates obtained by CMB ~~offline AMS~~ and marker-PMF always agreed with each

11 other ~~agreed well with each other, with 99% of the points being not statistically different~~

12 within ~~1σ~~3σ (Fig. 6). The two approaches confirm that TEOA is a minor source (Fig. 6). ~~at all~~

13 ~~three stations with on average higher concentrations in Vilnius (up to 0.8 μg m⁻³), than in~~

14 ~~Preila and Rūgšteliškis (up to 0.2 μg m⁻³).~~ ~~Hopane~~Consistently, hopane concentrations (used

15 in this work as TEOA treacers), ~~concentrations~~ were below detection limits (7 pg m^{-3}) for

16 66% of the collected samples. Similarly to NO_x, hopanes, ~~TEOA, similarly to hopanes and~~

17 ~~NO_x,~~ showed a clear spatial and seasonal variability with higher concentrations in Vilnius

18 during winter, suggesting an accumulation of traffic emissions in a shallower boundary layer

19 (Fig. 3b, NO_x data available only for Vilnius). During the grass burning event, we observed a

20 peak in the total hopane concentration, and therefore also a peak of the estimated TEOA (2.4

21 $\mu g\ m^{-3}$ maximum value). This relatively high concentration is most probably not due to a local

22 increase of TE, but rather due to a regional transport of polluted air masses from neighboring

23 countries (Poland and the Russian Kaliningrad enclave). By assuming an $(OM:OC)_{TEOA}$ ratio

24 of 1.2±0.1 (Aiken et al., 2008, Mohr et al., 2008, Docherty et al., 2011, Setyan et al., 2012),

25 we determined the corresponding organic carbon content (TEOC). Our TEOC concentration

26 was consistent within ~~1σ~~3σ with the average fossil primary OC over the whole episode as

27 estimated by Ulevicius et al. (~~2015~~2016)~~,~~ (0.4-2.1 $\mu g\ m^{-3}$) although on a daily basis the

28 agreement was relatively poor.

29 Overall, offline-AMS source apportionment and marker-PMF returned comparable results for

30 BBOA and similarly the TEOA estimate by markers-PMF and CMB were

31 comparable~~Overall, the offline AMS source apportionment and the marker PMF returned~~

32 ~~comparable results for TEOA and BBOA emissions~~, therefore not surprisingly the two

approaches yielded OA concentrations also for the Other-OA fractions which agreed within ~~1σ~~3σ for 90% of the points (Figure 6). This agreement was better for Rūgšteliškis and Preila (94% and 90%, respectively of the points not statistically different within 1σ), and worse for Vilnius (71% of the points not statistically different within 1σ).

4.4.2 Other-OA sources: offline-AMS and marker-source apportionment comparison

The marker-source apportionment, in comparison to the offline-AMS source apportionment enables resolving well-correlated sources (e.g. BBOA and NO_3^--related SOA) as well as minor sources (e.g. MSA-related SOA and PBOA) because source-specific markers were used as model inputs. By contrast, the offline-AMS source apportionment is capable of resolving OA sources for which no specific markers were available such as LOA, which was separated due to the distinct spatial and temporal trends of some N-containing AMS fragments. We first briefly summarize the Other-OA factor concentrations and their site-to-site differences retrieved by the two techniques; subsequently we compare the two source apportionment results.

The Other-OA$_{offline-AMS}$ factor time series are displayed in Fig. S13. The B-OOA factor showed relatively stable concentrations throughout the year with $0.9\pm0.8_{avg}$ µg m^{-3} during summer and $1.1\pm0.9_{avg}$ µg m^{-3} during winter. Although B-OOA concentrations were relatively stable throughout the year, higher contributions were observed in Preila and Rūgšteliškis compared to Vilnius. The extreme average seasonal concentrations were between 0.8 and 1.3 µg m^{-3} at Rūgšteliškis during fall and winter, between 0.9 and 1.1 µg m^{-3} at Preila during spring and winter, and between 0.4 and 0.6 µg m^{-3} in Vilnius during summer and winter. These values do not evidence clear seasonal trends, but highlight a site-to-site variability which will be further discussed in the following. S-OOA instead was the largest contributor to total OM during summer with an average concentration of 1.2 ± 0.8 µg m^{-3}, always agreeing between sites within a confidence interval of 95% (2 tails t-test). By contrast, during winter the S-OOA concentration dropped to an average value of 0.3 ± 0.2 µg m^{-3}, with 81% of the points not statistically different from 0 µg m^{-3} within 3σ. Finally, the LOA factor showed statistically significant contributions within 3σ only during summer and late spring in Vilnius. Despite its considerable day-to-day variability this ~~fraction~~ factor contributed 1.0 ± 0.8 µg m$^{-3}_{avg}$ in Vilnius during summer.

1   The markers source apportionment instead attributed $85\%_{avg}$ of the Other-OA$_{marker}$ mass to the

2   SO_4^{2-}-related SOA, while NO_3^--related SOA, MSA-related SOA, and PBOA explained

3   respectively $9\%_{avg}$, $5\%_{avg}$ and $1\%_{avg}$ of the Other-OA$_{marker}$ mass (Fig. S13). The SO_4^{2-}-related

4   SOA average concentration was 2.4 µg m^{-3} during summer and 1.7 µg m^{-3} during winter with

5   no significant differences from station to station, suggesting a regional origin of the factor.

6   The NO_3^--related SOA concentration was 0.4 µg m$^{-3}_{avg}$ during winter ~~and,~~ only 0.03_{avg} µg m^{-3},

7   during summer, corresponding to $10\%_{avg}$ and 1% of the OA, respectively. Moreover, the NO_3^-

8   -related SOA during winter showed the highest average concentrations in Vilnius with 0.5 µg

9   m^{-3} and the lowest in Rūgšteliškis with 0.3 µg m$^{-3}_{avg}$. The MSA-related SOA instead

10 manifested the highest concentrations during summer with an average of 0.12 µg m$^{-3}_{avg}$.

11 ~~Higher~~ The highest values were observed during summer at the rural coastal site of Preila

12 where the average concentration was 0.28 µg m$^{-3}_{avg}$ corresponding to $10\%_{avg}$ of the OM.

13 Finally, the PBOA factor exhibited the largest seasonal concentrations during spring at the

14 rural terrestrial site of Rūgšteliškis with an average of 0.05 µg m$^{-3}_{avg}$, while the summer

15 average concentration was 0.02 µg m^{-3} consistent with the low PBOA estimates reported in

16 Bozzetti et al. (2016) for the submicron fraction during summer.

17 Many previous studies reported a source apportionment of organic and inorganic markers

18 concentrations (Viana et al., 2008 and references therein). In these studies SO_4^{2-}, NO_3^-, and

19 NH_4^+ were typically used as tracers for secondary aerosol factors commonly associated with

20 regional background and long-range transport; here we compare the apportionment of the

21 SOA factors obtained from the marker source apportionment and the OOA factors separated

22 by the offline-AMS source apportionment. Moreover, contrasting the two source

23 apportionments may provide insight into the origin of the OOA factors retrieved from the

24 offline-AMS source apportionment, and into the origin of the SOA factors resolved by the

25 offline-AMS source apportionment. To our knowledge an explicit comparison has not yet

26 been reported in the literature.

27

28 ~~Table 2: Pearson correlation coefficients between Other-OA components from offline-AMS~~

29 ~~and marker source apportionment.~~

		Other-OA$_{marker}$			
		~~SO_4^{2-}-related SOA~~	~~MSA-related SOA~~	~~NO_3^--related SOA~~	~~PBOA~~
~~Other~~	~~LOA~~	~~0.33~~	~~0.16~~	~~-0.08~~	~~0.10~~
~~OA$_{offline}$~~	~~B-OOA~~	~~0.70~~	~~0.22~~	~~0.21~~	~~0.47~~

AMS	S-OOA	0.60	0.45	-0.47	0.05

Table 2 reports the correlations between the time series of the Other-OA$_{marker}$ factors and the Other-OA$_{offline-AMS}$ factors (Figs. 6 and S13). These correlations are mostly driven by seasonal trends as none of these sources shows clear spikes except for LOA during summer in Vilnius. Using the correlations coefficients we can identify the mostly related factors from the two source apportionments.

The SO$_4^{2-}$-related SOA explained the largest fraction of the Other-OA$_{marker}$ mass (85%$_{avg}$), and it was the only Other-OA$_{marker}$ factor always exceeding the individual concentrations of B-OOA and S-OOA, indicating that the variability explained by the SO$_4^{2-}$-related SOA in the marker-source apportionment is explained by both OOA factors in the offline-AMS source apportionment. Moreover, the SO$_4^{2-}$-related SOA seasonality seems consistent with the sum of S-OOA and B-OOA with higher concentrations in summer than in winter. This observation suggests that the OOA factors resolved by offline-AMS are mostly of secondary origin and the SO$_4^{2-}$-related SOA, typically resolved by the marker source apportionment, explains the largest fraction of the OOA factors apportioned by offline-AMS which includes both biogenic SOA and aged background OA.

The NO$_3^-$-related SOA and the PBOA were mostly related to the B-OOA factor as they showed higher correlations with B-OOA than with S-OOA (Table 2). The B-OOA factor therefore may explain a small fraction of primary sources (PBOA), which however represents only 0.6%$_{avg}$ of the total OA. The NO$_3^-$-related SOA and the PBOA were mostly related to the B-OOA factor as they showed higher correlations with B-OOA than with S-OOA. The B-OOA factor therefore may explain a small fraction of primary sources (PBOA), which however represents only 0.6%$_{avg}$ of the total OA. In detail, the NO$_3$-related SOA correlation with B-OOA was poor ($R = 0.21$), but the correlation with LOA and S-OOA was negative (Table 2), suggesting that the mass attributed by the markers source apportionment to NO$_3$-related SOA was fully attributed to the B-OOA factor in the offline-AMS source apportionment. This is also confirmed by the fact that the sum of LOA and S-OOA concentrations during winter (when the NO$_3$-related SOA substantially contributes) was much smaller than the NO$_3^-$-related SOA mass, which therefore was attributed to B-OOA.

The NO$_3^-$-related SOA and the PBOA were mostly related to the B-OOA factor as they showed higher correlations with B-OOA than with S-OOA. The B-OOA factor therefore may

explain a small fraction of primary sources (PBOA), which however represents only 0.6%avg of the total OA.

 The MSA-related SOA showed the highest correlation with the S-OOA factor, as the two sources exhibited the highest concentrations during summer, although the MSA-related SOA preferentially contributed at the rural coastal site of Preila. While we already discussed the probable secondary biogenic origin of S-OOA, the correlation with the MSA-related SOA suggests that the S-OOA factor, especially at the rural coastal site of Preila, explains also a large fraction of the marine biogenic SOA. The correlation between the two factors is therefore not surprising as the precursor emissions (dimethyl sulfide, isoprene and terpenes) are strongly related to the temperature leading to higher summer MSA-related SOA and S-OOA concentrations. Assuming all the MSA-related SOA to be explained by the S-OOA factor, we estimate a marine biogenic SOA contribution to S-OOA of 27%avg during summer at Preila, while this contribution is lower at the other stations (12%avg in Rūgšteliškis during summer, 7% in Vilnius during spring, no summer data for Vilnius Fig. S13). As already mentioned, here we assume all the MSA-related SOA to be related to marine secondary biogenic emissions, however other studies also report MSA from terrestrial biogenic emissions (Jardine et al., 2015), moreover a certain fraction of the MSA-related SOA can also be explained by the B-OOA factor. Overall these findings indicate that the terrestrial sources dominate the S-OOA composition, nevertheless the marine SOA sources may represent a non-negligible fraction, especially at the marine site.

Another advantage obtained in coupling the two source apportionment results is the possibility to study the robustness of the factor analyses by evaluating the consistency of the two approaches as we already discussed for the primary OA and Other-OA fractions. Figure S14b displays the ratio between PMF modelled WSOC and measured WSOC for the offline-AMS case. A clear bias between Vilnius and the rural sites can be observed, with a WSOC overestimate of ~5% in Preila and Rūgšteliškis. While this overestimate is negligible for the WSOC mass, it might have significant consequences on single factor concentrations. By contrast, for the markers source apportionment (Fig. S14a), OM residuals are more homogeneous. As we show in Fig. S6, these residuals marginally affect the apportionment of combustion sources, as suggested by the well comparing estimates of BBOA and TEOA using the two methods. Therefore, these residuals are more likely affecting non-combustion sources (LOA, S-OOA and B-OOA). For the common days, the S-OOA concentration is not

statistically different at the different stations during summer (confidence interval of 95%), indicating that the residuals are more likely affecting LOA and B-OOA, which instead show site-to-site differences. Now, the PMF WSOC residuals appear at all seasons, also during periods without significant LOA contribution in Vilnius. Therefore, we conclude that B-OOA is the factor most significantly affected by the difference in the WSOC residuals. We could best assess the residual effects by comparing the B-OOAoffline-AMS with that estimated using the other technique that seem to yield more homogeneous residuals: B-OOAmarker. Here B-OOAmarker is estimated as Other-OAmarkers - LOA - S-OOA. While B-OOAoffline-AMS shows site-to-site differences, B-OOAmarkers did not show statistically different concentrations at all stations within a confidence interval of 95%. Based on these observations, we conclude that observed site-to-site differences in B-OOA concentrations are likely to be related to model uncertainties. Another advantage obtained in coupling the two source apportionment results is the possibility to study the robustness of the factor analyses by evaluating the consistency of the two approaches as we already discussed for the primary OA and Other OA fractions. By subtracting LOA and S-OOA from Other OA$_{marker}$ we can estimate the equivalent B-OOA concentration from the marker source apportionment (B-OOA$_{marker}$). Unlike the B-OOA factor from offline AMS, whose contribution is lower at Vilnius, B-OOA$_{marker}$ did not show statistically different concentrations at all stations within a confidence interval of 95%. This discrepancy could indicate some PMF residual uncertainties or biases not considered in our error estimate for offline AMS and/or markers source apportionments for Vilnius, which could not be detected without coupling the 2 source apportionment approaches.

4.5 fCO$^+$ vs. fCO$_2^+$

Figure 7 displays the water-soluble fCO$^+$ vs. fCO$_2^+$ scatter plot. A certain correlation (R=0.63) is seenobserved, with fCO$^+$ values being systematically lower than fCO$_2^+$ (CO^{2+}:CO$^+$: 1st quartile 1.50, median 1.75, 3rd quartile 2.01), whereas a 1:1 CO$_2^+$:CO$^+$ ratio is assumed in standard AMS/ACSM analyses (Aiken et al., 2008; Canagaratna et al., 2007). Comparing the measured CO$_2^+$:CO$^+$ values for the bulk WSOM and for pure gaseous CO$_2$ might provide insight into the origin of the CO$^+$ fragment in the AMS. The fragmentation of pure gaseous CO$_2$ returned a CO$_2^+$:CO$^+$ ratio of 8.21$_{avg}$ which is significantly higher than our findings for the water-soluble bulk OA (1.75$_{med}$). Assuming thermal decarboxylation of organic acids as

the only source of CO_2^+ does not explain the observed $CO_2^+:CO^+$ ratio of 1.75_{med} and another large source of CO^+ has to be assumed. Therefore, the carboxylic acid decarboxylation can be considered as a minor source of CO^+. suggesting that the WSOM decarboxylation on the AMS vaporizer represents only a minor source of CO^+.

Figure 7b 7a and Fig. 8 show that not only does the water-soluble (WS) $CO_2^+:CO^+$ ratio systematically differ from 1, but it also varies throughout the year with higher $CO_2^+:CO^+$ values associated with warmer temperatures (Fig. 7b7c). The lower $CO_2^+:CO^+$ ratios in winter are primarily due to BB, as the WSBBOA factor profile showed the lowest $CO_2^+:CO^+$ ratio (1.20_{avg}) among all the apportioned WS factors (2.00_{avg} for B-OOA, 2.70_{avg} for S-OOA, and 2.70_{avg} for LOA). We observed a seasonal variation of the $CO_2^+:CO^+$ ratio also for the water-soluble OOA (S-OOA + B-OOA) mass spectral fingerprint. The $CO_2^+:CO^+$ ratio was slightly lower for B-OOA than for S-OOA (2.00_{avg} for B-OOA, 2.70 for S-OOA). Nevertheless, given the low S-OOA relative contribution during winter (Fig. 3), we note that the total OOA showed a slightly lower $CO_2^+:CO^+$ ratio during winter than in summer (Fig. S14S15), indicating that the OOA mass spectral fingerprint evolves over the year, possibly because of different precursor concentrations, and different photochemical activity.

Fig. 7a shows that most of the measured {fCO^+;fCO_2^+} combinations lies within the triangle defined by the BBOA, S-OOA and B-OOA {fCO^+;fCO_2^+} combinations. The LOA factor {fCO^+;fCO_2^+} combination lies within the triangle as well, but is anyways a minor source and thus unlikely to contribute to the CO_2^+/:CO^+ variability. We parameterized the CO^+ variability as a function of the CO_2^+, and $C_2H_4O_2^+$ fragment variabilities using a multi-parameter fit according to Eq. (8). CO_2^+ and $C_2H_4O_2^+$ were chosen as B-OOA and BBOA tracers, respectively, with B-OOA and BBOA being the factors that explained the largest fraction of the fCO^+ variability (85% together).

$$CO^+_i = a \cdot CO_2^+{}_i + b \cdot C_2H_4O_2^+{}_i \qquad (8)$$

Although this parameterization is derived from the WSOM fraction CO_2^+, $C_2H_4O_2^+$, and CO^+ originate from the fragmentation of oxygenated, i.e. mostly water-soluble compounds. Accordingly, this parameterization might also well represent the total bulk OA (as the offline-AMS recoveries of these oxygenated fragments are relatively similar: $R_{CO_2^+}$=0.74, $R_{C_2H_4O_2^+}$=0.61, Daellenbach et al., 2016). Note that this parameterization may represent very well the variation of CO^+ in an environment impacted by BBOA and OOA, but should be used with caution when other sources (such as COA) may contribute to CO^+, CO_2^+ and

69

1    $C_2H_4O_2^+$. In order to check the applicability of this parameterization to a PMF output, we

2   recommend monitoring the CO_2^+ and $C_2H_4O_2^+$ variability explained by the OOA and BBOA

3   factors. In case a large part of the CO_2^+ and $C_2H_4O_2^+$ variability is explained by OOA and

4   BBOA, the parameterization should ~~unlikely~~ return accurate ~~uncertain~~ CO^+ values. The

5   coefficients *a* and *b* of Eq. (8) were determined as 0.52 and 1.39 respectively, while the

6   average fit residuals were estimated to be equal to 10% (Fig. ~~S15~~S16). In contrast,

7   parameterizing CO^+ as proportional to CO_2^+ only (as done in the standard AMS analysis

8   scheme with coefficients updated to the linear fit between CO^+ and CO_2^+ (1.75)) yielded

9    $20\%_{avg}$ residuals, indicating that such a univariate function describes the CO^+ variation less

10   precisely.

11   An alternative parameterization is presented in the SI in which the contribution of moderately

12   oxygenated species (such as S-OOA) to CO^+ was also considered by using $C_2H_3O^+$ as an

13   independent variable. We show that the dependence of CO^+ on $C_2H_3O^+$ is statistically

14   significant (Fig. ~~7b~~7c) as also suggested by the PMF results (S-OOA contributes 12% to the

15   CO^+ variability). However, the parameter relating CO^+ to $C_2H_3O^+$ is negative, because the

16   $CO^+:CO_2^+$ and $CO^+:C_2H_4O_2^+$ ratios are lower in moderately oxygenated species compared to

17   species present in BBOA and B-OOA. While this parameterization captures the variability of

18   CO^+ across the seasons better compared to a 2-parameter fit for the present dataset, it may be

19   more prone to biases in other environments due to the known contributions of other factors to

20   $C_2H_3O^+$. For example, cooking-influenced organic aerosol (COA) often accounts for a

21   significant fraction of $C_2H_3O^+$. For ambient datasets we propose the use of CO_2^+ and $C_2H_4O_2^+$

22   only, which may capture less variation but is also less prone to biases. Although our results

23   suggest that the available CO^+ and O:C estimates (Aiken et al., 2008; Canagaratna et al.,

24   2015) may not well capture the CO^+ variability, our CO^+ parameterization should not be

25   applied to calculate the O:C ratios or recalculate the OA mass from AMS datasets, as those

26   are calibrated assuming a standard fragmentation table (i.e. $CO_2^+ = CO^+$).

27   In a recent work, Canagaratna et al. (2015) reported the Ar nebulization of water soluble

28   single compounds to study the HR-AMS mass spectral fingerprints in order to improve the

29   calculation of O:C and OM:OC ratios. Following the same procedure, we nebulized a subset

30   of the same standard compounds including malic acid, azalaic acid, citric acid, tartaric acid,

31   cis-pinonic acid, and D(+)-mannose. We obtained comparable $CO_2^+:CO^+$ ratios (within 10%)

32   to those of Canagaratna et al. (2015) for all the analyzed compounds, highlighting the

comparability of results across different instruments. With the exception of some multifunctional compounds (citric acid, malic acid tartaric acid, ketobutyric acid, hydroxyl methylglutaric acid, pyruvic acid, oxaloacetic acid, tartaric acid, oxalic acid and malonic acid), the water-soluble single compounds analyzed by Canagaratna et al. (2015) mostly showed CO_2^+:CO^+ ratios <1, systematically lower than the CO_2^+:CO^+ ratios measured for the bulk WSOM in Lithuania (1st quartile 1.50, median 1.75, 3rd quartile 2.01), which represents a large fraction of the total OM (bulk EE: median = 0.59, 1st quartile = 0.51, 3rd quartile = 0.72). Considering the relatively high extraction efficiency, and considering that the CO^+ and $CO_2^{\pm}$ fragmentation precursors tend to be more water soluble than the bulk OA, the aforementioned compounds could be representative of a large part of the CO^+ and CO_2^+ fragmentation precursors. ~~With the exception of some multifunctional compounds, the water soluble single compounds analyzed by Canagaratna et al. (2015) mostly showed CO_2^+:CO^+ ratios <1, systematically lower than the CO_2^+:CO^+ ratios measured for the bulk WSOM in Lithuania (1st quartile 1.50, median 1.75, 3rd quartile 2.01), which represents a large fraction of the total OM (bulk EE: median = 0.59, 1st quartile = 0.51, 3rd quartile = 0.72).~~ This indicates that the selection of appropriate reference compounds for ambient OA is non-trivial, and the investigation of multifunctional compounds is of high importance.

5   Conclusions

PM_1 filter samples were collected over an entire year (November 2013 to October 2014) at three different stations in Lithuania. Filters were analyzed by water extraction followed by nebulization of the liquid extracts and subsequent measurement of the generated aerosol with an HR-ToF-AMS (Daellenbach et al., 2016). For the first time, the nebulization step was conducted in Ar, enabling direct measurement of the CO^+ ion, which is typically masked by N_2^+ in ambient air and assumed to be equal to CO_2^+ (Aiken et al., 2008). CO_2^+:CO^+ values >1 were systematically observed, with a mean ratio of 1.7±0.3. This is likely an upper limit for ambient aerosol, as only the water-soluble OM fraction is measured by the offline-AMS technique. CO^+ concentrations were parameterized as a function of CO_2^+, and $C_2H_4O_2^+$, and this two-variable parameterization showed a superior performance to a parameterization based on CO_2^+ alone, because CO^+ and CO_2^+ show different seasonal trends.

PMF analysis was conducted on both the offline-AMS data described above and a set of molecular markers together with total OM. Biomass burning was found to be the largest OM

source in winter, while secondary OA was largest in summer. However, higher concentrations of primary anthropogenic sources (biomass burning and hopanes here used as traffic markerstraffic and biomass burning) were found at the urban background station of Vilnius. The offline-AMS and marker-based analyses also identified local emissions and primary biological particles, respectively, as factors with low overall but episodically important contributions to PM. Both methods showed traffic exhaust emissions to be only minor contributors to the total OM; which is not surprising given the distance of the three sampling stations from busy roads.

The two PMF analyses apportioned SOA to sources in different ways. The offline-AMS data yielded factors related to regional background (B-OOA) and temperature-driven (likely biogenic-influenced) emissions (S-OOA), while the marker-PMF yielded factors related to nitrate, sulfate, and MSA. For the offline-AMS PMF, S-OOA was the dominant factor in summer and showed a positive exponential correlation with the average daily temperature, similar to the behavior observed by Leaitch et al. (2011) in a Canadian boreal forest. Combining the two source apportionment techniques suggests that the S-OOA factor includes contributions from both terrestrial and marine secondary biogenic sources, while only small PBOA contributions to submicron OOA factors are possible. The analysis highlights the importance of regional meteorological conditions on air pollution in the southeastern Baltic region, as evidenced by simultaneous high BBOA levels at the three stations during three different episodes in winter and by statistically similar S-OOA concentrations across the three stations during summer.

Acknowledgements

References

Aiken, A. C., DeCarlo, P. F., Kroll, J. H., Worsnop, D. R., Huffmann, J. A., Docherty, K. S., Ulbrich, I. M., Mohr, C., Kimmel, J. R., Sueper, D., Sun, Y., Zhang, Q., Trimborn, A., Northway, M., Ziemann, P. J., Canagaratna, M. R., Onasch, T. B., Alfarra, M. R., Prevot, A. S. H., Dommen, J., Duplissy, J., Metzger, A., Baltensperger, U., and Jimenez J. L. O/C and OM:OC ratios of primary, secondary, and ambient organic aerosols with high-resolution time-of-flight aerosol mass spectrometry. Environ. Sci. Technol. 42, 4478-4485, 2008.

Aksoyoglu, S., Keller, J., Barmpadimos, I., Oderbolz, D., Lanz, V. A., Prévôt, A. S. H., and Baltensperger U.: Aerosol modelling in Europe with a focus on Switzerland during summer and winter episodes, Atmos. Chem. Phys., 11, 7355–7373, 2011.

Aksoyoglu, S., Keller, J., Ciarelli, G., Prévôt, A. S. H., and Baltensperger, U.: A model study on changes of European and Swiss particulate matter, ozone and nitrogen deposition between 1990 and 2020 due to the revised Gothenburg protocol, Atmos. Chem. Phys., 14, 13081-13095, doi:10.5194/acp-14-13081-2014, 2014.

Alfarra, M. R., Prévôt, A. S. H., Szidat, S., Sandradewi, J., Weimer, S., Lanz, V. A., Schreiber, D., Mohr, M., and Baltensperger, U.: Identification of the mass spectral signature of organic aerosols from wood burning emissions, Environ. Sci. Technol., 41, 5770–5777, 2007.

Allan, J. D., Delia, A. E., Coe, H., Bower, K. N., Alfarra, M. R., Jimenez, J. L., Middlebrook, A. M., Drewnick, F., Onasch, T. B., and Canagaratna, M. R.: A generalized method for the extraction of chemically resolved mass spectra from Aerodyne aerosol mass spectrometer data, J. Aerosol Sci. 35 , 909-922, 2004.

Allan, J. D., Jimenez, J. L., Williams, P. I., Alfarra, M. R., Bower, K. N., Jayne, J. T., Coe, H., and Worsnop, D. R.: Quantitative sampling using an Aerodyne aerosol mass spectrometer: 1. Techniques of data interpretation and error analysis, J. Geophys. Res.-Atmos., 108, 4090, 2003.

Baklanov, A., Schlünzen, K., Suppan, P., Baldasano, J., Brunner, D., Aksoyoglu, S., Carmichael, G., Douros, J., Flemming, J., Forkel, R., Galmarini, S., Gauss, M., Grell, G., Hirtl, M., Joffre, S., Jorba, O., Kaas, E., Kaasik, M., Kallos, G., Kong, X., Korsholm, U., Kurganskiy, A., Kushta, J., Lohmann, U., Mahura, A., Manders-Groot, A., Maurizi, A., Moussiopoulos, N., Rao, S. T., Savage, N., Seigneur, C., Sokhi, R. S., Solazzo, E.,

Solomos, S., Sørensen, B., Tsegas, G., Vignati, E., Vogel, B., and Zhang, Y.: Online coupled regional meteorology chemistry models in Europe: current status and prospects, Atmos. Chem. Phys., 14, 317-398, doi:10.5194/acp-14-317-2014, 2014.

Besombes, J.-L., Maître, A., Patissier, O., Marchand, N., Chevron, N., Stoklov, M., Masclet, P.: Particulate PAHs observed in the surrounding of a municipal incinerator. Atmos. Environ. 35, 6093–6104, 2001.

Birch, M. E. and Cary, R. A.: Elemental carbon-based method for monitoring occupational exposures to particulate diesel exhaust, Aerosol Sci. and Tech., 25, 221–241, 1996.

Bozzetti, C., Daellenbach, K., R., Hueglin, C., Fermo, P., Sciare, J., Kasper-Giebl, A., Mazar, Y., Abbaszade, G., El Kazzi, M., Gonzalez, R., Shuster Meiseles, T., Flasch, M., Wolf, R., Křepelová, A., Canonaco, F., Schnelle-Kreis, J., Slowik, J. G., Zimmermann, R., Rudich, Y., Baltensperger, U., El Haddad, I., and Prévôt, A. S. H.: Size-Resolved Identification, Characterization, and Quantification of Primary Biological Organic Aerosol at a European Rural Site, Environ. Sci. Technol., doi: 10.1021/acs.est.5b05960, 2016.

Bressi, M., Sciare, J., Ghersi, V., Mihalopoulos, N., Petit, J.-E., Nicolas, J. B., Moukhtar, S., Rosso, A., Féron, A., Bonnaire, N., Poulakis, E., and Theodosi, C.: Sources and geographical origins of fine aerosols in Paris (France), Atmos. Chem. Phys., 14, 8813–8839, 2014.

Brown, S. G., Eberly, S., Paatero, P., and Norris, G. A., Methods for estimating uncertainty in PMF solutions: Examples with ambient air and water quality data and guidance on reporting PMF results, Sci. Tot. Environ. 518-519, 626-635, 2015.

Bruns, E. A., Krapf, M., Orasche, J., Huang, Y., Zimmermann, R., Drinovec, L., Močnik, G., El-Haddad, I., Slowik, J. G., Dommen, J., Baltensperger, U. and Prévôt, A. S. H.: Characterization of primary and secondary wood combustion products generated under different burner loads, Atmos. Chem. Phys., 15, 2825–2841, 2015.

Budisulistiorini, S. H., Canagaratna, M. R., Croteau, P. L., Marth, W. J., Baumann, K., Edgerton, E. S., Shaw, S. L., Knipping, E. M., Worsnop, D. R., Jayne, J. T., Gold, A., and Surratt, J. D.: Real-Time Continuous Characterization of Secondary Organic Aerosol Derived from Isoprene Epoxydiols in Downtown Atlanta, Georgia, Using the Aerodyne Aerosol Chemical Speciation Monitor, Environ Sci Technol, 47, 5686-5694, Doi 10.1021/Es400023n, 2013.

Formatted: Font color: Auto

1   Byčenkienė, S., Ulevicius, V., Plauškaitė, K., Bozzetti, C., Fröhlich, R., Mordas, G., Slowik,

2   J. G., El Haddad, I., Canonaco, F., and Prévôt A. S. H.: Source apportionment of the

3   carbonaceous aerosols during wintertime over urban environment, *in prep*.

4   Canagaratna, M. R., Jayne, J. T., Jimenez, J. L., Allan, J. D., Alfarra, M. R., Zhang, Q.,

5   Onasch, T. B., Drewnick, F., Coe, H., Middlebrook, A., Delia, A., Williams, L. R., Trimborn,

6   A. M., Northway, M. J., DeCarlo, P. F., Kolb, C. E., Davidovits, P. and Worsnop, D. R.:

7   Chemical and microphysical characterization of ambient aerosols with the Aerodyne aerosol

8   mass spectrometer, Mass Spectrom. Rev. 26:185-222, 2007.

9   Canagaratna, M. R., Jimenez, J. L., Kroll, J. H., Chen, Q., Kessler, S. H., Massoli, P.,

10 Hildebrandt Ruiz, L., Fortner, E., Williams, L. R., Wilson, K. R., Surratt, J. D.,

11 Donahue, N. M., Jayne, J. T., and Worsnop, D. R.: Elemental ratio measurements of organic

12 compounds using aerosol mass spectrometry: characterization, improved calibration, and

13 implications, Atmos. Chem. Phys., 15, 253-272, doi:10.5194/acp-15-253-2015, 2015.

14 Canonaco, F., Crippa, M., Slowik, J. G., Baltensperger, U., and Prévôt, A. S. H.: SoFi, an

15 IGOR-based interface for the efficient use of the generalized multilinear engine (ME-2) for

16 the source apportionment: ME-2 application to aerosol mass spectrometer data, Atmos. Meas.

17 Tech., 6, 3649-3661, 2013.

18 Canonaco, F., Slowik, J. G., Baltensperger, U., and Prévôt, A. S. H.: Seasonal differences in

19 oxygenated organic aerosol composition: implications for emissions sources and factor

20 analysis. Atmos. Chem. Phys. 15, 6993-7002, 2015.

21 Cavalli, F., Viana, M., Yttri, K. E., Genberg, J., and Putaud, J. P.: Toward a standardised

22 thermal-optical protocol for measuring atmospheric organic and elemental carbon: the

23 EUSAAR protocol, Atmos. Meas. Tech., 3, 79-89, 2010.

24 Chow, J., Watson, J., Ashbaugh, L. L., and Magliano, K. L.: Similarities and differences in

25 PM10 chemical source profiles for geological dust from the San Joaquin Valley, California.

26 Atmos. Environ. 37, 1317-1340, 2003.

27 Crippa, M., Canonaco, F., Lanz, V. A., Äijälä, M., Allan, J. D., Carbone, S., Capes, G.,

28 Ceburnis, D., Dall'Osto, M., Day, D. A., DeCarlo, P. F., Ehn, M., Eriksson, A., Freney, E.,

29 Hildebrandt Ruiz, L., Hillamo, R., Jimenez, J. L., Junninen, H., Kiendler-Scharr, A.,

30 Kortelainen, A. M., Kulmala, M., Laaksonen, A., Mensah, A. A., Mohr, C., Nemitz, E.,

31 O'Dowd, C., Ovadnevaite, J., Pandis, S. N., Petäjä, T., Poulain, L., Saarikoski, S., Sellegri, K.,

Swietlicki, E., Tiitta, P., Worsnop, D. R., Baltensperger, U., and Prévôt, A. S. H.: Organic aerosol components derived from 25 AMS data sets across Europe using a consistent ME-2 based source apportionment approach, Atmos. Chem. Phys., 14, 6159–6176, 2014.

Crippa, M., El Haddad, I., Slowik, J. G., DeCarlo, P.F., Mohr, C., Heringa, M. F., Chirico, R., Marchand, N., L., Sciare, J., Baltensperger, U., and Prévôt, A. S. H.: Identification of marine and continental aerosol sources in Paris using high resolution aerosol mass spectrometry, J. Geophys. Res., 118, 1950-1963, 2013.

Daellenbach, K. R., Bozzetti, C., Krepelova, A., Canonaco, F., Huang, R.-J., Wolf, R., Zotter, P., Crippa, M., Slowik, J., Zhang, Y., Szidat, S., Baltensperger, U., Prévôt, A. S. H., and El Haddad, I.: Characterization and source apportionment of organic aerosol using offline aerosol mass spectrometry, Atmos. Meas. Tech., 9, 23-39, 2016.

Davison, A. C. and Hinkley, D. V.: Bootstrap Methods and Their Application, Cambridge University Press, Cambridge, UK, 582 pp., 1997.

DeCarlo, P. F., Kimmel, J. R., Trimborn, A., Northway, M. J., Jayne, J. T., Aiken, A. C., Gonin, M., Fuhrer, K., Horvath, T., Docherty, K. S., Worsnop, D. R., and Jimenez, J. L.: Field-deployable, high-resolution, time-of-flight aerosol mass spectrometer, Anal. Chem., 78, 8281–8289, 2006.

Dockery, D. W., Luttmann-Gibson, H., Rich, D. Q., Link, M. S., Mittleman, M. A., Gold, D. R., Koutrakis, P., Schwartz, J. D., and Verrier, R. L.: Association of air pollution with increased incidence of ventricular tachyarrhythmias recorded by implanted cardioverter defibrillators, Environ. Health Perspect. 113:670-674, 2005.

Docherty, K. S., Aiken, A. C., Huffman, J. A., Ulbrich, I. M., DeCarlo, P. F., Sueper, D., Worsnop, D. R., Snyder, D. C., Peltier, R. E., Weber, R. J., Grover, B. D., Eatough, D. J., Williams, B. J., Goldstein, A. H., Ziemann, P. J., and Jimenez, J. L.: The 2005 Study of Organic Aerosols at Riverside (SOAR-1): instrumental intercomparisons and fine particle composition, Atmos. Chem. Phys., 11, 12387-12420, doi:10.5194/acp-11-12387-2011, 2011.

Dudoitis, V., Byčenkienė, S., Plauškaitė, K., Bozzetti, C., Fröhlich, R., Mordas, G., and Ulevicius V.: Spatial distribution of carbonaceous aerosol in the southeastern Baltic region (event of grass fires), Acta Geophys., 64, 711-731, 2016.

Dudoitis, V., Byčenkienė, S., Plauškaitė, K., Bozzetti, C., Fröhlich, R., Mordas, G., and Ulevicius V.: Spatial distribution of carbonaceous aerosol in the southeastern Baltic region (event of grass fires), Acta Geophys., *in press*, 2015.

El Haddad, I., D'Anna, B., Temime-Roussel, B., Nicolas, M., Boreave, A., Favez, O., Voisin, D., Sciare, J., George, C., Jaffrezo, J.-L., Wortham, H., and Marchand, N.: Towards a better understanding of the origins, chemical composition and aging of oxygenated organic aerosols: case study of a Mediterranean industrialized environment, Marseille, Atmos. Chem. Phys., 13, 7875-7894, doi:10.5194/acp-13-7875-2013, 2013.

El Haddad, I., Marchand, N., Dron, J., Temime-Roussel, B., Quivet, E., Wortham, H., Jaffrezo, J. L., Baduel, C., Voisin, D., Besombes, J. L., and Gille, G.: Comprehensive primary particulate organic characterization of vehicular exhaust emissions in France, Atmos. Environ., 43, 6190–6198, 2009.

Elser, M., Bozzetti, C., El-Haddad, I., Maasikmets, M., Teinemaa, E., Richter, R., Wolf, R., Slowik, J. G., Baltensperger, U., and Prévôt, A. S. H.: Urban increments of gaseous and aerosol pollutants and their sources using mobile aerosol mass spectrometry measurements, Atmos. Chem. Phys. Discuss., doi:10.5194/acp-2016-31, 2016.

Elser, M., Huang, R.-J., Wolf, R., Slowik, J. G., Wang, Q., Canonaco, F., Li, G., Bozzetti, C., Daellenbach, K. R., Huang, Y., Zhang, R., Li, Z., Cao, J., Baltensperger, U., El-Haddad, I., and Prévôt, A. S. H.: New insights into PM2.5 chemical composition and sources in two major cities in China during extreme haze events using aerosol mass spectrometry, Atmos. Chem. Phys., 16, 3207-3225, doi:10.5194/acp-16-3207-2016, 2016.

Fraser, M. P., Cass, G. R., and Simoneit, B. R. T.: Gas-phase and particle-phase organic compounds emitted from motor vehicle traffic in a Los Angeles roadway tunnel, Environ. Sci. Technol. 14, 2051-2060, 1998.

Fröhlich, R., Cubison, M. J., Slowik, J. G., Bukowiecki, N., Prevot, A. S. H., Baltensperger, U., Schneider, J., Kimmel, J. R., Gonin, M., Rohner, U., Worsnop, D. R. and Jayne J. T.: The ToF-ACSM: a portable aerosol chemical speciation monitor with TOFMS detection, Atmos. Meas. Tech., 6, 3225-3241, 2013.

Golly, B., Brulfert, G., Berlioux G., Jaffrezo J.-L., Besombes, J.-L.: Large chemical characterisation of PM10 emitted from graphite material production: Application in source apportionment, Sci. Tot. Environ., 538, 634–643, 2015.

1 Guenther, A., Karl, T., Harley, P., Wiedinmyer, C., Palmer, P. I., and Geron, C.: Estimates of
2 global terrestrial isoprene emissions using MEGAN (Model of Emissions of Gases and
3 Aerosols from Nature), Atmos. Chem. Phys., 6, 3181-3210, doi:10.5194/acp-6-3181-2006,
4 2006.

5 He, L.-Y., Hu, M., Zhang, Y.-H., Huang, X.-F. and Yao, T.-T: Chemical characterization of
6 fine particles from on-road vehicles in the Wutong tunnel in Shenzhen, China, Chemosphere
7 62, 1565-1573, 2006.

8 He, L.-Y., Hu, M., Zhang, Y.-H., Huang, X.-F., and Yao, T.-T. Fine particle emissions from
9 onroad vehicles in the Zhujiang tunnel, China, Environ. Sci. Technol., 42, 4461-4466, 2008.

10 Herich, H., Gianini, M. F. D., Piot, C., Močnik, G., Jaffrezo, J. L., Besombes, J. L., Prévôt, A.
11 S. H., and Hueglin, C.: Overview of the impact of wood burning emissions on carbonaceous
12 aerosols and PM in large parts of the Alpine region, Atmos. Environ., 89, 64–75,
13 doi:10.1016/j.atmosenv.2014.02.008, 2014.

14 Huang, R.-J., Zhang, Y., Bozzetti, C., Ho, K.-F., Cao, J., Han, Y., Dällenbach, K. R., Slowik,
15 J. G., Platt, S. M., Canonaco, F., Zotter, P., Wolf, R., Pieber, S. M., Bruns, E. A., Crippa, M.,
16 Ciarelli, G., Piazzalunga, A., Schwikowski, M., Abbaszade, G., Schnelle-Kreis, J.,
17 Zimmermann, R., An, Z., Szidat, S., Baltensperger, U., Haddad, I. E., and Prévôt, A. S. H.:
18 High secondary aerosol contribution to particulate pollution during haze events in China,
19 Nature, 514, 2014.

20 Jaffrezo, J.-L., Aymoz, G., Delaval, C., and Cozic J.: Seasonal evolution of the soluble
21 fraction of particulate organic carbon in Alpine Valleys. Atmos. Chem. Phys., 5, 2809-2821,
22 2005.

23 Jaffrezo, J. L., Calas, T., and Bouchet, M.: Carboxylic acids measurements with ionic
24 chromatography, Atmos. Environ., 32, 2705–2708, 1998.

25 Jardine, K., Yañez-Serrano, A. M., Williams, J., Kunert, N., Jardine, A., Taylor, T., Abrell,
26 L., Artaxo, P., Guenther, A., Hewitt, C. N., House, E., Florentino, A. P., Manzi, A., Higuchi,
27 N., Kesselmeier, J., Behrendt, T, Veres, P. R., Derstroff, B., Fuentes, J. D., Martin, S. T., and
28 Andreae, M. O.: Dimethyl Sulfide in the Amazon Rain Forest, Global Biogeochem. Cy., 29,
29 19-32, 2015.

30 Klein, F., Platt, S. M., Farren, N. J., Detournay, A., Bruns, E. A., Bozzetti, C., Daellenbach,
31 K. R., Kilic, D., Kumar, N. K., Pieber, S. M., Slowik, J. G., Temime-Roussel, B., Marchand,

N., Hamilton, J. F., Baltensperger, U., Prévôt, A. S. H., and El Haddad, I.: Characterization of gas-phase organics using proton transfer reaction time-of-flight mass spectrometry: cooking emissions, Environ. Sci. Technol., 50, 1243–1250, 2016.

Laden, F., Neas, L. M., Dockery, D. W., and Schwartz, J.: Association of fine particulate matter from different sources with daily mortality in six US cities, Environ. Health Perspect. 108:941-947, 2000.

Lanz, V. A., Alfarra, M. R., Baltensperger, U., Buchmann, B., Hueglin, C., and Prévôt, A. S. H.: Source apportionment of submicron organic aerosols at an urban site by factor analytical modelling of aerosol mass spectra, Atmos. Chem. Phys., 7, 1503-1522, doi:10.5194/acp-7-1503-2007, 2007.

Lanz, V. A., Prévôt, A. S. H., Alfarra, M. R., Weimer, S., Mohr, C., DeCarlo, P. F., Gianini, M. F. D., Hueglin, C., Schneider, J., Favez, O., D'Anna, B., George, C., and Baltensperger, U.: Characterization of aerosol chemical composition with aerosol mass spectrometry in Central Europe: an overview, Atmos. Chem. Phys., 10, 10453–10471, 2010.

Leaitch, W. R. Macdonald, A. M., Brickell, P. C., Liggio, J., Sjostedt, S. J., Vlasenko, A., Bottenheim, J. W., Huang, L., Li, S.-M., Liu, P. S. K., Toom-Sauntry, D., Hayden, K. A., Sharma, S., Shantz, N. C., Wiebe H. A., Zhang, W., Abbatt, J. P. D., Slowik, J. G., Chang, Rachel, Y.-W., Russell, L. M., Schwartz, R. E., Takahama, S., Jayne, J. T., Ng, N. L.: Temperature response of the submicron organic aerosol from temperate forests, Atmos. Environ., 45, 6696-6704, 2011.

Lee, A. K. Y., Herckes, P., Leaitch, W. R., Macdonald, A. M., and Abbatt, J. P. D.: Aqueous OH oxidation of ambient organic aerosol and cloud water organics: Formation of highly oxidized products, Geoph. Res. Lett., 38, L11 805, 2011.

Li, S.M., Talbot, R.W., Barrie, L.A., Harriss, R.C., Davidson, C.I. and Jaffrezo, J.-L.: Seasonal and geographic variations of methanesulfonic acid in the Arctic troposphere, Atmos. Environ., 27A, 3011-3024, 1993.

Lohmann, U., Broekhuizen, K., Leaitch, R., Shantz, N., and Abbatt, J.: How efficient is cloud droplet formation of organic aerosols?, Geophys. Res. Lett. 31, L05108, 2004.

Manish K. S., Subramanian, R., Rogge, W. F., and Robinson, A. L.: Sources of organic aerosol: Positive matrix factorization of molecular marker data and comparison of results from different source apportionment models, Atmos. Environ., 41, 9353-9369, 2007.

Field Code Changed

Field Code Changed

McMeeking, G. R., Bart, M., Chazette, P., Haywood, J. M.,, Hopkins, J. R., McQuaid, J. B., Morgan, W. T., Raut, J.-C., Ryder, C. L., Savage, N., Turnbull, K., and Coe, H.: Airborne measurements of trace gases and aerosols over the London metropolitan region, Atmos. Chem. Phys., 12, 5163–5187, 2012.

Mihara, T. and Mochida, M.: Characterization of solvent-extractable organics in urban aerosols based on mass spectrum analysis and hygroscopic growth measurement, Envir. Sci. Tech., 45, 9168–9174, 2011.

Minguillón, M. C., Perron, N., Querol, X., Szidat, S., Fahrni, S. M., Alastuey, A., Jimenez, J. L., Mohr, C., Ortega, A. M., Day, D. A., Lanz, V. A., Wacker, L., Reche, C., Cusack, M., Amato, F., Kiss, G., Hoffer, A., Decesari, S., Moretti, F., Hillamo, R., Teinila, K., Seco, R., Penuelas, J., Metzger, A., Schallhart, S., Muller, M., Hansel, A., Burkhart, J. F., Baltensperger, U., and Prevot, A. S. H.: Fossil versus contemporary sources of fine elemental and organic carbonaceous particulate matter during the DAURE campaign in Northeast Spain, Atmos. Chem. Phys., 11, 12067-12084, 2011.

Mohr, C., DeCarlo, P. F., Heringa, M. F., Chirico, R., Slowik, J. G., Richter, R., Reche, C., Alastuey, A., Querol, X., Seco, R., Penuelas, J., Jimenez, J. L., Crippa, M., Zimmermann, R., Baltensperger, U., and Prevot, A. S. H.: Identification and quantification of organic aerosol from cooking and other sources in Barcelona using aerosol mass spectrometer data, Atmos. Chem. Phys., 12, 1649-1665, 2012.

Mordas, G., Plauškaitė, K., Prokopčiuk, N., Dudoitis, V., Bozzetti, C. and Ulevicius, V.: Observation of new particle formation on Curonian Spit located between continental Europe and Scandinavia, J Aerosol Sci, 97, 38-55, 2016.

Ng, N. L., Herndon, S. C., Trimborn, A., Canagaratna, M. R., Croteau, P. L., Onasch, T. B. Sueper, D., Worsnop, D. R., Zhang, Q., Sun, Y. L. and Jayne, J. T.: An Aerosol Chemical Speciation Monitor (ACSM) for routine monitoring of the composition and mass concentrations of ambient aerosol, Aerosol Sci. Tech., 45, 770-784, 2011.

Paatero, P.: Least squares formulation of robust non-negative factor analysis, Chemom. Intell. Lab. Syst., 37, 23–35, 1997.

Paatero, P.: The multilinear engine - A table-driven, least squares program for solving multilinear problems, including the n-way parallel factor analysis model, J. Comput. Graph. Stat., 8, 854-888, 1999.

Formatted: Font color: Auto

80

1 Paatero, P. and Tapper, U.: Positive matrix factorization - a nonnegative factor model with
2 optimal utilization of error-estimates of data values, Environmetrics, 5, 111-126, 1994.

3 Rocke, D. M., and Lorenzato, S.: A two-component model for measurement error in
4 analytical chemistry, Technometrics, 37, 176-184, 1995.

5 Rutter, A. P., Snyder, D. C., Schauer, J. J., DeMinter, J. and Shelton, B.: Sensitivity and bias
6 of molecular marker-based aerosol source apportionment models to small contributions of
7 coal combustion soot, Environ. Sci. Technol., 43, 7770-7777, 2009.

8 Schauer, J. J., Kleeman, M. J., Cass, G. R., and Simoneit, B. T.: Measurement of emissions
9 from air pollution sources. 3. C1-C29 organic compounds from fireplace combustion of
10 wood, Environ. Sci. Technol., 35, 1716-1728, 2001.

11 Schwarze, P. E., Ovrevik, J., Lag, M., Refsnes, M., Nafstad, P., Hetland, R. B., and Dybing,
12 E.: Particulate matter properties and health effects: consistency of epidemiological and
13 toxicological studies, Hum. Exp. Toxicol. 25, 559-579, 2006.

14 Setyan, A., Zhang, Q., Merkel, M., Knighton, W. B., Sun, Y., Song, C., Shilling, J. E.,
15 Onasch, T. B., Herndon, S. C., Worsnop, D. R., Fast, J. D., Zaveri, R. A., Berg, L. K.,
16 Wiedensohler, A., Flowers, B. A., Dubey, M. K., and Subramanian R.: Characterization of
17 submicron particles influenced by mixed biogenic and anthropogenic emissions using high-
18 resolution aerosol mass spectrometry: results from CARES, Atmos. Chem. Phys., 12, 8131-
19 8156, 2012.

20 Subramanian, R., Donahue, N. M., Bernardo-Bricker, A., Rogge, W. F., and Robinson, A. L.:
21 Contribution of motor vehicle emissions to organic carbon and fine particle mass in
22 Pittsburgh, Pennsylvania: Effects of varying source profiles and seasonal trends in ambient
23 marker concentrations, Atmos. Environ., 40, 8002-8019, 2006.

24 Subramanian, R., Donahue, N. M., Bernardo-Bricker, A., Rogge, W. F., and Robinson, A. L.:
25 Insights into the primary-secondary and regional-local contributions to organic aerosol and
26 PM $_{2.5}$ mass in Pittsburgh, Pennsylvania, Atmos. Environ., 41, 7414-7433, 2007.

27 Sun, Y., Zhang, Q., Zheng, M., Ding, X., Edgerton, E. S., and Wang, X.: Characterization and
28 source apportionment of water-soluble organic matter in atmospheric fine particles (PM2.5)
29 with High-Resolution Aerosol Mass Spectrometry and GC-MS, Envir. Sci. Tech., 45, 4854–
30 4861, 2011.

Ulbrich, I. M., Canagaratna, M. R., Zhang, Q., Worsnop, D. R., and Jimenez, J. L.: Interpretation of organic components from positive matrix factorization of aerosol mass spectrometric data, Atmos. Chem. Phys., 9, 2891-2918, 2009.

Ulevicius, V., Byčenkienė, S., Bozzetti, C., Vlachou, A., Plauškaitė, K., Mordas, G., Dudoitis, V., Abbaszade, G., Remeikis, V., Garbaras, A., Masalaite, A., Blees, J., Fröhlich, R., Dällenbach, K. R., Canonaco, F., Slowik, J. G., Dommen, J., Zimmermann, R., Schnelle-Kreis, J., Salazar, G. A., Agrios, K., Szidat, S., El Haddad, I., and Prévôt, A. S. H.: Fossil and non-fossil source contributions to atmospheric carbonaceous aerosols during extreme spring grassland fires in Eastern Europe. Atmos. Chem. Phys., 16, 5513-5529, 2016.

Viana, M., Kuhlbusch, T. A. J., Querol, X., Alastuey, A., Harrison, R. M., Hopke, P. K., Winiwarter, W., Vallius, M., Szidat, S., Prévôt, A. S. H., Hueglin, C., Bloemen, H., Wåhlin, P., Vecchi, R., Miranda, A. I., Kasper-Giebl, A., Maenhaut, W., and Hitzenberger, R.: Source apportionment of particulate matter in Europe: a review of methods and results, J. Aerosol Sci., 39, 827–849, doi:10.1016/j.jaerosci.2008.05.007, 2008.

Waked, A., Favez, O., Alleman, L. Y., Piot, C., Petit, J. E., Delaunay, T., Golly, B., Besombes, J.-L., Jaffrezo, J.-L., and Leoz-Garziandia, E.: Source apportionment of PM10 in an urban site using a PMF model applied on inorganic and organic chemical species. Atmos. Chem. Phys., 14, 3325-3346, 2014.

Xu, L., Guo, H., Boyd, C. M., Klein, M., Bougiatioti, A., Cerully, K. M., Hite, J. R., Isaacman-VanWertz, G., Kreisberg, N. M., Knote, C., Olson, K., Koss, A., Goldstein, A. H., Hering, S. V., de Gouw, J., Baumann, K., Lee, S.-H., Nenes, A., Weber, R. J., and Ng, N. L.: Effects of anthropogenic emissions on aerosol formation from isoprene and monoterpenes in the southeastern United States, Proceedings of the National Academy of Sciences, 112, 37-42, 10.1073/pnas.1417609112, 2015.

Xu, L., Williams, L. R., Young, D. E., Allan, J. D., Coe, H., Massoli, P., Fortner, E., Chhabra, P., Herndon, S., Brooks, W. A., Jayne, J. T., Worsnop, D. R., Aiken, A. C., Liu, S., Gorkowski, K., Dubey, M. K., Fleming, Z. L., Visser, S., Prévôt, A. S. H., and Ng, N. L.: Wintertime aerosol chemical composition, volatility, and spatial variability in the greater London area, Atmos. Chem. Phys., 16, 1139-1160, 10.5194/acp-16-1139-2016, 2016.

Formatted: Font color: Auto

1 Zhang, Q., Jimenez, J. L., Canagaratna, M. R., Ulbrich, I. M., Ng, N. L., Worsnop, D. R., and

2 Sun Y.: Understanding atmospheric organic aerosols via factor analysis of aerosol mass

3 spectrometry: a review. Anal Bioanal. Chem., 401, 3045-3067, 2011.

4 Zotter, P., Ciobanu, V. G., Zhang, Y. L., El Haddad, I., Macchia, M., Daellenbach, K. R.,

5 Salazar, G. A., Huang, R.-J., Wacker, L., Hueglin, C., Piazzalunga, A., Fermo, P.,

6 Schwikowski, M., Baltensperger, U., Szidat, S., and Prévôt, A. S. H.: Radiocarbon analysis of

7 elemental and organic carbon in Switzerland during winter-smog episodes from 2008 to 2012

8 – Part 1: Source apportionment and spatial variability, Atmos. Chem. Phys., 14, 13551–

9 13570, doi:10.5194/acp-14-13551-2014, 2014.

10

1   **Figures main text**
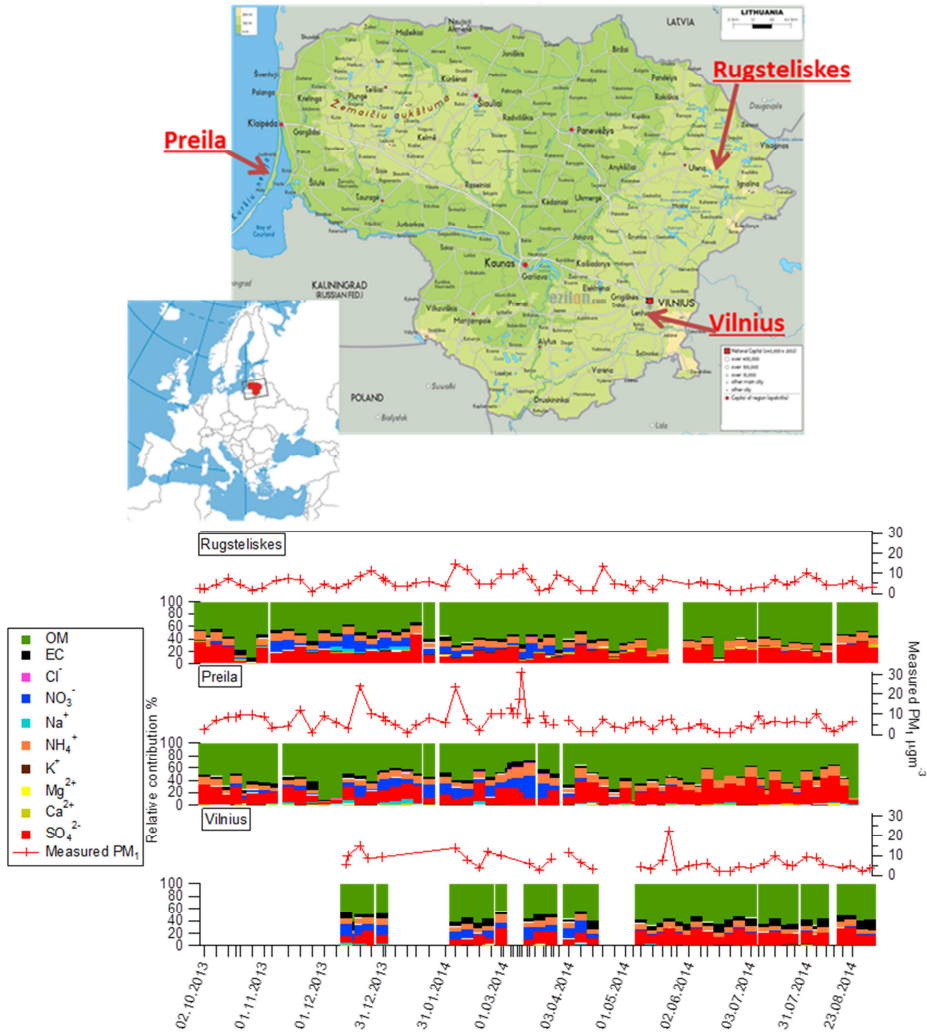
2
3   Figure 1. Sampling locations, and measured PM$_1$ composition. Ion concentrations from IC.
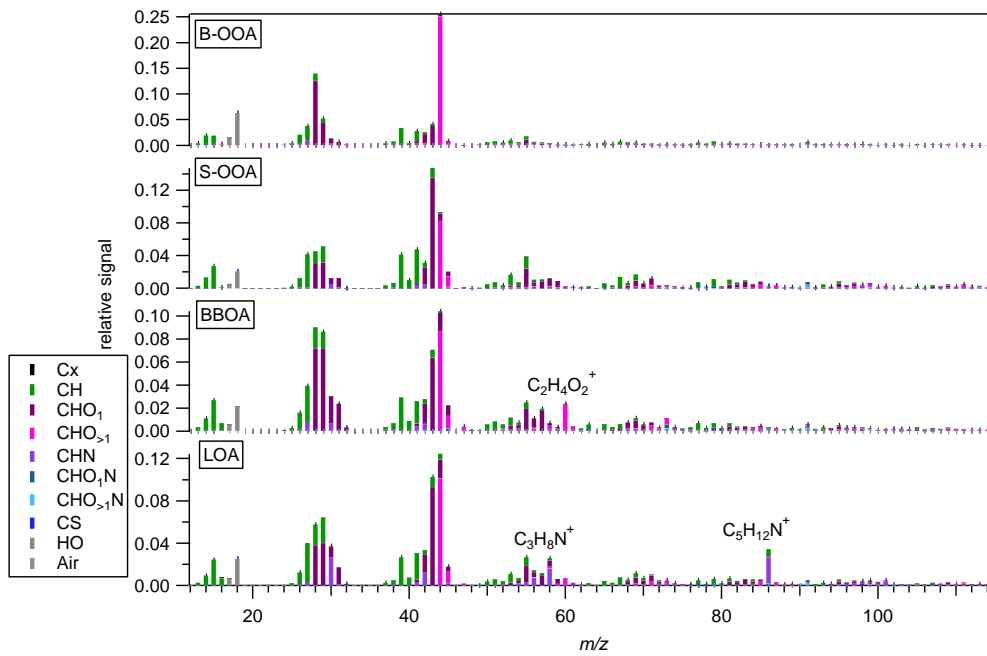
1

2 Figure 2. Offline-AMS PMF factor profiles: background oxygenated OA (B-OOA), summer

3 oxygenated OA (S-OOA), biomass burning OA (BBOA), local OA (LOA).

4

5
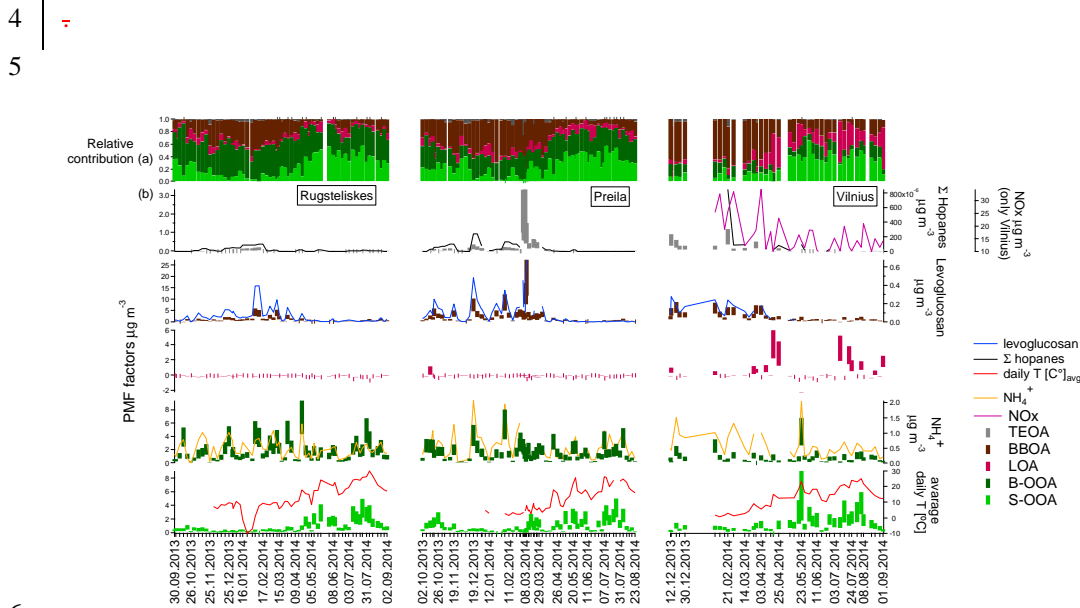
6

7 Figure 3. a) Temporal evolutions of relative contributions to the OA factors; b) OA sources

8 and corresponding tracers: concentrations and uncertainties (shaded areas).

1
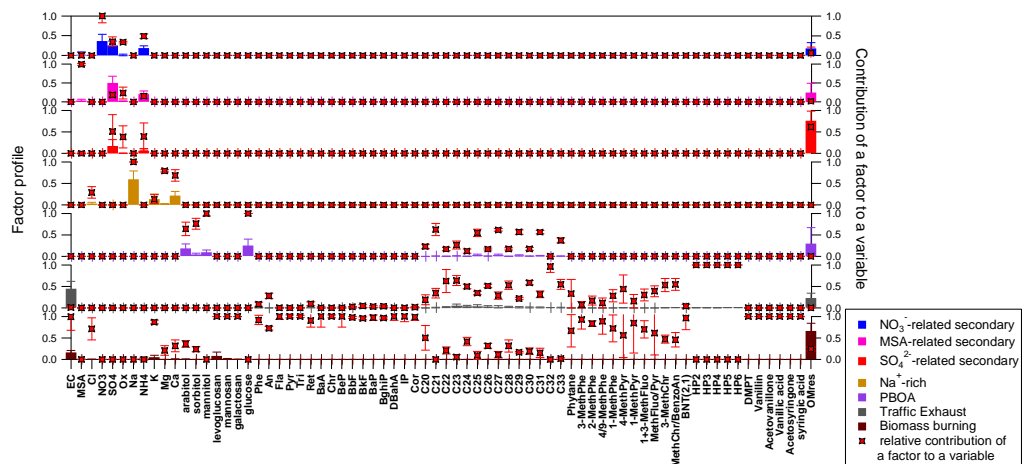
2

3 Figure 4. Marker-PMF factor profiles (bars) and relative contributions of the factors to the

4 measured variables (symbols). Factor list and abbreviations: NO_3^--related secondary aerosol

5 (NO_3^- related SA), SO_4^{2-}-related-SA, MSA-related-SA, Na^+-rich aerosol, primarybiological

6 organic aerosol (PBOA), traffic exhaust (TE), biomass burning (BB).

Formatted: Font color: Auto
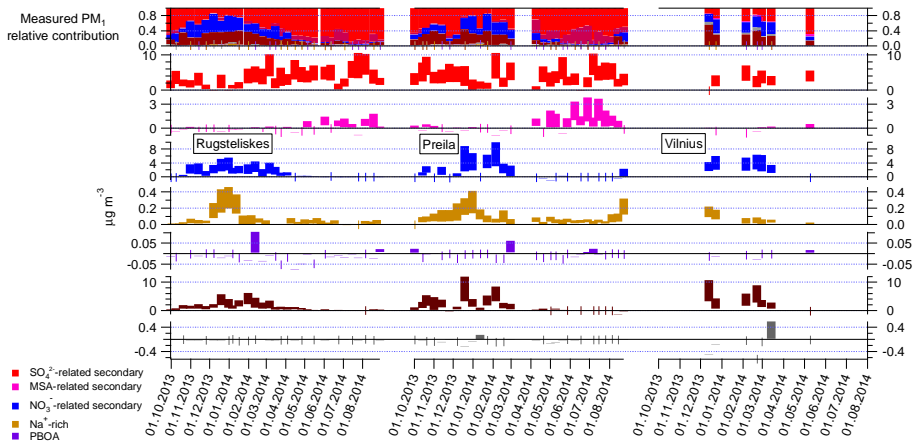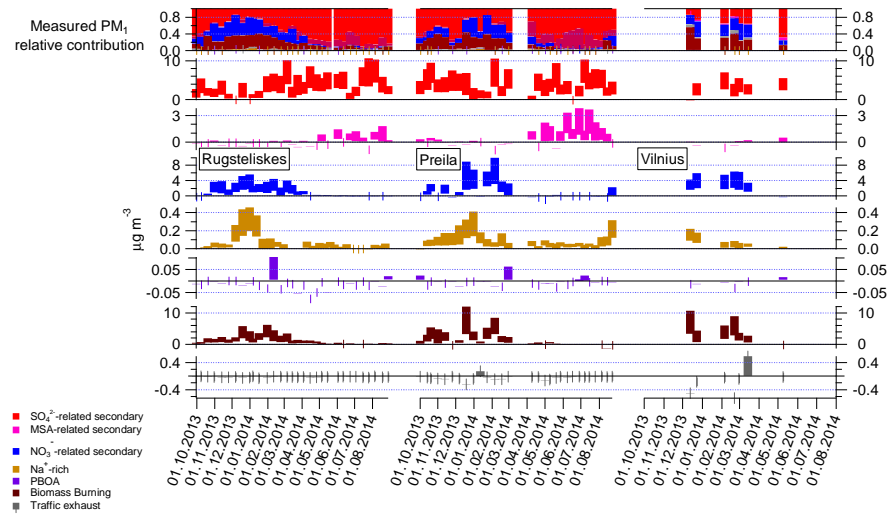
Figure 5. PM$_1$ marker source apportionment: factor time series and relative contributions. Shaded areas indicate uncertainties (standard deviation) of 20 bootstrap runs.
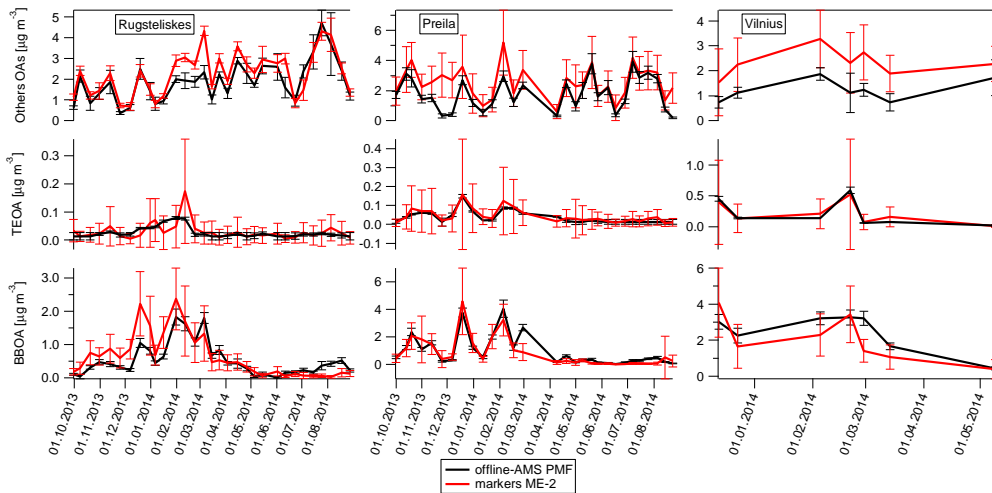
Figure 6. Marker-PMF and offline-AMS OM source apportionment comparison.
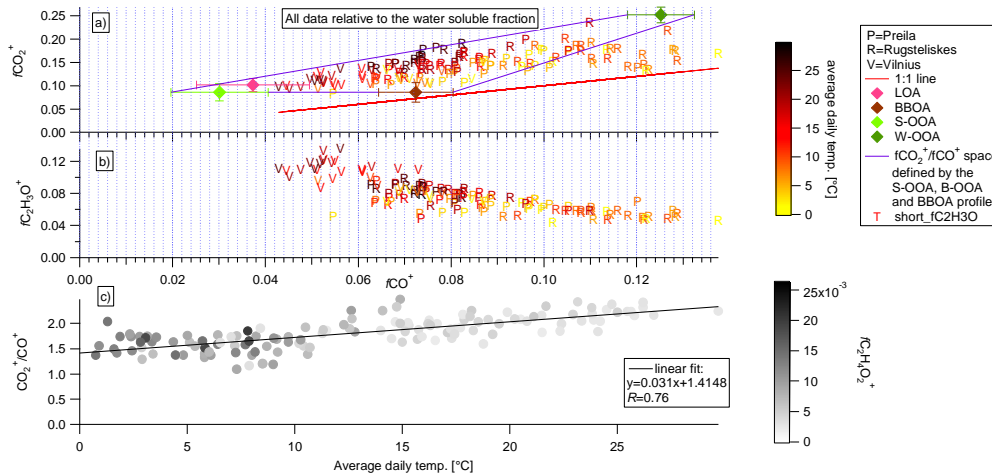
Figure 7. a) water-soluble fCO$_2^+$ vs fCO$^+$ scatter plot. Color code denotes the average daily temperature [°C], diamonds indicate the fCO$_2^+$/fCO$^+$ ratio for different PMF factor profiles. The 1:1 line is displayed in red. Few points from Rūgšteliškis lie outside the triangle, suggesting they are not well explained by our PMF model. However, Fig. S5 displays flat residuals for Rūgšteliškis, indicating an overall good WSOM explained variability by the model. b) water-soluble fC$_2$H$_3$O$^+$ vs fCO$^+$ scatter plot. Color code denotes the average daily temperature [°C] c) Scatter plot of the water-soluble CO^{2+} to CO$^+$ ratio *vs.* average daily temperature. Grey code denotes fC$_2$H$_4$O$_2^+$.
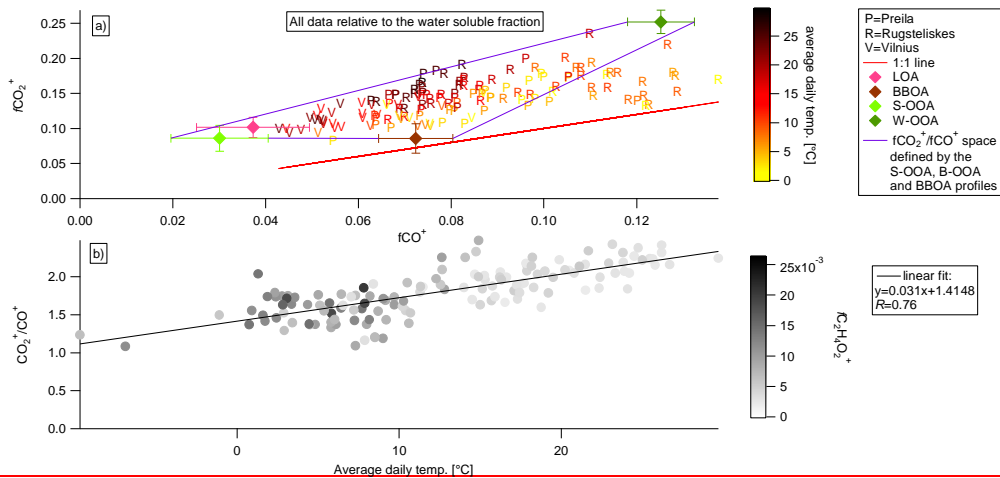
Figure 7. a) water-soluble fCO_2^+ vs fCO^+ scatter plot. Color code denotes the average daily temperature [°C], diamonds indicate the fCO_2^+/fCO^+-ratio for different PMF factor profiles. The 1:1 line is displayed in red. Few points from Rūgšteliškis lie outside the triangle, suggesting they are not well explained by our PMF model. However, Fig. S5 displays flat residuals for Rūgšteliškis, indicating an overall good WSOM explained variability by the model. b) Scatter plot of the water-soluble CO^{2+} to CO^+ ratio vs. average daily temperature. Grey code denotes $fC_2H_4O_2^+$.
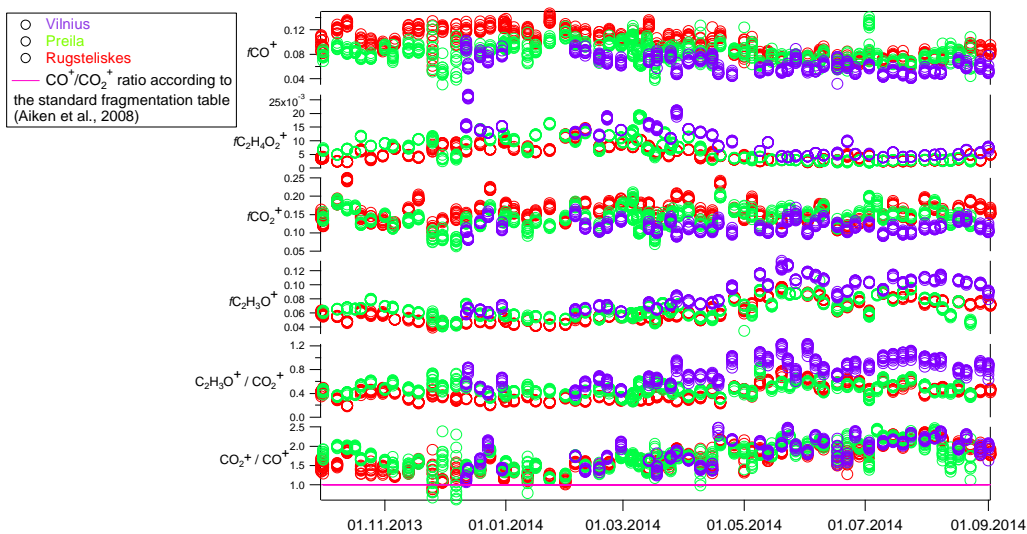
Figure 8. Time-dependent fractional contributions (*f*) of typical AMS tracers.

1